

August 2016

## Resource Allocation for Interference Management in Wireless Networks

Raghd El Bardan  
*Syracuse University*

Follow this and additional works at: <https://surface.syr.edu/etd>



Part of the [Engineering Commons](#)

---

### Recommended Citation

El Bardan, Raghd, "Resource Allocation for Interference Management in Wireless Networks" (2016).  
*Dissertations - ALL*. 663.  
<https://surface.syr.edu/etd/663>

This Dissertation is brought to you for free and open access by the SURFACE at SURFACE. It has been accepted for inclusion in Dissertations - ALL by an authorized administrator of SURFACE. For more information, please contact [surface@syr.edu](mailto:surface@syr.edu).

## ABSTRACT

Interference in wireless networks is a major problem that impacts system performance quite substantially. Combined with the fact that the spectrum is limited and scarce, the performance and reliability of wireless systems significantly deteriorates and, hence, communication sessions are put at the risk of failure. In an attempt to make transmissions resilient to interference and, accordingly, design robust wireless systems, a diverse set of interference mitigation techniques are investigated in this dissertation.

Depending on the rationale motivating the interfering node, interference can be divided into two categories, communication and jamming. For communication interference such as the interference created by legacy users (e.g., primary user transmitters in a cognitive radio network) at non-legacy or unlicensed users (e.g., secondary user receivers), two mitigation techniques are presented in this dissertation. One exploits permutation trellis codes combined with  $M$ -ary frequency shift keying in order to make SU transmissions resilient to PUs' interference, while the other utilizes frequency allocation as a mitigation technique against SU interference using Matching theory. For jamming interference, two mitigation techniques are also investigated here. One technique exploits time and structures a jammer mitigation framework through an automatic repeat request protocol. The other one utilizes power and, following a game-theoretic framework, employs a defense strategy against jamming based on a strategic power allocation. Superior performance of all of the proposed mitigation techniques is shown via numerical results.

RESOURCE ALLOCATION FOR INTERFERENCE  
MANAGEMENT IN WIRELESS NETWORKS

By

Raghd El Ahmad El Bardan

B. E., Lebanese American University, 2007  
M. Sc., Lebanese American University, 2009

DISSERTATION

Submitted in partial fulfillment of the requirements for the degree of  
Doctor of Philosophy in Electrical and Computer Engineering

Syracuse University  
August 2016

Copyright © 2016 Raghed Ahmad El Bardan

All rights reserved

# ACKNOWLEDGMENTS

I would like to thank my Ph.D advisor, Professor Pramod K. Varshney, for supporting me during the past couple of years. I am truly fortunate to have had the opportunity to work with him. I am grateful to him for his scientific knowledge, methodical advice, and many keen suggestions and discussions. Professor Varshney is someone you will instantly love and never forget. He is the funniest advisor and one of the smartest people I know. I hope that I could be as spirited and exuberant as him and to someday be able to command an audience as well as he can. I will forever be thankful to him.

I would also like to thank my committee members, Professors Mustafa Cenk Gursoy, Yingbin Liang, Jian Tang, Qi Cheng, and H. Ezzat Khalifa for the thought-instigating suggestions, constructive feedback, valuable guidance, and genuine collegiality that each of them provided. Along the same lines, I would like to recognize the faculty members in the department of Electrical Engineering and Computer Science at Syracuse University with whom I interacted, for the contributions that they made to my intellectual growth during my years of study at Syracuse University.

I am also thankful to a handful of collaborators, Drs. Yunghsiang Sam Han, Walid Saad, Swastik Brahma, Engin Masazade, and Onur Ozdemir, for their insightful discussions and feedback about my research.

Furthermore, I was lucky enough to be a member of the "Sensor Fusion" Lab at Syracuse University. I am very grateful to Aditya, Arun, Bhavya, Hao, Nianxia, Sid, Sijia, and all the current and past members of the Lab. Our friendship means a lot to me.

I especially thank my mom, dad, and brother. My parents have sacrificed their lives

for my brother and I and have always provided unconditional love and care. In simple words, I would not have made it this far without them. I know that I always have them to count on.

*To Marwa, Ahmad, and Rawad  
for their endless support and unconditional love.*

# TABLE OF CONTENTS

<b>Acknowledgments</b>	<b>v</b>
<b>List of Tables</b>	<b>x</b>
<b>List of Figures</b>	<b>xi</b>
<b>1 Introduction</b>	<b>1</b>
1.1 Challenges . . . . .	3
1.2 State-of-the-art Defense Techniques . . . . .	4
1.2.1 Forward Error-correction Coding . . . . .	5
1.2.2 Re-transmission Protocols . . . . .	5
1.2.3 Power/Frequency Allocation . . . . .	5
1.3 Major Contributions and Dissertation Outline . . . . .	6
1.4 Bibliography . . . . .	8
<b>2 Mitigation of Primary User Interference via Permutation Trellis Codes</b>	<b>10</b>
2.1 Literature Review . . . . .	11
2.2 Motivation, Novelty, and Contributions . . . . .	13
2.3 System Model . . . . .	15
2.4 Bit Error Rate Analysis . . . . .	21
2.4.1 Computation of likelihoods in the absence of PU . . . . .	27
2.4.2 Computation of likelihoods in the presence of PU . . . . .	28
2.5 Throughput Analysis . . . . .	30



2.5.1	Licensed Channel Dynamic Occupancy Model . . . . .	30
2.5.2	Throughput Analysis . . . . .	31
2.6	Numerical Results and Discussion . . . . .	32
2.6.1	Approximate BER with Single Permanent PU Interference . . . . .	32
2.6.2	Throughput Analysis of $H$ -FSK . . . . .	34
2.6.3	SU Link's Resiliency in the Presence of Multiple PUs . . . . .	38
2.7	Summary . . . . .	40
<b>3</b>	<b>Mitigation of SU Interference via a Matching-based Frequency Allocation</b>	<b>42</b>
3.1	Literature Review . . . . .	43
3.2	Motivation, Novelty, and Contributions . . . . .	44
3.3	System Model . . . . .	44
3.4	Spectrum Allocation as a Matching Game . . . . .	49
3.4.1	Matching Concepts . . . . .	49
3.4.2	Preferences and Proposals of the SUs . . . . .	50
3.4.3	Preferences of the PUs . . . . .	51
3.5	Solution Concept and Proposed Algorithm . . . . .	52
3.6	Numerical Results . . . . .	55
3.7	Summary . . . . .	58
<b>4</b>	<b>Mitigation of Jamming Interference via ARQ Protocols</b>	<b>59</b>
4.1	Literature Review . . . . .	60
4.2	Motivation, Novelty, and Contributions . . . . .	60
4.3	System Model and Problem Formulation . . . . .	61
4.3.1	Problem Formulation . . . . .	62
4.4	Approximate Minimax Energy Allocations for a fixed $\mathcal{T}$ . . . . .	63
4.4.1	Upper-bound . . . . .	66
4.4.2	Lower-bound . . . . .	67

4.4.3	Equilibrium Analysis of Problem 4.P2-B . . . . .	68
4.4.4	Discussion: Impact of Retransmissions on System-Performance . . . . .	69
4.5	Minimization of the Number of Transmission Attempts for Successful Communi- cation . . . . .	70
4.6	Numerical Results . . . . .	71
4.7	Summary . . . . .	73
<b>5</b>	<b>Mitigation of Jamming Interference via a Strategic Power Allocation</b>	<b>74</b>
5.1	Literature Review . . . . .	74
5.2	Motivation, Novelty, and Contributions . . . . .	77
5.3	System Model and Problem Formulation . . . . .	78
5.4	Equilibrium Analysis: Channels are available . . . . .	82
5.4.1	Solution of 5.P1 . . . . .	83
5.4.2	Solution of 5.P2 . . . . .	85
5.5	Optimal Power Allocation for Different Instantiations and Knowledge Level . . . . .	86
5.5.1	Multi-path Fading Model with Incomplete Knowledge of Channel Gains . . . . .	88
5.5.2	Simplified Path-Loss Model and Incomplete Knowledge of $d_{J_i}$ . . . . .	90
5.6	Sensing-based Spectrum Access . . . . .	93
5.6.1	Problem Formulation . . . . .	93
5.6.2	Equilibrium Analysis . . . . .	96
5.7	Numerical Results . . . . .	97
5.8	Summary . . . . .	103
<b>6</b>	<b>Conclusion</b>	<b>106</b>
6.1	Summary . . . . .	106
6.2	Future Work . . . . .	108
	<b>References</b>	<b>110</b>

# LIST OF TABLES

1.1	List of technical challenges and the corresponding defense techniques . . . . .	8
2.1	Mapping of symbols into permutation code matrices ( $M = H = 2$ ) . . . . .	17
2.2	Mapping of symbols into permutation code matrices ( $M = 4, H = 3$ ) . . . . .	18
2.3	A comparison of the time needed to compute BER between exhaustive search [28] and approximation approach for different PTC ( $H = 2, 3, \text{ and } 4$ ) . . . . .	34

# LIST OF FIGURES

1.1	A cognitive radio network with one PU transmitter-receiver pairs and two SU transmitter-receiver pairs in the presence of a jammer. . . . .	4
2.1	A simple cognitive radio network with $H = 3$ independent PU transmitter-receiver pairs and one SU transmitter-receiver pair. . . . .	15
2.2	Block diagram of the Coded multi-level FSK System . . . . .	16
2.3	Finite State Machine of a ( $R = \frac{1}{2}$ ) convolutional coded PTC system. . . . .	22
2.4	A ( $R = \frac{1}{2}$ ) convolutional code trellis for our PTC-based system in which a 0 or a 1 denotes the input bit and a permutation of symbols 1, 2, and 3 denotes the output symbol as shown next to each arrow. . . . .	23
2.5	Two-state Markov chain model for a given PU $j$ activity over its licensed frequency. . . . .	30
2.6	BER approximations for PTC with $H = 3$ . . . . .	32
2.7	$ BER - BER_{apx} $ for different PTC ( $H = 2, 3, \text{ and } 4$ ) and SNR = 7 dB. . . . .	33
2.8	Throughput Comparison of $H$ -FSK and uncoded opportunistic $M$ -FSK as well as convolutionally coded BPSK schemes for SNR = 7 dB, packet size = 256 bits, and $R_p = 100$ packets/sec. . . . .	35
2.9	Approximate BER performance of different PTCs with respect to PUs that are <i>always</i> ON and transmitting. . . . .	37
2.10	Approximate BER versus Simulated BER for a PTC with $H = 2, 3, \text{ and } 4$ , $n = 1, 2, \text{ and } 3$ , and $P_{ch}^{ON} = 0.35$ . . . . .	37
2.11	Approximate BER performance of a PTC ( $H = 4$ ) with respect to dynamically varying PUs activities and PUs that are <i>always</i> ON. . . . .	38

2.12	A BER comparison between the proposed PTC scheme with $H = 4$ and a $1/2$ rate (64800,32400) LDPC encoding with a 4-FSK modulation system with respect to static ( $P_{ch}^{On} = 1$ ) and dynamic ( $P_{ch}^{On} = 0.75$ ) activities of a PU. . . . .	39
3.1	An illustration of the system model. An arrow portrays the sensing mechanism of PUs activities performed at the transmitter's side of each SU pair. . . . .	45
3.2	The sum of SUs' rates with respect to the number of SUs in the network, $O$ , for $H = \{3, 4\}$ . . . . .	55
3.3	The number of iterations required for an algorithm to converge with respect to the number of SUs, $O$ , when $H = 4$ . . . . .	56
3.4	The sum of PUs' payoffs with respect to the number of SUs in the network, $O$ , for $H = 3$ and 4. . . . .	57
4.1	A P2P communication system in the presence of a jammer. . . . .	61
4.2	A state diagram showing the transitions of a data packet transmission. . . . .	64
4.3	Energy allocation of the transmitter when $\mathcal{T} = 3$ . . . . .	71
4.4	Energy allocation of the jammer when $\mathcal{T} = 3$ . . . . .	71
4.5	The behavior of $f(\mathcal{T})$ with respect to $\mathcal{T}$ . . . . .	72
4.6	The variation of $\mathcal{T}^*$ with respect to $\delta$ . . . . .	72
5.1	A CRN with one SU Tx-Rx pair in the presence of a jammer. . . . .	78
5.2	[a, b] presents the support over which the marginal CDFs of the SU are defined when $H = 2$ in the absence of a power budget. The red-shaded region denotes all power allocations of the SU that satisfy a power budget $P$ , if it exists. The blue region, on the other hand, corresponds to those allocations that don't. Solving for KKT multipliers in the power budget will guarantee the existence of a power allocation strategy that always lies in the red shaded region. . . . .	87
5.3	A set of $H$ PUs and a single-hop CRN with one SU Tx-Rx pair in the presence of a jammer. . . . .	94
5.4	Marginal CDFs of both players under incomplete knowledge of the jammer's location. . . . .	97

5.5	SU's Marginal CDFs with complete and incomplete knowledge of channels' fading gains, $g_k$ for all $k$ . . . . .	98
5.6	Jammer's Marginal CDFs with complete and incomplete knowledge of the jammer's location.	99
5.7	SU's expected utility with respect to $P$ and different power allocation schemes. . . . .	100
5.8	SU's expected utility versus $P$ under complete and incomplete knowledge of jammer's location. . . . .	101
5.9	SU's expected utility with respect to increasing values of $\beta$ and different power allocation schemes. . . . .	102
5.10	SU's expected utility versus $\beta$ for different values of $R$ . . . . .	103
5.11	SU's expected utility versus $J$ for different power allocation schemes. . . . .	104
5.12	SU's expected utility versus $\alpha_k$ . . . . .	105

# CHAPTER 1

## INTRODUCTION

Over the last century, the world has witnessed many advances in wireless technologies [2, 8, 12, 22, 24, 30, 66, 70, 71, 85], the impact of which has been and will continue to be great and immense. Among its fastest growing segments, cellular technology ranks first. It has captured a lot of attention from media as well as researchers. The number of subscribers (users) has tremendously increased due to the many exciting services and features that such networks offer. Consequently, a huge demand on spectrum, which is already limited, has surfaced. This rapid growth, combined with the continuous generation of new wireless technologies, has advocated a vivid future for wireless systems, both as standalone and as part of the larger network infrastructure. However, such a swift growth and generation have also highlighted interference<sup>1</sup> and spectrum scarcity as two major issues which, if not handled properly, would critically affect the continuous operability and existence of the different technologies.

In order to accommodate the growing needs for wireless communication, impact and mitigation of interference needs to be addressed. In most existing wireless systems, interference is dealt with by using powerful forward error-correcting codes (FEC) or by coordinating users to orthogonalize their transmissions in time or frequency or by increasing the transmission power and treating

---

<sup>1</sup>Interference is a basic characteristic of wireless communication systems resulting from multiple transmissions that often take place simultaneously over a shared communication medium or nature that introduces noise, shadowing, scattering, etc.

each other's interference as noise. A number of sophisticated receiver designs have also been proposed for interference suppression under various settings, e.g., multiuser detection. Furthermore, interference can be classified into two categories based on its source as follows:

- **Communication interference:** This is the interference that nature causes or a transmitter accidentally creates at another receiver that is in its vicinity and shares the same communication medium and band when sending information to its corresponding receiver.
- **Jamming interference:** This is the interference that a jammer creates at one or more receivers in order to bring down the communication sessions when the corresponding transmitters and the jammer share the same communication medium and band.

This classification is based on the fact that, in the case of communication interference, the primary source is either nature or co-existence of other users on the same frequency band and the transmitter's main objective in this case is to ensure a successful reception (decoding) of its information at the corresponding receiver. On the other hand, in the case of a jammer, the jammer is a malicious entity and its main objective is to intentionally disrupt the on-going communication sessions in the network.

The traditional static spectrum assignment policy that is adopted by the Federal Communications Commission (FCC) leads to spectrum scarcity given the dramatic increase in spectrum demands. At the same time, there exists an inefficient spectrum utilization due to the fact that a large portion of the licensed spectrum is still not in use or severely underutilized [1]. Hence, spectrum scarcity and the inefficiency in the spectrum usage necessitate a new communication paradigm to opportunistically exploit the existing wireless spectrum. This new communication paradigm is referred to as Dynamic Spectrum Access (DSA) and radios implementing this access mechanism are called cognitive radios (CRs). Supplied with the inherent capabilities of the CR, cognitive radio networks (CRNs) are expected to yield an optimum spectrum-aware communication paradigm in wireless networks. We root this to the fact that the cognitive radio technology is envisaged to solve problems in wireless networks resulting from the inefficiency in the spectrum



usage and the limited available spectrum. The CR concept was first introduced by Mitola [60]. The idea he proposed was to make the licensed spectrum available to unlicensed or non-legacy users (i.e., secondary users) only when the licensed (legacy) users (i.e., primary users) are not using their frequency bands. Nevertheless, such a spectrum access agreement does not hold between multiple secondary users (SUs) in the absence of a primary user (PU). In other words, SUs are highly likely expected to interfere with each other upon transmitting over the same frequency band. As a matter of fact, the open nature of DSA is expected to stimulate such a behavior of the SUs in a CRN. It is important, at this point, to mention that communication interference in a CRN can be classified into two subcategories:

- PU interference: This is the interference that a PU creates at an SU's receiver when both the SU and the PU coexist over the same frequency band.
- SU interference: This is the interference that an SU creates at other SUs' receivers (a PU's receiver) when two or more SUs (an SU and a PU) coexist over the same frequency band.

## 1.1 Challenges

There are many technical challenges when designing robust wireless networks. Among these challenges, we mention the interference created by one or more PUs' transmissions at one or more SUs' receivers. Also, the competition for spectrum between multiple SUs constitutes another challenge that needs to be addressed. Equivalently, the latter can be described through interference that the corresponding SU transmitters would create at others' receivers. Another challenge lies in the security issues related to the availability of information at one or more SUs' receivers which, in turn, can also be interpreted by how much interference the jammer creates at one or more SUs' receivers. For more details on these challenges in addition to others in general, we refer the readers to [4, 33, 41, 47, 52, 54, 97, 102].

In Fig. 1.1, we show a general network model that summarizes the aforementioned issues assuming that the network's nodes share the same communication medium and frequency bands.

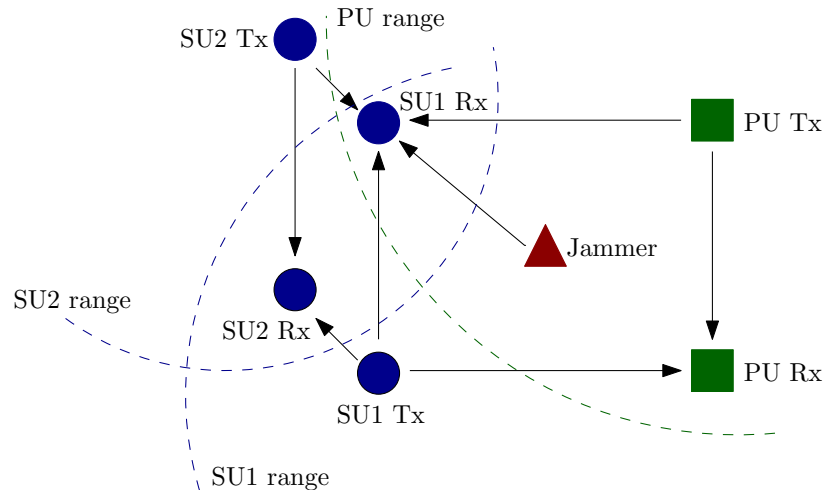


Fig. 1.1: A cognitive radio network with one PU transmitter-receiver pairs and two SU transmitter-receiver pairs in the presence of a jammer.

Here, the receiver of SU1 may suffer from communication interference created by either PU's transmitter or SU2's transmitter since the former is located within the communication range of the latter two. Additionally, upon the jammer's presence, SU1's receiver may also suffer from jamming interference. In this respect, SU2's receiver may suffer from communication interference created by SU1's transmitter as it is located within the latter's communication range.

## 1.2 State-of-the-art Defense Techniques

Managing interference, including communication and jamming, has been the subject of very active research up until today. Traditionally, interference prevention and mitigation techniques have been suggested to prevent the disruption of the network. In fact, several techniques [4, 47, 57] have been proposed to either prevent interference from deteriorating the network performance or mitigate it and still maintain a functional network. In this section, we confine our interest to only a subset of interference management techniques, for which we next present a brief overview.

### **1.2.1 Forward Error-correction Coding**

The performance of a wireless system deteriorates significantly more in the presence of interference. This is due to the fact that more data may be received in degraded form in this case than in the usual noisy communication systems and, accordingly, the receiver's output becomes more erroneous. When the number of output errors exceeds that number the decoder is capable of correcting, the transmitted data cannot be reconstructed correctly and, as a result, the probability of bit or symbol error increases. In other words, as the number of errors increases due to the presence of an interferer, i.e., the signal to interference-plus-noise ratio (SINR) at a particular receiver decreases, the probability of bit or symbol error increases. Therefore, in its attempt to adapt to interference that degrades its performance, a transmitter adds some type of controlled redundancy to its original data through the use of a forward error-correcting code (FEC). This technique is able to mitigate the impact of interference depending on the error correction capability of the code used.

### **1.2.2 Re-transmission Protocols**

A re-transmission protocol is considered an error-control mechanism that uses acknowledgments and timeouts to achieve a reliable data transmission over an unreliable service [18]. This technique ensures accurate delivery of information to the destination despite errors that occur during transmission. For instance, in a wireless system that employs a stop-and-wait Automatic Repeat Request (ARQ) protocol, the sender re-transmits the same information until it receives an acknowledgment or exceeds a predefined number of re-transmissions. This is another interference mitigation technique used as a defense strategy against an interferer.

### **1.2.3 Power/Frequency Allocation**

A power or frequency allocation approach constitutes a feasible technique for managing interference. This is because transmissions of multiple transmitters, who are trying to access the spectrum with fixed power and/or over a fixed frequency band, are expected to severely interfere with each

other in the overlapping portions of the spectrum. Hence, there is a necessity to efficiently manage transmissions of multiple transmitters over the same spectrum before sending their messages. In this respect, power as well as frequency allocation provide potential solutions that the wireless transmitter can exploit in its transmission strategy in order to mitigate interference.

In a framework where power allocation is employed in either a centralized or a distributed manner, transmitters adapt their transmit power levels over the shared spectrum in order to maximize some performance metric, e.g., SINR. Furthermore, when frequency allocation is implemented, transmitters are able to adapt to harmful interference in the environment by selecting, or getting assigned through a central entity, the best available frequency band that satisfies its quality-of-service requirements (e.g., minimizes interference at its receiver).

### **1.3 Major Contributions and Dissertation Outline**

The focus of this dissertation is on how to efficiently and effectively manage interference in wireless networks. In order to achieve this, we propose different interference management techniques that are based on Coding theory, Matching theory, and Game theory.

In the case of PUs' interference at an SU receiver in a CRN, we propose a novel spectrum underlay approach for SUs in Chapter 2, where PTCs are employed in conjunction with multi-level FSK signaling in the presence of multiple and dynamic narrowband PUs. Our proposed approach derives its resilience to the interference caused by PUs and noise disturbances via dispersal of the information in SU's messages over multiple frequencies and time intervals. This underlay-design improves the SU data rate by accumulating a large amount of spectrum from several PUs, while simultaneously operating at low power to minimize the interference caused at PUs' receivers. We evaluate our system performance in terms of bit error rate (BER) and throughput by approximating the actual BER using properties of the Viterbi decoder and, accordingly, show that the proposed coded system is robust to heavy interference caused by PUs.

In our attempt to address competition for spectrum between multiple SUs in a CRN, a novel

spectrum allocation approach is proposed in Chapter 3. Based on a measure of inference performance as well as on a measure of quality-of-service, the association between SUs in the network and frequency bands licensed to PUs is investigated. The problem is formulated as a matching game between SUs and PUs, where SUs employ hypothesis testing to detect PUs' signals and rank them based on the logarithm of the *a posteriori* probability ratios. A valuation that captures the ranking metric and rate over the PU-owned frequency bands is proposed to PUs in the form of credit or rewards by SUs. Using this proposal, a PU evaluates a utility function that it uses to build its association preferences. Furthermore, a distributed algorithm that allows both SUs and PUs to interact and self-organize into a stable and optimal matching is presented.

For jamming interference in wireless point-to-point (P2P) communication links with perfect feedback channels, where transmissions occur over an additive white Gaussian noise channel subject to Inter-symbol Interference (ISI), we investigate the design and performance of a novel ARQ-based system in Chapter 4. We define system-latency as the number of transmission attempts at the transmitter to achieve a successful transfer of a data packet to the receiver. We attempt to minimize it by modeling this as a constrained optimization problem where the system-latency is minimized such that the probability of successfully receiving a data packet at the receiver satisfies a prescribed guarantee. In this respect, a game-theoretic formulation is provided.

For the case of jamming interference in a CRN, the distributed competitive interactions between a SU transmitter-receiver pair and a jammer are investigated in Chapter 5 using a game-theoretic framework under physical interference restrictions, power budget constraints, and incomplete knowledge of channel gains. In this game, the SU transmitter is expected to choose its power strategy with the objective of satisfying a minimum SINR at the corresponding receiver. Similarly, the jammer's objective is to strategically allocate its power so that the SINR constraint of the SU is not satisfied. Due to a lack of complete information, this strategic power allocation problem between the two players is modeled as a Bayesian game for which the self-enforcing strategies of the SU transmitter-receiver pair and the jammer are analyzed. In this respect, probability distributions are further employed by the corresponding players to model the incomplete nature of the game.

Equilibrium analysis is carried out by considering the mixed strategy solution space.

Finally, in Chapter 6, we present a summary of our work in this dissertation along with some future directions that can be pursued.

## 1.4 Bibliography

In this section, we present the following table that lists the technical challenges we address in this dissertation along with the techniques that we utilize to manage such challenges.

Table 1.1: List of technical challenges and the corresponding defense techniques

Technical Challenge	Defense Strategy
PU interference	PTC [C1], [J1]
SU interference	Frequency allocation [C2]
Jammer interference in P2P systems	ARQ protocols [C3]
Jammer interference in CRNs	Power allocation [C4], [J2]

- Journal Papers

- [J1] R. El-Bardan, E. Masazade, O. Ozdemir, Y. S. Han and P. K. Varshney, "Permutation Trellis Coded Multi-Level FSK Signaling to Mitigate Primary User Interference in Cognitive Radio Networks," *IEEE Transactions on Communications*, vol. 64, no. 1, pp. 104-116, Jan. 2016.
- [J2] R. El-Bardan, S. Brahma, P. K. Varshney, "Strategic Power Allocation with Incomplete Information in the Presence of a Jammer," *IEEE Transactions on Communications*, vol. 64, no. 8, pp. 3467-3479, Aug. 2016.

- Conference Papers

- [C1] R. El-Bardan, E. Masazade, O. Ozdemir, and P. K. Varshney, "Performance of permutation trellis codes in cognitive radio networks," *Proc. of the 35th IEEE Sarnoff Symposium*, Newark, NJ, 2012, pp. 1-6.

- [C2] R. El-Bardan, W. Saad, S. Brahma and P. K. Varshney, “Matching theory for cognitive spectrum allocation in wireless networks,” *Proc. of the 50th Annual Conference on Information Science and Systems (CISS)*, Princeton, NJ, 2016, pp. 466-471.
- [C3] R. El-Bardan, V. S. S. Nadendla, S. Brahma and P. K. Varshney, “On ARQ-based wireless communication systems in the presence of a strategic jammer,” *Proc. of the IEEE Global Conference on Signal and Information Processing*, Atlanta, GA, 2014, pp. 273-277.
- [C4] R. El-Bardan, S. Brahma and P. K. Varshney, “Power control with jammer location uncertainty: A Game Theoretic perspective,” *Proc. of the 48th Annual Conference on Information Sciences and Systems (CISS)*, Princeton, NJ, 2014, pp. 1-6.

# CHAPTER 2

## MITIGATION OF PRIMARY USER INTERFERENCE VIA PERMUTATION TRELLIS CODES

According to [39], there are three main CRN paradigms<sup>1</sup>: interweave<sup>2</sup>, overlay, and underlay. The SUs in an interweave system opportunistically sense the spectrum looking for spectral holes to exploit in order to communicate without disrupting other transmissions. An overlay approach allows the SUs to use sophisticated signal processing and coding to maintain or improve the communication of PUs while also obtaining some additional bandwidth for their own communication. In underlay systems, SUs operate if the interference they cause to PUs is below a given threshold [19, 32, 51, 93]. However, an important question that remains yet to be answered satisfactorily is how to deal with the interference that one or more PUs create at SUs' receivers in an underlay system.

In this chapter, we investigate the use of Permutation Trellis Codes (PTCs) [34, 88] combined with multi-level FSK modulation systems in spectrum underlay CRNs where the special challenge

---

<sup>1</sup>The authors provide a detailed description on each of the paradigms in [39], including the associated regulatory policy as well as the underlying assumptions about what channel side information is available, and the practicality of obtaining such information.

<sup>2</sup>An interweave system is what Mitola proposed in [59, 60].



is to guarantee reliable communication by SUs in the presence of intermittent transmissions by narrowband PUs that stay active for an unknown duration without the need of detecting them. The emphasis of the proposed PTC based framework in this chapter is on robustness of SU transmissions against PUs' interference, rather than on data rate<sup>3</sup> or bandwidth use. The proposed approach derives its resilience to the interference caused by PUs and noise via dispersal of the information in SU's messages over multiple frequencies and time intervals in conjunction with PTCs. The proposed framework is quite general and is applicable to many systems beyond CRNs where interference is an issue. For example, the framework has been applied to power line communications [34, 88] where strong interferers are assumed to be always present. Here, we show a much wider applicability of the PTC based framework as an interference mitigation approach.

## 2.1 Literature Review

Orthogonal frequency division multiplexing (OFDM) has been suggested as a multi-carrier communication candidate for CR systems where the available spectrum is divided into sub-carriers each of which carries a low rate data stream [50, 58, 63, 81, 100]. A typical approach for a CR using OFDM is to sense the PU activity over the sub-carriers and then adjust its communication parameters accordingly. The goal is to protect PUs as well as intended SU receivers from possible collisions resulting from the use of the same sub-carriers. Continuous spectrum sensing and re-formation of wireless links may result in substantial performance degradation for SUs [90]. For instance, the throughput of the secondary system is affected by the time spent for channel sensing. When an SU spends more time on spectrum sensing, a smaller number of information bits will be transmitted over a shorter interval of time resulting in reduced system throughput. On the other hand, decreasing sensing duration may result in a larger probability of making incorrect decisions, thereby decreasing the throughput of both SUs and PUs. The authors in [65] numerically ana-

---

<sup>3</sup>However, it is important to mention that this underlay design improves the SU data rate by accumulating a large amount of spectrum from several PUs, while simultaneously operating at low power to minimize the interference caused at PUs' receivers.

lyze the trade-offs between throughput and sensing duration in addition to coding blocklength and buffer constraints. In [55], the authors study the problem of designing a sensing slot duration to maximize the achievable throughput for the SUs under the constraint that the PUs are sufficiently protected.

In [81], it is assumed that an SU transmitter vacates the band once a PU is detected. Due to the sudden appearance of a PU, rateless codes have been considered to compensate for the packet loss in SU data which is transmitted through parallel subchannels. The authors in [100] consider the design of two efficient anti-jamming coding techniques for the recovery of lost transmitted packets via parallel channels, namely rateless and piecewise coding. Similar to the spectrum model defined in [81], their performance is compared in terms of throughput and goodput. For an OFDM-based CRN presented in [50], SU transmitters and receivers continuously sense the spectrum, exchange information and decide on the available and unavailable portions of the frequency spectrum. Depending on frequency availability, an appropriate Reed-Solomon coding scheme is used to retrieve the bits transmitted over the unavailable portions of the frequency spectrum. The authors in [63] further explore Low-Density-Parity-Check (LDPC) codes in an OFDM scheme where a switching model is considered for dynamic and distributed spectrum allocation. They also analyze the effects of errors during PU detection on channel capacity and system performance. The switch is assumed to be open for each SU detecting a PU. When the switch is open, the channel is modeled as a binary erasure channel (BEC) and the SU continues to transmit its message allowing bits to be erroneous when received. Another major application of the FEC schemes is presented in [80] where the authors study the performance of cooperative relaying in cognitive radio networks using a rateless coding error-control mechanism. They assume that an SU transmitter participates in PU's transmission as a relay instead of vacating the band in order to reduce the channel access time by a PU. Since the use of rateless codes allows an SU receiver to decode data regardless of which packets it has received as long as enough encoded packets are received, these codes are very suitable for cooperative schemes. The authors in [9] propose an end-to-end hybrid ARQ scheme in CRNs consisting of unidirectional opportunistic links to reduce the number of re-transmissions with a fixed

throughput offset. Their error control approach is based on coded cooperation among paths and amplify-and-forward relaying of packets within a path such that this hybrid ARQ works for CRNs even if some coded data are missing. The authors implement their scheme using convolutional codes combined with BPSK modulation.

## 2.2 Motivation, Novelty, and Contributions

The motivation for approach proposed in this chapter is to overcome the tremendous degrading effect of multiple PUs' interference on an SU transmission and to provide a stable level of reliable information reception regardless of how severe or prolonged the dynamic PUs' activities are and without requiring their accurate detection. This is achieved via the dispersion of information in SU's messages over multiple frequencies and time intervals. In our model, an SU transmits its own information using low power concurrently with PUs' transmissions without the need to relay PUs' traffic [80] or to vacate the band [81].

Different from [50], we assume that no information exchange or control channel negotiation takes place between the SU transmitter-receiver pair. Our proposed scheme is different from existing work where communication sessions are carried out over parallel frequencies [50, 63, 81, 100]. This is due to the fact that our scheme is based on multi-level FSK modulation with PTC using a single frequency at a time. By using PTC, continuous channel sensing by the SU transmitter-receiver pair is no longer required, since an appropriate PTC can cope with high levels of PUs' interference on a given SU link. Thus, SUs no longer suffer from the huge overhead created by continuous sensing of the spectrum. We consider a similar system model as devised in [34, 88] and carry out a thorough performance analysis in terms of BERs and throughput for dynamically varying interference. In [34, 88], the authors were interested in the design of PTCs that mitigate the impact of interferences that always exist in power line communications. In their work, they conducted a simulation study and presented results on the performance of different PTCs with respect to the probability of an element of the code matrix being in error in the presence of

different noises on one or more channels. They also investigated the choice of distance increasing/conservative/reducing mappings for a given PTC with respect to narrowband interference that *always* exists on one band in the presence of background noise in terms of BER. The authors in [34, 88] provide a BER performance analysis via simulations and not analytically.

An analytical BER evaluation of a PTC coded M-FSK system is imperative to determine its link quality which is a useful tool for cross-layer design. Given that the PU stays active once it starts transmitting, the exact bit error rate (BER) is derived using an exhaustive search in [28]. Hence, the analytical evaluation of BER becomes computationally prohibitive for large codes. Rather than using an exhaustive search, in this chapter, we develop an approximation of BER using the properties of the Viterbi decoder. Also, in [28], a very special case is considered where a PU stays active once it starts transmission. In this chapter, we consider a more practical scenario where a 2-state Markov chain is employed to model each of the *dynamic* PUs' activities in terms of alternating On-Off periods. It should be noted that the work in [34] and [88] also considered an extreme case where the authors assumed that the interference was always present and did not consider dynamically varying interference. In the more general framework presented in this chapter, the performance results provided, e.g., BER, are intuitive and more useful in comparison to the worst-case guaranteed performance presented in [28].

In summary, the main contributions of the chapter are as follows:

- To mitigate interference created by the dynamic PUs, we propose the use of PTC-based multi-level FSK signaling that incurs no overhead costs for sensing as no channel sensing is required before SU transmissions.
- We consider a more practical scenario in which we represent each PU's activity in the network using a dynamic channel occupancy model and investigate the performance of the SU both analytically and through simulations in terms of BER and throughput for both static and dynamic activities of multiple PUs.
- Using the proposed PTC based framework, the SU transmissions are shown to achieve *ro-*

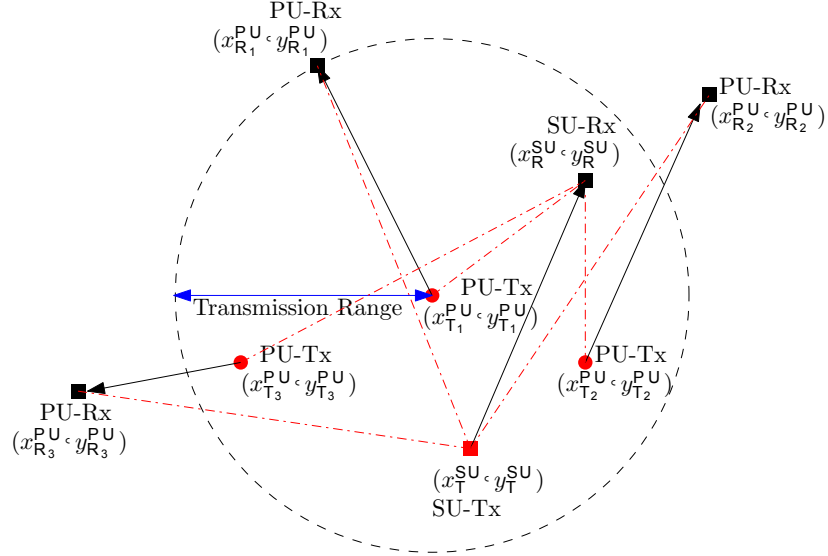


Fig. 2.1: A simple cognitive radio network with  $H = 3$  independent PU transmitter-receiver pairs and one SU transmitter-receiver pair.

*bustness* against the dynamic PUs' interference and noise disturbances and improved *resiliency* of SU links.

## 2.3 System Model

We consider a cognitive radio network which consists of  $H$  independent PU transmitter-receiver pairs, each operating on a different licensed frequency band, and an SU transmitter-receiver pair that may operate on one or more frequencies from the set of all PU-licensed bands  $\mathcal{F} = \{1, 2, \dots, H\}$ .

Fig. 2.1 shows an example of this simple network for  $H = 3$ .

Let  $(x_{T_j}^{PU}, y_{T_j}^{PU})$  and  $(x_{R_j}^{PU}, y_{R_j}^{PU})$ ,  $1 \leq j \leq H$ , denote the location coordinates of PU  $j$ 's transmitter and receiver respectively. Similarly, we denote the location coordinates of the SU transmitter and receiver as  $(x_T^{SU}, y_T^{SU})$  and  $(x_R^{SU}, y_R^{SU})$  respectively. Note that the SU pair may be located within the transmission range of any of the  $H$  PUs in the network. The transmission range shown in Fig. 2.1 is the maximum distance covered by PU  $j$ 's transmission such that the SINR at the corresponding PU receiver equals a minimum threshold value,  $SINR_{PU_j}^*$ . In this model, we assume a free space path loss model and a Line-Of-Sight (LOS) AWGN channel. The power in the

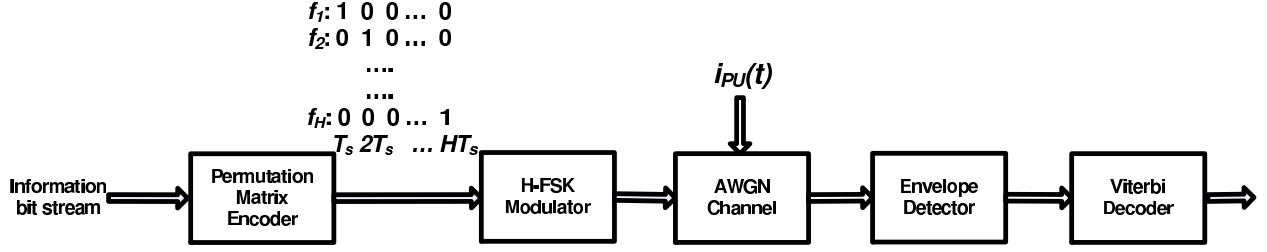


Fig. 2.2: Block diagram of the Coded multi-level FSK System

transmitted signal is  $P_T$ , so the received power over frequency  $f_j$  is given by [40]

$$P_{R_j} = P_T \frac{c_j}{d_{TR}^2}, \quad (2.1)$$

where  $c_j$  denotes the power attenuation factor for frequency  $f_j$  and  $d_{TR}$  is the distance between the transmitter and the receiver. Each PU in the network is licensed to use a single unique frequency in  $\mathcal{F}$  while SU transmissions occur over all the PU-licensed set of frequencies. One further assumption made here is that interference, created by an SU, that deteriorates the QoS of PUs is negligible compared to the received PUs' powers at their corresponding receivers. This is due to the fact that the transmission power of each PU is much larger than the transmission power of SU, i.e.,  $P_T^{SU} \ll P_T^{PU_j}, \forall j$ . In our approach, the SINR at PU  $j$ 's receiver [29] given in (2.2) satisfies  $SINR \geq SINR_{PU_j}^*$ , that is,

$$SINR = \frac{P_{R_j}^{PU}}{N_0 + P_{I_j}^{SU}} \geq SINR_{PU_j}^*, \quad (2.2)$$

where  $P_{I_j}^{SU}$  is the SU interference at PU  $j$ 's receiver and  $SINR_{PU_j}^*$  is the minimum threshold above which PU  $j$ 's transmission is received successfully. It is assumed that the SU transmitter knows the location of its corresponding receiver possibly by means of extra signaling.

An overview of the signal processing model that combines the PTC scheme with the multi-level FSK communication system is provided in Fig. 2.2.  $m$  information bits are loaded in parallel into a permutation matrix encoder which, in turn, is composed of a rate  $R = \frac{m}{n}$  convolutional encoder, e.g., a  $R = \frac{1}{2}$  with a two-stage shift register and generator 7, 5 (octal) [34], and a mapper that maps

each of the convolutional coded output symbols to a certain code matrix<sup>4</sup> to be transmitted over both time and frequency. For illustration purposes, we present an example in which the mapped symbol “213”, that is to be transmitted in both time and frequency domains, results in a  $3 \times 3$  ( $H \times H$ ) binary code matrix as given below.

$$\mathbf{T}_i = \begin{bmatrix} 0 & 1 & 0 \\ 1 & 0 & 0 \\ 0 & 0 & 1 \end{bmatrix}, \quad (2.3)$$

where  $1 \leq i \leq M$ ,  $M = 2^n$  denotes the total number of possible  $n$ -tuples at the output of the convolutional encoder, and  $H$  defines the number of frequency bands as well as the number of time steps used in transmitting the outputs of the encoder. In this chapter, we define the PTC-based multi-level FSK system as the  $H$ -FSK system since the PTC-based multi-level FSK modulated system leads to an  $H \times H$  binary code matrix. According to (2.3), transmission takes place on  $f_2$ ,  $f_1$ , and  $f_3$  (first, second and third columns of  $\mathbf{T}_i$ ) corresponding to the time steps  $T_s$ ,  $2T_s$ , and  $3T_s$  respectively. Tables 2.1 and 2.2 present the symbol (with 1 bit and 2 bits) mappings onto the corresponding unique permutation code matrices respectively [34]. For mapping tables for larger values of  $H$ , we refer the reader to [34]. For  $M$  different symbols,  $\mathbf{T}_i$  denotes the set of

Table 2.1: Mapping of symbols into permutation code matrices ( $M = H = 2$ )

Label	Symbol	Permutation code matrix
$\mathbf{T}_1$	0	12
$\mathbf{T}_2$	1	21

---

<sup>4</sup>It is important to mention that the Hamming distance between the permutation trellis matrices is lower-bounded by that of the convolutional coded output symbols used in the mapping procedure provided in [34].

Table 2.2: Mapping of symbols into permutation code matrices ( $M = 4, H = 3$ )

Label	Symbol	Permutation code matrix
$\mathbf{T}_1$	00	123
$\mathbf{T}_2$	01	132
$\mathbf{T}_3$	10	213
$\mathbf{T}_4$	11	231

transmitted code matrices such that  $\mathbf{T}_i \in \{\mathbf{T}_1, \dots, \mathbf{T}_M\}$  has the following general form:

$$\mathbf{T}_i = \begin{bmatrix} q_{1,1} & \cdots & q_{1,H} \\ \vdots & \ddots & \vdots \\ q_{H,1} & \cdots & q_{H,H} \end{bmatrix}, \quad (2.4)$$

where  $q_{j,k} \in \{0, 1\}$  denotes the  $(j, k)$  binary element in  $i$ -th transmitted code matrix,  $j$  indicates the output of the detector for frequency  $f_j$  at time step  $k$  in the code matrix. At the  $k$ -th time step, let  $j^*$  denote the row index for which  $q_{j^*,k} = 1$ . Note that  $q_{j,k} = 0, \forall j^* \neq j$  since PTC is a permutation matrix. At every time step, each entry in the column of the coded matrix is transmitted using ON-OFF keying over  $H$  parallel frequencies. In other words, a "1" in the  $j$ -th row of the coded matrix is modulated and transmitted over  $f_j$ , while no signal is transmitted in case of a "0". At a given time, only one frequency band is used for transmission.

Using the  $H$ -FSK scheme, the transmitted signal, assumed to be sufficiently narrowband, over  $j$ -th frequency and  $k$ -th time step where  $j, k \in \{1, 2, \dots, H\}$ , is given by:

$$s_k(t) = q_{j^*,k} \sqrt{2 \frac{E_s/H}{T_s}} \cdot \cos(2\pi f_{j^*} t),$$

$$(k-1)T_s \leq t \leq kT_s,$$

$$f_{j^*} = f_1 + \frac{j^* - 1}{T_s}, \quad (2.5)$$

where  $E_s$  denotes the transmitted signal energy per information symbol and  $T_s$  is the symbol



duration. In this model, we assume a strong LOS path between a stationary SU transmitter and a stationary receiver. Therefore, channel noise is modeled as Additive White Gaussian Noise (AWGN) with zero-mean and variance  $\frac{N_0}{2}$ . Since path loss is a function of the operating frequency, we need to ensure that the received signal power over the different frequency channels is the same,  $P_{R_1}^{SU} = \dots = P_{R_H}^{SU} = P_R^{SU}$ , in order to maintain a fixed signal-to-noise ratio,  $E_s/N_0$  at the receiver. Therefore, we adjust each SU's transmitting power over each frequency,  $P_T^{SU}(f_j)$ , according to the free space path loss model given in (2.1). This requires the SU transmitter to know the location of its corresponding receiver or the distance from its corresponding receiver. At the input of the SU demodulator, the received signal at the  $k$ -th time step is given by:

$$r_k(t) = s_k^r(t) + \sum_{j=1}^H i_j^{PU}(t) + w(t) ,$$

where

$$i_j^{PU}(t) = \begin{cases} \sqrt{2\frac{E_{I_j}^{PU}/H}{T_s}} \cos(2\pi f_j t + \phi_j), & \text{if PU } j \text{ is active} \\ 0, & \text{otherwise} \end{cases}$$

and  $s_k^r(t) = q_{j^*,k} \sqrt{2\frac{E_s^r/H}{T_s}} \cos(2\pi f_{j^*} t + \theta)$  where  $E_s^r$  is defined as the symbol energy at the receiver.  $E_{I_j}^{PU} \triangleq P_{I_j}^{PU} T_s$  and  $P_{I_j}^{PU}$  are defined as the interference energy per coded symbol and the interference power due to PU  $j$ 's transmitter at the SU receiver, respectively, and  $w(t)$  represents the channel noise at the receiver. It should be mentioned that PUs' transmitters can employ any modulation scheme while transmitting their signals and are not limited to the use of FSK-modulated signals. The fact that PUs' powers are very high compared to that of the SU implies that the received signal at the SU receiver is dominated by PUs' signals which, in turn, determine the behavior of the system.

In this chapter, we assume perfect synchronization in that each transmission time slot of the SU is aligned with that of the active PUs. We also assume that the bits to be transmitted in every PU's transmission are independent. In this case, the interference caused by PUs can be treated as being independent for each bit in SU's transmission. This might not be true when synchronization

is not perfect or channel coding is performed by a PU.

At the receiver side, non-coherent detection is employed using a bank of  $H$  quadrature receivers so that each consists of two correlation receivers corresponding to the in-phase and quadrature components of the signal. The in-phase component of the signal received,  $r_{I_{j,k}}$ , is given by:

$$r_{I_{j,k}} = \begin{cases} q_{j,k} \frac{E_s^r}{H} \cos \theta + \frac{E_{I_j}^{PU}}{H} \cos \phi_j + w, & \text{if PU exists on } f_j \text{ at time } k; \\ q_{j,k} \frac{E_s^r}{H} \cos \theta + w, & \text{otherwise,} \end{cases} \quad (2.6)$$

where  $\theta$  and  $\phi_j \forall j$  are uniformly distributed<sup>5</sup> over  $[0, 2\pi]$ , i.e.,  $\theta, \phi_j \forall j \sim \mathcal{U}(0, 2\pi)$ , and denote the random phase components of the SU and the PU signals, respectively. The noise term  $w$  in (2.6) is modeled as AWGN, i.e.,  $w \sim \mathcal{N}(0, \frac{N_0}{2})$ .  $E_s^r$  is the received symbol energy over a given signaling interval. Similarly,  $x_{Q_{j,k}}$  is the received signal's quadrature component defined as follows:

$$r_{Q_{j,k}} = \begin{cases} q_{j,k} \frac{E_s^r}{H} \sin \theta + \frac{E_{I_j}^{PU}}{H} \sin \phi_j + w, & \text{if PU exists on } f_j \text{ at time } k; \\ q_{j,k} \frac{E_s^r}{H} \sin \theta + w, & \text{otherwise.} \end{cases} \quad (2.7)$$

The envelope of each quadrature receiver over frequency  $j$  and time step  $k$ ,  $l_{j,k}$ , is defined as the square root of the sum of the squared in-phase and quadrature components of the correlator output as

$$l_{j,k} = \sqrt{r_{I_{j,k}}^2 + r_{Q_{j,k}}^2}. \quad (2.8)$$

At the receiver, a hard decision decoding scheme is used where the envelope value of each of the  $H$  quadrature receivers is compared to a threshold value,  $l_{th}$ . In this chapter, we do not perform formal optimization to find the threshold and instead we perform a sensitivity analysis by finding BER for different threshold values. We employ the threshold value  $l_{th} = 0.6\sqrt{E_s^r}$  that is shown to yield excellent performance in terms of BER. This value is the same as that used by the

---

<sup>5</sup>In the case of mobile networks, if the motion dynamics of all the transmitting nodes are deterministic and known, then the expected values of  $\theta$  and  $\phi_j$  shift by a fixed quantity. By including these quantities, our analysis can also handle mobile networks.

authors in [34]. It would certainly be desirable to determine the optimum value of the threshold such that the performance of the system is optimized. However, it is a difficult problem which will be considered in future work.

The received code matrix  $\mathbf{R}_i$  is of the form,

$$\mathbf{R}_i = \begin{bmatrix} b_{1,1} & b_{1,2} & \dots & b_{1,H} \\ \vdots & \vdots & \ddots & \vdots \\ b_{H,1} & b_{H,2} & \dots & b_{H,H} \end{bmatrix}, \quad (2.9)$$

where  $b_{j,k} \in \{0, 1\}$  and can be determined from,

$$b_{j,k} = \begin{cases} 1, & l_{j,k} \geq l_{th}, \\ 0, & \text{otherwise.} \end{cases} \quad (2.10)$$

## 2.4 Bit Error Rate Analysis

We employ BER as the QoS metric to characterize the communication performance for an SU. We consider the system model presented in Fig. 2.2 and obtain an approximation for BER. This system model is the same as the one considered in [34, 88] where the PTC encoder includes a convolutional encoder and the corresponding decoder uses Viterbi algorithm for decoding.

Here, we assume that the PTC encoder uses a rate- $\frac{1}{2}$  convolutional code whose output is converted to a symbol which, in turn, is mapped onto a permutation matrix to be transmitted. We recall that the mapping procedure from convolutional coded output symbols onto PTC matrices has to satisfy the distance preserving property discussed in [34]. In this case, the Hamming distance between any two PTC matrices is lower-bounded by the Hamming distance between the convolutional coded output symbols used in the mapping procedure. Since the exact BER analysis of the proposed system is computationally prohibitive, we approximate BER using some properties of the Viterbi decoder.

The encoder of the binary convolutional code with a given rate is viewed as a finite state ma-

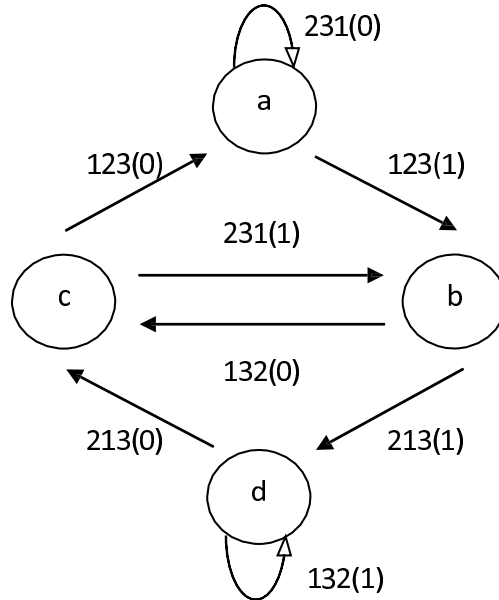


Fig. 2.3: Finite State Machine of a  $(R = \frac{1}{2})$  convolutional coded PTC system.

chine as shown in Fig. 2.3. This state diagram, corresponding to the PTC shown in Table 2.2, results in the trellis presented in Fig. 2.4. In order to optimally decode the received information, we employ the Viterbi algorithm which reconstructs the maximum-likelihood path given the input information sequence. In this case, an error event may occur if for a transmitted path in the trellis the overall number of differences with the demodulator outputs is larger than or equal to that of a competing path. The probability of bit error of a convolutional code is upper-bounded according to [56, 69] as

$$P_e \leq \sum_{d=d_{\text{free}}}^{\infty} a_d P_2(d), \quad (2.11)$$

where  $d_{\text{free}}$  is the free distance of the convolutional code,  $a_d$  is the number of paths that differ by  $d$  bits from the transmitter codeword, and  $P_2(d)$  is the probability that the decoded path differs by  $d$  bits from the transmitted codeword. In particular,  $a_d$  and  $P_2(d)$  are independent of the transmitted codeword. In fact, they can be calculated assuming that an all-zero codeword is transmitted. Knowing that all the code matrices to be sent include  $H$  non-zero elements, we next obtain a similar upper-bound for the system given in Fig. 2.2.

Now, let  $\mathbf{c}$  be a codeword of the convolutional code and  $\mathcal{P}(\mathbf{c})$  be the corresponding expanded

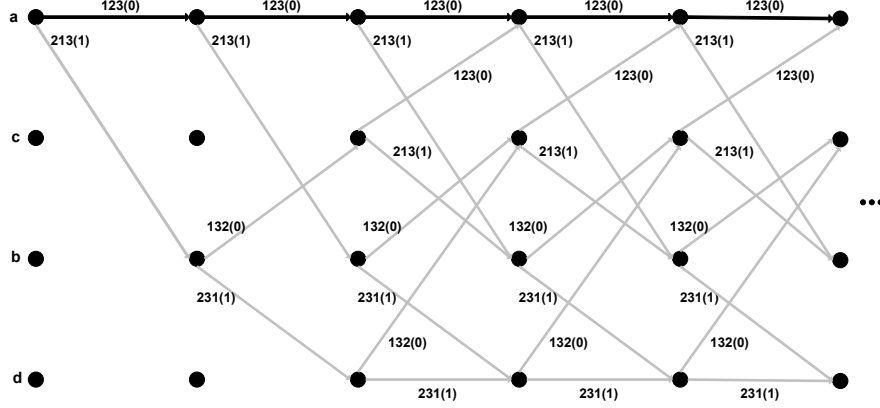


Fig. 2.4: A ( $R = \frac{1}{2}$ ) convolutional code trellis for our PTC-based system in which a 0 or a 1 denotes the input bit and a permutation of symbols 1, 2, and 3 denotes the output symbol as shown next to each arrow.

codeword comprising the permutation code matrices mapped from  $\mathbf{c}$ . The length of  $\mathcal{P}(\mathbf{c})$  is  $(L + m)H^2$ , where  $L$  denotes the size of the packet to be transmitted and  $L + m$  the number of branches in the trellis.

Let  $P_e(\mathcal{P}(\mathbf{c}))$  denote the probability of a bit error when  $\mathcal{P}(\mathbf{c})$  is the transmitted codeword. Knowing that  $\mathcal{P}(\mathbf{c})$  is a one-to-one mapping from the codeword  $\mathbf{c}$ , using (2.11), we have

$$P_e(\mathcal{P}(\mathbf{c})) \leq \sum_{d=d_{\text{free}}^*}^{\infty} a_d^{\mathcal{P}(\mathbf{c})} P_2^{\mathcal{P}(\mathbf{c})}(d), \quad (2.12)$$

where  $d_{\text{free}}^*$  is the free distance of the expanded code, and  $a_d^{\mathcal{P}(\mathbf{c})}$  and  $P_2^{\mathcal{P}(\mathbf{c})}(d)$  are the number of paths and the probability that the paths differ by  $d$  bits from the transmitted codeword  $\mathcal{P}(\mathbf{c})$ , respectively. In order to calculate (2.12), we need to prove that the upper-bound given in (2.12) is independent of the transmitted expanded codeword.

Let  $d_H(\mathbf{T}_i, \mathbf{T}_{j'})$  denote the number of different corresponding elements in  $\mathbf{T}_i$  and  $\mathbf{T}_{j'}$ , where  $\mathbf{T}_i$  and  $\mathbf{T}_{j'}$  are code matrices defined in (2.4). Furthermore, let  $\mathbf{S}_i \in \mathcal{S}$  be the corresponding symbol for  $\mathbf{T}_i$  such that  $\mathcal{P}(\mathbf{S}_i) = \mathbf{T}_i$ , where  $\mathcal{S}$  is the set of all symbols. We define a permutation

code matrix to be *geometrically uniform* if the following property is satisfied<sup>6</sup>.

$$\begin{aligned} & d_H(\mathcal{P}(\mathbf{S}_i \oplus \mathbf{S}_{k'}), \mathcal{P}(\mathbf{S}_i \oplus \mathbf{S}_{j'})) \\ = & d_H(\mathcal{P}(\mathbf{S}_{k'}), \mathcal{P}(\mathbf{S}_{j'})) \text{ for all } \mathbf{S}_i, \mathbf{S}_{j'}, \mathbf{S}_{k'} \in \mathcal{S}. \end{aligned} \quad (2.13)$$

For any  $\mathbf{S}_i \in \mathcal{S}$ ,  $\mathbf{S}_i \oplus \mathbf{S}_{k'}$  and  $\mathbf{S}_i \oplus \mathbf{S}_{j'}$  can be evaluated. The result of each Exclusive-Or operation is then mapped to a unique PTC. As such, it can easily be verified that the Hamming distance of the mappings is the same for all  $\mathbf{S}_i$ 's. Therefore, the permutation code matrix given in Table 2.2 is geometrically uniform. Under this condition, we have the following proposition in which we identify the sufficient condition that allows the use of the all-zero codeword (all-123 code matrix) in calculating the upper bound given in (2.12).

**Proposition 2.1.** *The bound in (2.12) is independent of the transmitted codeword if the permutation code matrix obtained upon expanding codewords is geometrically uniform.*

*Proof.* We need to prove that

$$\begin{aligned} & d_H(\mathcal{P}(\mathbf{c}_i \oplus \mathbf{c}_{k'}), \mathcal{P}(\mathbf{c}_i \oplus \mathbf{c}_{j'})) \\ = & d_H(\mathcal{P}(\mathbf{c}_{k'}), \mathcal{P}(\mathbf{c}_{j'})) \text{ for all } \mathbf{c}_i, \mathbf{c}_{j'}, \mathbf{c}_{k'} \in \mathcal{C}, \end{aligned}$$

where  $\mathcal{C}$  contains all codewords of the convolutional code. Since the convolutional code is linear,  $\mathbf{c}_i \oplus \mathbf{c}_{k'}$  and  $\mathbf{c}_i \oplus \mathbf{c}_{j'}$  are also codewords in  $\mathcal{C}$  and

---

<sup>6</sup>A general definition of geometrically uniform codes can be found in [36].

$$\begin{aligned}
& d_H(\mathcal{P}(\mathbf{c}_i \oplus \mathbf{c}_{k'}), \mathcal{P}(\mathbf{c}_i \oplus \mathbf{c}_{j'})) \\
&= \sum_{\ell=1}^{\infty} d_H(\mathcal{P}(\bar{\mathbf{c}}_{i,\ell} \oplus \bar{\mathbf{c}}_{k',\ell}), \mathcal{P}(\bar{\mathbf{c}}_{i,\ell} \oplus \bar{\mathbf{c}}_{j',\ell})) \tag{2.14}
\end{aligned}$$

$$= \sum_{\ell=1}^{\infty} d_H(\mathcal{P}(\mathbf{S}_{i,\ell} \oplus \mathbf{S}_{k',\ell}), \mathcal{P}(\mathbf{S}_{i,\ell} \oplus \mathbf{S}_{j',\ell})) \tag{2.15}$$

$$= \sum_{\ell=1}^{\infty} d_H(\mathcal{P}(\mathbf{S}_{k',\ell}), \mathcal{P}(\mathbf{S}_{j',\ell})) \text{ by (2.13)} \tag{2.16}$$

$$= \sum_{\ell=1}^{\infty} d_H(\mathcal{P}(\bar{\mathbf{c}}_{k',\ell}), \mathcal{P}(\bar{\mathbf{c}}_{j',\ell})) \tag{2.17}$$

$$= d_H(\mathcal{P}(\mathbf{c}_{k'}), \mathcal{P}(\mathbf{c}_{j'})), \tag{2.18}$$

where  $\bar{\mathbf{c}}_{i,\ell}$  is the  $\ell$ -th branch (stage) output code bits of  $\mathbf{c}_i$ . Both (2.15) and (2.17) are derived from the fact that the output code bits are the corresponding symbols.  $\square$

The fact that we have no information regarding the length of the transmitted bits sequence means that the calculation of the upper bound, in (2.11), involves an infinite sum over all possible error events which will render the process of evaluating the error bound computationally prohibitive for applications such as link adaptation. Therefore, it is important to approximate BER using a suitably selected finite number of trellis paths. It is most likely that the first few error events (paths) in the trellis dominate all the remaining ones. In this manner, the approximate BER can be written as

$$\hat{P}_e \approx \sum_{d=d_{\text{free}}^*}^{d_{\text{free}}^*+z} a_d^{\mathcal{P}(\mathbf{c})} P_2^{\mathcal{P}(\mathbf{c})}(d), \tag{2.19}$$

where  $z \in \mathbb{N}$  and  $z + 1$  denotes the number of paths involved in the BER approximation for which numerical results are presented in Section 2.6. At this point, it is important to mention that a path (error event) is composed of  $\mathcal{V}$  stages. Let  $\mathbf{T}$  be the concatenation of  $\mathbf{T}^1, \mathbf{T}^2, \dots, \mathbf{T}^{\mathcal{V}}$  and  $\mathbf{R}$  be the concatenation of  $\mathbf{R}^1, \mathbf{R}^2, \dots, \mathbf{R}^{\mathcal{V}}$ , where  $\mathbf{T}^u$  and  $\mathbf{R}^u$  denote the transmitted and received code matrices at stage  $u$  in the trellis respectively. Furthermore, let  $\mathcal{D}_d$  be the set of code matrices that

differ from  $\mathbf{T}$  in the first  $d$  bits. Accordingly,  $P_2^{\mathcal{P}(c)}(d)$  can be written as

$$P_2^{\mathcal{P}(c)}(d) = \begin{cases} \sum_{\substack{d_H(\mathbf{R}, \mathbf{T}) = \frac{d+1}{2} \\ \mathbf{R} \in \mathcal{D}_d}}^d \prod_{u=1}^{\nu} P(\mathbf{R}^u | \mathbf{T}^u), & d \text{ is odd,} \\ \sum_{\substack{d_H(\mathbf{R}, \mathbf{T}) = \frac{d}{2} + 1 \\ \mathbf{R} \in \mathcal{D}_d}}^d \prod_{u=1}^{\nu} P(\mathbf{R}^u | \mathbf{T}^u) \\ + \frac{1}{2} \prod_{u=1}^{\nu} P(\mathbf{R}^u | \mathbf{T}^u) \Big|_{\substack{d_H(\mathbf{R}, \mathbf{T}) = \frac{d}{2} \\ \mathbf{R} \in \mathcal{D}_d}}, & d \text{ is even.} \end{cases} \quad (2.20)$$

Given the transmitted code matrix at stage  $u$  ( $\mathbf{T}^u$ ), the conditional distribution of the received code matrix  $\mathbf{R}^u$  solely depends on the noise distribution and PU interference and, therefore, is independent in both time and frequency domains. Thus, we have

$$\begin{aligned} P(\mathbf{R}^u | \mathbf{T}^u) &= \prod_{j=1}^H \prod_{k=1}^H P(b_{j,k}^u | q_{j,k}^u) \\ &= \prod_{j=1}^H \prod_{k=1}^H [P(b_{j,k}^u | q_{j,k}^u, PU_j) P(PU_j) \\ &\quad + P(b_{j,k}^u | q_{j,k}^u, \bar{P}U_j) P(\bar{P}U_j)], \end{aligned} \quad (2.21)$$

where  $q_{j,k}^u$  and  $b_{j,k}^u$  are the  $(j, k)$  binary elements given by (2.4) and (2.9) respectively in the  $u$ -th stage of the trellis and  $PU_j$  and  $\bar{P}U_j$  denote the presence and absence of PU activity over channel  $f_j$  respectively. Note that the last step in (2.21) is justifiable since the conditional distribution of the received code matrix  $\mathbf{R}^u$  solely depends on the noise distribution and interference caused by multiple PUs given the transmitted code matrix  $\mathbf{T}^u$ . Here we note that  $P(PU_j)$  and  $P(\bar{P}U_j)$  depend on channel  $f_j$ 's occupancy model which will be discussed in Section 2.5.1.

At each stage of the trellis, the absence and presence of PU need to be taken into consideration when computing the likelihoods in (2.21) that also depend on the code matrix to be transmitted. Next, we compute the likelihoods given in (2.21). We recall that an SU uses an ON-OFF modula-



tion scheme to transmit its information over each licensed frequency according to (2.5).

### 2.4.1 Computation of likelihoods in the absence of PU

Suppose there is no PU transmission over frequency band  $j$  at time step  $k$ . If the SU is transmitting a bit '1', then the demodulator in-phase component  $r_{I_{j,k}} \sim \mathcal{N}(\sqrt{\frac{E_s^r}{H}} \cos \theta, \frac{N_0}{2})$  and the demodulator quadrature component  $r_{Q_{j,k}} \sim \mathcal{N}(\sqrt{\frac{E_s^r}{H}} \sin \theta, \frac{N_0}{2})$ . The fact that  $r_{I_{j,k}}$  and  $r_{Q_{j,k}}$  are statistically independent random variables with non-zero means, then implies  $l_{j,k} \sim \text{Rice}(\sqrt{\frac{E_s^r}{H}}, \sqrt{\frac{N_0}{2}})$ . Accordingly,  $P(b_{j,k} = 0 | q_{j,k} = 1, \bar{P}U_j)$  can be computed as

$$\begin{aligned}
P(b_{j,k} = 0 | q_{j,k} = 1, \bar{P}U_j) &= P(l_{j,k} < l_{th} | q_{j,k} = 1, \bar{P}U_j) \\
&= F_{L_{j,k}}(l_{th}) \\
&= 1 - Q_1\left(\sqrt{2\frac{E_s^r/H}{N_0}}, 0.6\sqrt{2\frac{E_s^r}{N_0}}\right), \tag{2.22}
\end{aligned}$$

where  $F_{L_{j,k}}(l_{th})$  is the cumulative distribution function (CDF) of  $l_{j,k}$  evaluated at  $l_{th}$ ,  $Q_1(v, v')$  is the Marcum's Q-function defined as [83],

$$Q_1(v, v') = \int_{v'}^{\infty} x \exp\left\{-\frac{x^2 + v^2}{2}\right\} I_0(vx) dx \tag{2.23}$$

and  $I_0(vx)$  is the zeroth order modified Bessel function.  $P(b_{j,k} = 1 | q_{j,k} = 1, \bar{P}U_j)$ , in this case, is nothing but the complement of (2.22) and is given by

$$\begin{aligned}
P(b_{j,k} = 1 | q_{j,k} = 1, \bar{P}U_j) &= P(l_{j,k} \geq l_{th} | q_{j,k} = 1, \bar{P}U_j) \\
&= 1 - F_{L_{j,k}}(l_{th}) \\
&= Q_1\left(\sqrt{2\frac{E_s^r/H}{N_0}}, 0.6\sqrt{2\frac{E_s^r}{N_0}}\right). \tag{2.24}
\end{aligned}$$

If the SU is transmitting a bit ‘0’ on subchannel  $j$  at time step  $k$ , then,  $r_{I_{j,k}} \sim \mathcal{N}(0, \frac{N_0}{2})$  and  $r_{Q_{j,k}} \sim \mathcal{N}(0, \frac{N_0}{2})$ , and we have  $l_{j,k} \sim \text{Rayleigh}(\sqrt{\frac{N_0}{2}})$ . Then,  $P(b_{j,k} = 1|q_{j,k} = 0, \bar{P}U_j)$  and  $P(b_{j,k} = 0|q_{j,k} = 0, \bar{P}U_j)$  can be computed as,

$$\begin{aligned}
& P(b_{j,k} = 1|q_{j,k} = 0, \bar{P}U_j) \\
&= P(l_{j,k} \geq l_{th}|q_{j,k} = 0, \bar{P}U_j) \\
&= 1 - F_{L_{j,k}}(l_{th}) \\
&= \exp\left(-0.36 \frac{E_s^r}{N_0}\right)
\end{aligned} \tag{2.25}$$

and

$$\begin{aligned}
& P(b_{j,k} = 0|q_{j,k} = 0, \bar{P}U_j) \\
&= P(l_{j,k} < l_{th}|q_{j,k} = 0, \bar{P}U_j) \\
&= F_{L_{j,k}}(l_{th}) \\
&= 1 - \exp\left(-0.36 \frac{E_s^r}{N_0}\right).
\end{aligned} \tag{2.26}$$

## 2.4.2 Computation of likelihoods in the presence of PU

In the presence of PU activity in its licensed frequency  $f_j$  at time step  $k$  during SU’s transmission of bit ‘1’, the signal received at the input of the demodulator has two significant terms besides noise. One corresponds to the actual signal energy of the transmitted symbol and the other is created by the PU activity. It is assumed that the SU transmitting power is sufficiently small so that QoS of the PU session is maintained. Therefore, the SU signal is negligible as compared to that of the PU. In this case,  $r_{I_{j,k}} \sim \mathcal{N}(\sqrt{\frac{E_{I_j}^{PU}}{H}} \cos \phi, \frac{N_0}{2})$  and  $r_{Q_{j,k}} \sim \mathcal{N}(\sqrt{\frac{E_{I_j}^{PU}}{H}} \sin \phi, \frac{N_0}{2})$ . Thus,  $l_{j,k} \sim \text{Rice}(\sqrt{\frac{E_{I_j}^{PU}}{H}}, \sqrt{\frac{N_0}{2}})$ .  $P(b_{j,k} = 0|q_{j,k} = 1, PU_j)$  and  $P(b_{j,k} = 1|q_{j,k} = 1, PU_j)$ , in this

scenario, are calculated according to,

$$\begin{aligned}
& P(b_{j,k} = 0 | q_{j,k} = 1, PU_j) \\
&= P(l_{j,k} < l_{th} | q_{j,k} = 1, PU_j) \\
&= F_{L_{j,k}}(l_{th}) \\
&= 1 - Q_1 \left( \sqrt{2 \frac{E_{I_j}^{PU}}{N_0}}, 0.6 \sqrt{2 \frac{E_s^r}{N_0}} \right)
\end{aligned} \tag{2.27}$$

and

$$\begin{aligned}
& P(b_{j,k} = 1 | q_{j,k} = 1, PU_j) \\
&= P(l_{j,k} \geq l_{th} | q_{j,k} = 1, PU_j) \\
&= 1 - F_{L_{j,k}}(l_{th}) \\
&= Q_1 \left( \sqrt{2 \frac{E_{I_j}^{PU}}{N_0}}, 0.6 \sqrt{2 \frac{E_s^r}{N_0}} \right).
\end{aligned} \tag{2.28}$$

If the SU transmits a ‘0’ on subchannel  $j$  at time step  $k$ , the output of the demodulator has the noisy signal received from the PU. In that case, and similar to the analysis approach followed earlier,  $r_{I_{j,k}} \sim \mathcal{N}(\sqrt{\frac{E_{I_j}^{PU}}{H}} \cos \phi, \frac{N_0}{2})$  and  $r_{Q_{j,k}} \sim \mathcal{N}(\sqrt{\frac{E_{I_j}^{PU}}{H}} \sin \phi, \frac{N_0}{2})$ . Consequently,  $l_{j,k} \sim Rice(\sqrt{\frac{E_{I_j}^{PU}}{H}}, \sqrt{\frac{N_0}{2}})$ . So, the following probabilities  $P(b_{j,k} = 0 | q_{j,k} = 0, PU_j)$  and  $P(b_{j,k} = 1 | q_{j,k} = 0, PU_j)$  are the same as  $P(b_{j,k} = 0 | q_{j,k} = 1, PU_j)$  and  $P(b_{j,k} = 1 | q_{j,k} = 1, PU_j)$ , respectively.

Once the probabilities presented above are evaluated, we can calculate (2.21) for each stage of the  $\mathcal{V}$  stages in the trellis and, eventually, approximate the BER of the proposed scheme as given in (2.19).

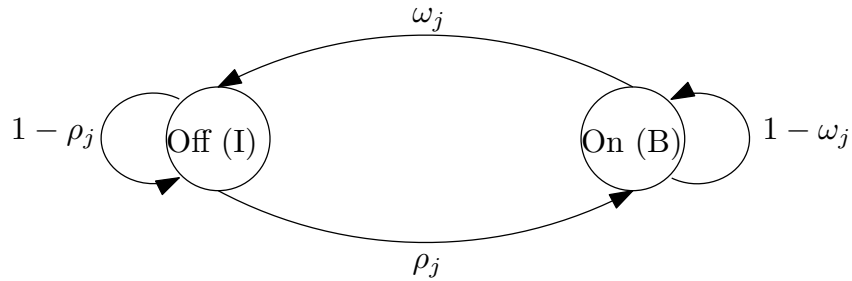


Fig. 2.5: Two-state Markov chain model for a given PU  $j$  activity over its licensed frequency.

## 2.5 Throughput Analysis

So far, we have computed the BER approximately and evaluated the performance of the  $H$ -FSK system in the presence of interference caused by multiple PUs. To further explore the performance of the proposed  $H$ -FSK communication system and validate its effectiveness, we perform a throughput analysis based on the approximate BER provided in Section 2.4. Accordingly, an SU, adopting the proposed  $H$ -FSK communication scheme, is expected to provide a level of reliable information reception which is better than what the SU could achieve otherwise under heavy PU interference.

### 2.5.1 Licensed Channel Dynamic Occupancy Model

To characterize the dynamic behavior of a PU, we model each PU's spectrum usage as a two-state Markov chain, which is depicted in Fig. 2.5. Note that our model is different from [28] where we assumed the licensed channel to be *always* occupied by the PU. In this model, the channel has two alternative states denoted by On (Busy) and Off (Idle). This assumption is practical in the sense that the licensed spectrum occupancy will experience alternating On-Off periods rather than the assumption of the channel being *always* occupied (a given PU being *always* present once it starts transmission during an SU transmission). The periods during which the licensed spectrum's state is idle or busy, also known as holding times, are geometrically distributed with known independent parameters  $r_j$  and  $p_j$  as shown in Fig. 2.5. An On state represents the state in which the licensed band  $f_j$  is occupied by a PU resulting in degraded BER performance for SU transmissions, while an

Off (idle) state represents the state in which the primary band is idle. The steady state probabilities of any primary channel,  $f_j$ , state being *Off* or *On* are given respectively as

$$P_{ch_j}^{Off} = \frac{\omega_j}{\omega_j + \rho_j} \quad (2.29)$$

and

$$P_{ch_j}^{On} = \frac{\rho_j}{\omega_j + \rho_j}. \quad (2.30)$$

It is important, at this point, to mention that  $P(\bar{P}U_j) = P_{ch_j}^{Off}$  and  $P(PU_j) = P_{ch_j}^{On}$ .

## 2.5.2 Throughput Analysis

In order to examine the effectiveness of the proposed *H*-FSK approach, we conduct a throughput analysis by computing the average throughput of the SU communication session in the presence of multiple PUs whose activities are modeled as a 2-state Markov chain. It is assumed that the SU transmitter has no information regarding the presence or absence of PUs in the network. The expected throughput, in this case, is defined as

$$Th_e = \left(1 - PER\right) \times R_p \times L, \quad (2.31)$$

where  $PER = 1 - (1 - P_e)^L$  is the packet error rate (PER) at the SU receiver and  $R_p$  is the rate at which information packets are sent. As stated earlier, since the closed-form expression of  $P_e$  is computationally prohibitive, we approximate the expected throughput of the *H*-FSK communication scheme as follows, using an approximate value of  $P_e$  given in (2.19):

$$Th_e \approx \left(1 - \hat{P}_e\right)^L \times R_p \times L. \quad (2.32)$$

Empirically, we define expected throughput as the average number of correctly received packets per unit time. For simplicity, we do not consider header and overhead bits when computing the

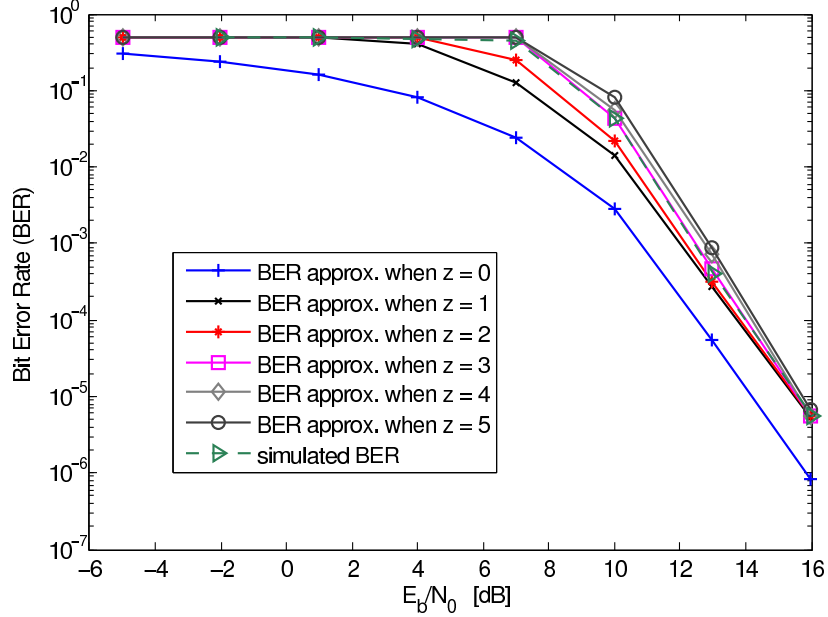


Fig. 2.6: BER approximations for PTC with  $H = 3$ .

link throughput.

## 2.6 Numerical Results and Discussion

### 2.6.1 Approximate BER with Single Permanent PU Interference

For the coded  $H$ -FSK communication system shown in Fig. 2.2, the following values of the physical parameters are assumed. The transmit power of the SU is varied between  $[25 \mu W, 4 mW]$  and the noise power density is selected as  $N_0 = 2.5 \times 10^{-14}$ . These values are chosen in such a way so as to not create destructive interference to PUs' transmissions. We select the lowest frequency band in the available frequency spectrum,  $f_1$ , to be 56 MHz, and the bandwidth spacing between any two subchannels is selected as 6 MHz. Furthermore,  $c_j = \left(\frac{\lambda_j}{4\pi}\right)^2$  where  $\lambda_j$  is the signal wavelength defined as the ratio of the speed of light to the center frequency of the band in operation  $\frac{c}{f_j}$ . Among PUs existing in the network, only the PU operating at the licensed frequency  $f_2$  is assumed active and has a total transmitting power of 1 MW. The distances between the PU transmitter and SU receiver and that between the SU transmitter-receiver pair are selected as 10 m,

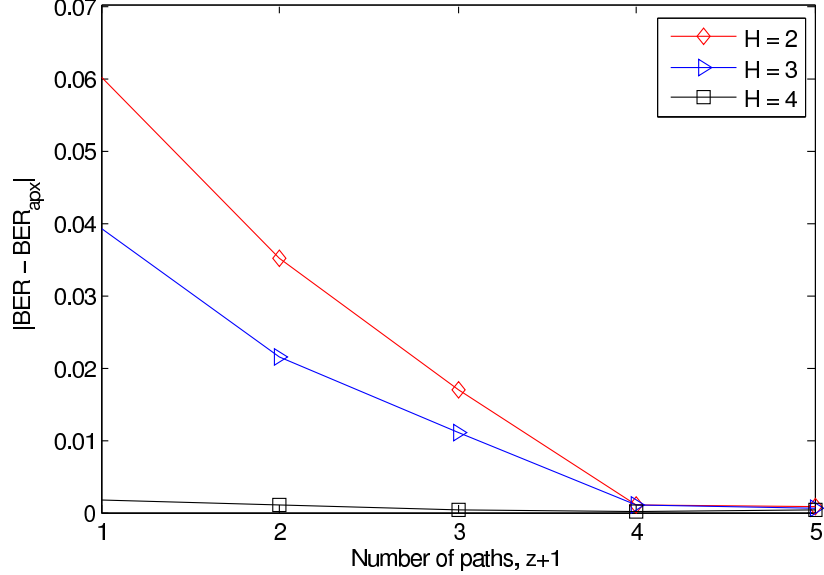


Fig. 2.7:  $|BER - BER_{apx}|$  for different PTC ( $H = 2, 3,$  and  $4$ ) and  $SNR = 7$  dB.

in order to analyze the quality of the SU link under a high interference scenario. The remaining parameter values used in the simulation are chosen in accordance with the IEEE 802.22 standard [86].

In Fig. 2.6, we fix  $H = 3$  and compare the simulated BER with its approximations using different number of paths used in the approximation, i.e.,  $z + 1$ . It is clear from the figure that  $z = 3$  approximates BER well for  $H = 3$ . At the same time, we observe that the BER curve surpasses the simulated BER for  $z \geq 4$ . In other words,  $\hat{P}_e$  serves as an upper-bound in this case.

In Fig. 2.7, we fix  $SNR = 7$  dB and compare the absolute error of the BER approximation for different values of  $H$ . It is again clear that  $z = 3$ , i.e., using only  $z + 1 = 4$  paths of the convolutional code's trellis, provides good BER approximation for different sizes of PTC. This is due to the fact that the first few error events with a few errors in the trellis dominate all the remaining transitions. This result confirms what we have mentioned earlier regarding the domination of a small number of paths in the trellis over all the remaining paths that may evolve due to incoming bits. The approximate BER we provide in the section could be used as a QoS metric in an adaptive scenario where certain parameters of the system such as  $H$  could be adapted in an online manner using this approximation. In Table 2.3, we present results on the performance based on exhaus-

tive search<sup>7</sup> compared to the proposed approximation approach in this chapter in terms of the time needed to compute BER for different PTC. As shown in Table 2.3, it takes much shorter time to

Table 2.3: A comparison of the time needed to compute BER between exhaustive search [28] and approximation approach for different PTC ( $H = 2, 3,$  and  $4$ )

PTC	Exhaustive Search Approach	Approximate Approach
$H = 2$	0.33s	0.31s
$H = 3$	42.21s	7.24s
$H = 4$	26274.99s	245.32s

compute the BER approximately as compared to its exact calculation.

## 2.6.2 Throughput Analysis of $H$ -FSK

For comparison purposes, we first consider a competing scenario where an SU does not employ any coding technique in its spectrum interweaved transmission strategy. It is assumed to be based on  $M$ -FSK modulated signals. In this scenario, an SU makes use of the CR channel sensing feature in order to determine if there is an active PU in the network or not. Depending on the channel sensing measurements of the licensed spectrum, a decision is made on whether or not the SU should vacate the band. When the SU detects a white space, it adapts the transmission parameters to utilize the full spectrum available and achieve the maximum throughput. On the other hand, when a PU is detected an SU vacates the band and adjusts its transmission parameters accordingly by employing a modified FSK modulation scheme supporting the transmission of  $M'$  symbols where  $M' < M$ . In order to gain more insight regarding the throughput performance comparison of the PTC-based multi-level FSK with the uncoded-opportunistic (adaptive)  $M$ -FSK system, we assume that packet transmissions take place over an observation window of length  $T$  seconds divided into  $x$  time slots. In each time slot,  $P_{ch}^{On}$  can be obtained using the channel's steady

<sup>7</sup>Using this technique, decisions on the transmitted code matrices are made by the permutation trellis decoder which decides in favor of the transmitted code matrix, i.e., among  $2^m$  possible code matrices, which has the minimum Hamming distance with respect to the received one. In order to determine all the decisions for every possible code matrix, a brute force method is used to compare each possible received code matrix to every code matrix. This method needs roughly  $2^{H^2+m}$  comparisons [28].



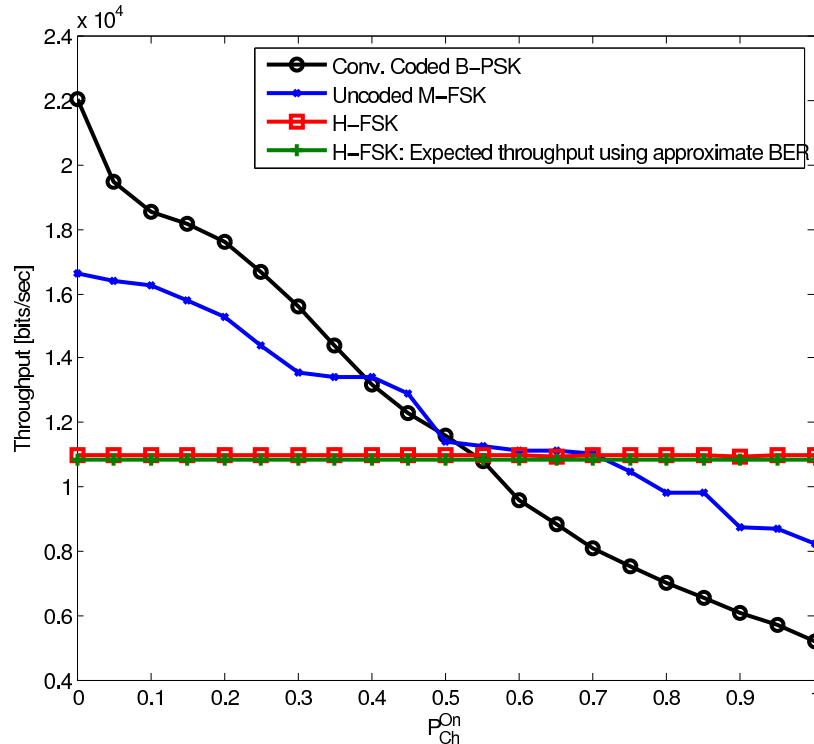


Fig. 2.8: Throughput Comparison of  $H$ -FSK and uncoded opportunistic  $M$ -FSK as well as convolutionally coded BPSK schemes for SNR = 7 dB, packet size = 256 bits, and  $R_p = 100$  packets/sec.

state probabilities. Then, the probability of packet error is evaluated by averaging the results over a 100000 Monte-Carlo runs.<sup>8</sup> As a result, the SU's throughput is computed and analyzed. We further assume that the available spectrum consists of four frequency bands. With the use of the PTC-based multi-level FSK approach, an SU does not need to sense the channel or adapt its wireless links. In the uncoded opportunistic system, an SU senses the licensed frequency band at the beginning of a time slot. Assuming zero-cost perfect detection of a licensed user's activity, an SU decides on which  $M$ -FSK modulated signals are to be transmitted. In the case where an SU detects a spectrum hole, it utilizes the full available spectrum (4 bands) using a 4-FSK modulation scheme. When a PU is detected, an SU vacates the licensed band and utilizes the remaining spectrum (2 frequency bands out of the 4 bands assumed to comprise the spectrum) using BFSK modulated signals. Different from [103], the licensed channel can change its state at any instant in a time slot. In Fig. 2.8, we present the average throughput of  $H$ -FSK and that of an uncoded opportunistic

<sup>8</sup>In each Monte-Carlo run, the channel's steady state probabilities vary.

$M$ -FSK system as a function of  $P_{ch}^{On}$  for  $H = M = 4$  where the packet size  $L = 256$  bits,  $R_p = 100$  packets/sec, and SNR is 7 dB. Fig. 2.8 illustrates that the average throughput in  $H$ -FSK is constant regardless of  $P_{ch}^{On}$  values while the average throughput of the uncoded opportunistic  $M$ -FSK decreases as  $P_{ch}^{On}$  increases and it matches the theoretical approximation given in (2.32). The throughput of  $H$ -FSK is constant because we assume that there is only one frequency over which the PU interferes with the SU with a probability,  $P_{ch}^{On}$ . Since PTC is a permutation of the identity matrix, the interfered row in the received coded matrix can be deterministically found from the other rows. Therefore, we observe a flat throughput response for the proposed PTC-based communication scheme. As shown, there exists a probability  $p_1^* \approx 0.7$  such that for  $P_{ch}^{On} \geq p_1^*$  the  $H$ -FSK approach outperforms the uncoded opportunistic scheme in terms of throughput performance. Thus, the use of the proposed  $H$ -FSK communication scheme for values of  $P_{ch}^{On}$  less than  $p_1^*$  is not beneficial because higher throughput values are obtained using the uncoded opportunistic scheme. In other words, the  $H$ -FSK system is effective for situations where the PU activity is relatively high. In practice, the throughput evaluated for the uncoded  $M$ -FSK system is expected to be lower than what is shown in Fig. 2.8 due to channel sensing intervals. It should be noted that the proposed  $H$ -FSK communication scheme does not need the channel sensing mechanism that might not be available for some applications.

We also compare the average throughput of the proposed  $H$ -FSK scheme to a rate- $\frac{1}{2}$  convolutionally coded BPSK modulated OFDM system. We assume that the latter transmits a BPSK modulated signal in parallel over the available frequency bands in a given time window as discussed above. For a fair comparison, neither scheme carries out sensing, i.e., they transmit at all times. It is worth noting that the throughput performance of this BPSK OFDM system is investigated assuming the same transmission bandwidth, power, and time frame as that of the  $H$ -FSK system. As shown in Fig. 2.8, the average throughput of the convolutionally coded BPSK system also decreases as  $P_{ch}^{On}$  increases. Similar to the previous throughput comparison, there exists a probability  $p_2^* \approx 0.55$  such that for  $P_{ch}^{On} \geq p_2^*$  the  $H$ -FSK system outperforms the convolutionally coded BPSK scheme in terms of SU's average throughput. Therefore, the use of the proposed

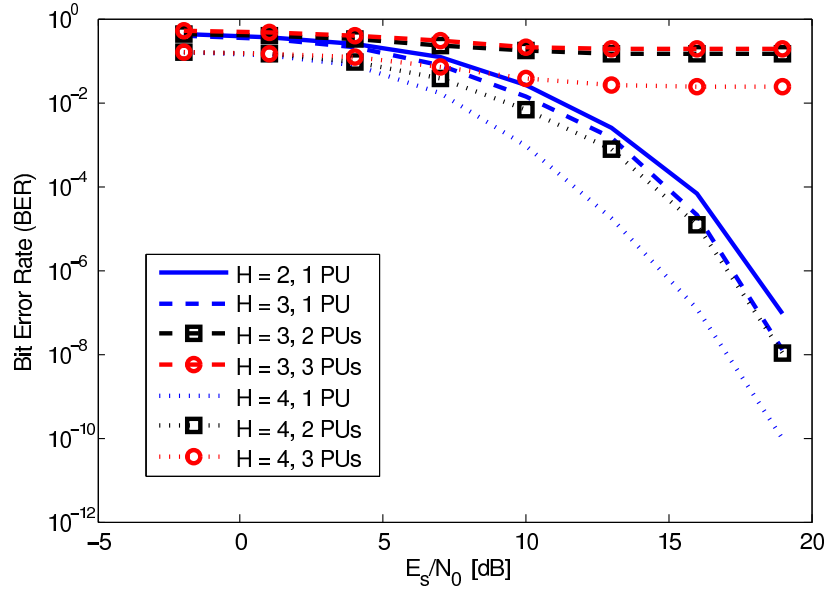


Fig. 2.9: Approximate BER performance of different PTCs with respect to PUs that are *always* ON and transmitting.

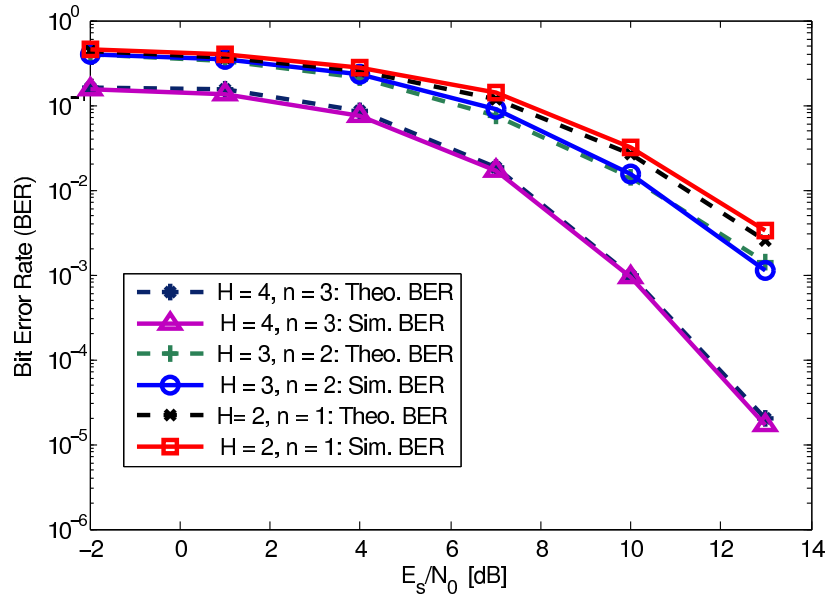


Fig. 2.10: Approximate BER versus Simulated BER for a PTC with  $H = 2, 3,$  and  $4, n = 1, 2,$  and  $3,$  and  $P_{ch}^{ON} = 0.35.$

$H$ -FSK communication scheme for values of  $P_{ch}^{ON}$  less than  $p_2^*$  is not beneficial because higher throughput values would be obtained using the other coded scheme.

### 2.6.3 SU Link's Resiliency in the Presence of Multiple PUs

In this section, we further carry out our performance analysis and examine the resiliency of the network (SU's link) to interference provided by the proposed PTC based framework in the presence of multiple PUs when i) PUs *always* transmit and ii) PUs are *dynamic* and their activities vary dynamically. It is worth noting here that the PUs are located 10 m away from the SU receiver in order to analyze the quality of the SU link under a high interference scenario.

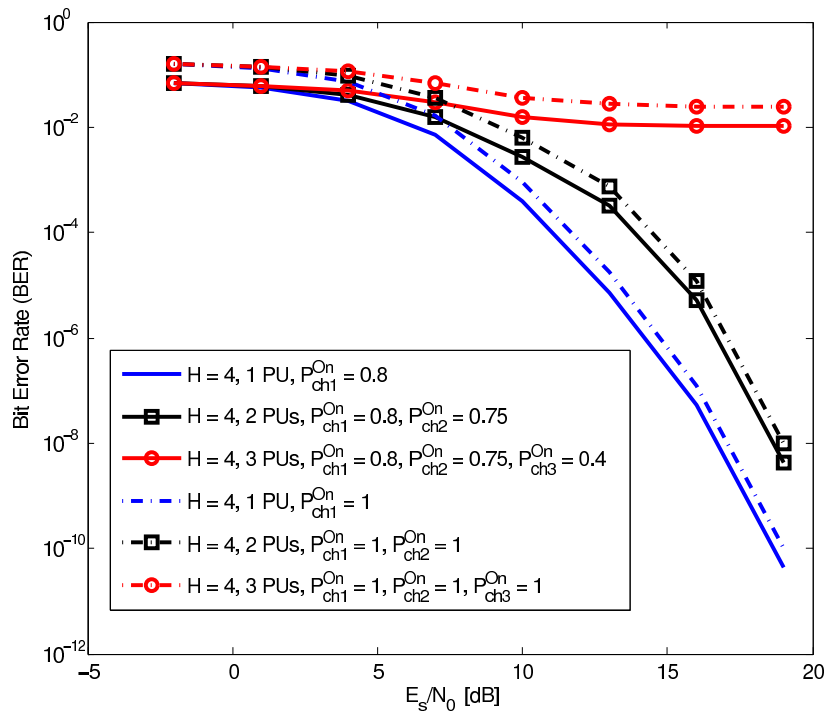


Fig. 2.11: Approximate BER performance of a PTC ( $H = 4$ ) with respect to dynamically varying PUs activities and PUs that are *always* ON.

First, we consider multiple PUs that are *always* active in the network during SU communication. In Fig. 2.9, we plot the approximate BER performance of the SU link for different PTCs in the presence of multiple PUs. The results obtained in the presence of multiple PUs that are *always* ON are similar to those presented in [34, 88]. These results show that the use of larger PTC (higher value of  $H$ ) adds more robustness to SU communications, i.e., BER decreases as the value of  $H$  increases. It is also shown that the approximate BER performance of an SU link degrades as the number of PUs in the network increases. Of course, this is achieved at the expense of larger

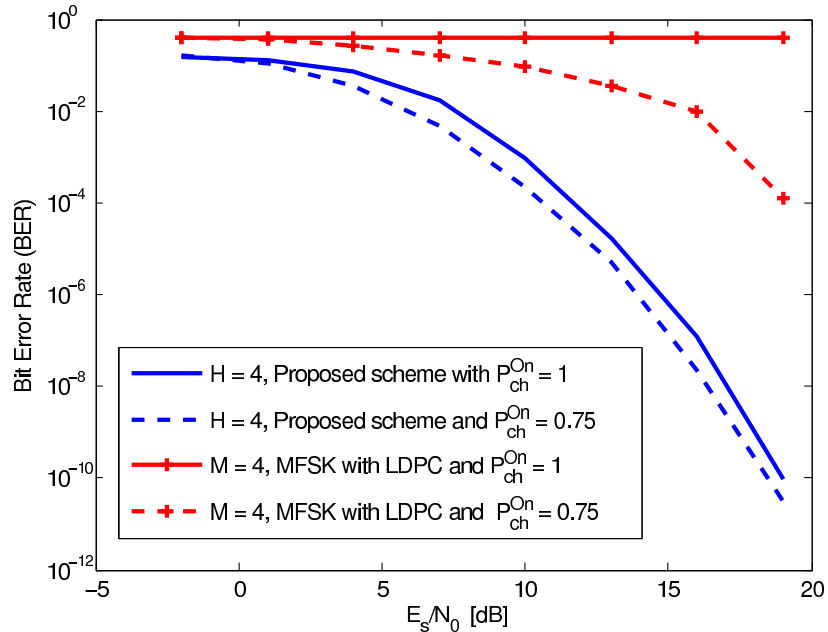


Fig. 2.12: A BER comparison between the proposed PTC scheme with  $H = 4$  and a  $1/2$  rate (64800,32400) LDPC encoding with a 4-FSK modulation system with respect to static ( $P_{ch}^{On} = 1$ ) and dynamic ( $P_{ch}^{On} = 0.75$ ) activities of a PU.

overhead when larger values of  $H$  are used.

The case of *static* PUs that *always* transmit is more of a pessimistic scenario as presented above. In this chapter, as discussed earlier, we have extended the work in [34, 88] and have considered a more practical scenario to model the intermittent *dynamic* activities of PUs in the network. Using a 2-state Markov chain to model channels' occupancy by PUs, we have provided a more realistic characterization of system performance and verify the approximate BER in the presence of a dynamically transmitting PU with simulated BER for a given PTC and known parameters of the channel occupancy model. In Fig. 2.10, we present the approximate BER performance of the proposed framework as a function of  $\frac{E_s}{N_0}$  for different PTC schemes, i.e.,  $H = 2, 3$ , and 4, and  $P_{ch}^{ON} = 0.35$ . Both analytical and simulation results are presented which match each other quite well.

In addition, in Fig. 2.11, we further examine the approximate BER performance of SU communications for a given PTC, i.e.,  $H = 4$ , in the presence of one, two, and three PUs that i) are *static* in nature and *always* transmit and ii) *dynamic* in nature. The results obtained in Fig. 2.11

clearly show that there exists a gap between the performance of the systems in both cases. Our analysis based on a more practical occupancy model is able to predict SU communication performance more accurately and which is better than the pessimistic case of PUs being *always* ON. For example, the approximate BER value in the presence of one *dynamic* PU is lower than when a PU is *always* transmitting. This is intuitive because only a fraction of the transmitted information packets are affected by interference from the *dynamic* PU when it is transmitting compared to the *static* PU case when all the transmitted information packets experience continuous interference. In fact, this is also observed for the case of 2 and 3 PUs being active in the network.

Next, for the same energy per information bit, transmission bandwidth, and transmission time, let us compare the performance of our proposed PTC-based communication system with another system based on LDPC codes using a simple example where  $|\mathcal{F}| = 4$  frequency bands. In the case of LDPC-based communication system, we construct a coded message using a 1/2 rate (64800,32400) LDPC code as given in Matlab toolbox. This coded message of length 64800 is grouped into matrices of size  $4 \times 4$  and transmitted using the same modulation scheme as in the proposed communication system. Fig. 2.12 illustrates how the proposed PTC-based communication system outperforms the LDPC-based system for both static and dynamic activities of a PU in terms of error probability for different SNR values.

## 2.7 Summary

In this chapter, we employed a PTC based framework to mitigate the impact of PUs modeled using a practical *dynamic* channel occupancy model in CRNs. We computed the SU link's BER approximately which was shown to be quite accurate. This approximation allows one to use BER as a QoS metric to determine the link quality of an SU link for applications such as link adaptation. Furthermore, in order to assess the effectiveness of the proposed PTC based multi-level FSK communication scheme, we compared the performance to that of an uncoded opportunistic  $M$ -FSK system, a coded  $M$ -FSK system, a coded BPSK modulated system deploying parallel transmissions, and

a  $\frac{1}{2}$ -rate LDPC encoding with an  $M$ -FSK modulation system. Based on these comparisons, we showed that the proposed scheme outperforms the latter two under relatively heavy PU interference. We also presented results that exhibit the resiliency of an SU link to interference for PTCs in the presence of multiple *dynamic* PUs activities.

In order to mitigate the interference created by multiple intermittent PUs in a CRN, a novel spectrum underlay design, based on PTCs in conjunction with multi-level FSK signaling, was presented in this chapter. In the future, we propose to consider a novel spectrum allocation mechanism to mitigate interference created by multiple SUs in a CRN.

# CHAPTER 3

## MITIGATION OF SU INTERFERENCE VIA A MATCHING-BASED FREQUENCY ALLOCATION

The proliferation of new wireless technologies has led to an increasing demand for the scarce radio spectrum resources, thus motivating operators and governmental agencies to rethink the way in which existing fixed spectrum allocation policies are defined [1].

In order to reap the benefits of CRNs, it is imperative to design smart and agile spectrum allocation mechanisms that can achieve better management and utilization of spectral resources. In this chapter, we design a novel and distributed spectrum allocation approach in a CRN when SUs have non-identical spectrum availability measures. We consider a CRN in which each SU perceives the availability of the spectrum differently. We formulate a matching game [37] in which the SUs and PUs are the players that need to rank one another in order to find suitable associations. The key advantage of the proposed approach lies in the fact that the SU-PU associations are achieved through distributed decisions at each SU and PU. To solve the proposed matching game, we introduce a novel distributed algorithm according to which the SUs and PUs self-organize into a stable and optimal matching.



### 3.1 Literature Review

For spectrum allocation in a CRN, two fundamental architectures have recently been studied [5, 45, 72]. One is centralized where a central entity, such as a central controller or spectrum broker, is in charge of allocating the spectrum or part of it to different SUs [14]. Based on this scheme, SUs forward their spectrum sensing measurements to a central entity which constructs a spectrum allocation map. Naturally, a centralized approach can lead to high communication overhead and is not scalable. Alternatively, a distributed architecture can be adopted, for example, when the construction of a centralized infrastructure is not possible and/or for quick adaptation to network dynamics. Therefore, we focus our attention on distributed architectures in this chapter.

Distributed spectrum allocation, in the context of wireless networks, has received considerable attention recently [16, 53, 61, 82]. The authors in [82] developed a distributed algorithm for multi-user channel allocation in CRNs that is based on the learning of the behavior of PUs through a multi-agent learning concept. However, in [82], for the network nodes to learn and take decisions, they must have precise and timely information such as channel information or interference patterns that might be hard to gather in a distributed setting. In [16], the authors introduced an adaptive and distributed local bargaining approach where mobile users self-organize into bargaining groups and adapt their previous spectrum assignment to approximate a new optimal assignment. Nevertheless, their approach is highly centralized. The work in [53] studies the problem of channel allocation in wireless networks using a matching theory-based mechanism that is solved via a variant of the so-called Gale-Shapley deferred acceptance algorithm [37]. They analyze the performance of the proposed solution from the user's perspective and provide tight lower and upper bounds on both the stable allocation and the optimal centralized allocation performance. In [61], the authors use matching theory to find a stable multi-channel allocation for each SU assuming the existence of a central coordinator responding on behalf of the PUs. They investigate cooperative channel assignments that require direct communication between SUs and prove the existence of an equilibrium solution. However, in [61], the scheme is not fully distributed and it incurs additional communication overhead.

## 3.2 Motivation, Novelty, and Contributions

Compared to existing works such as [16] and [61], the proposed approach is fully distributed as it requires no cluster-head to determine the assignment, no central entity to perform bargaining, no coordinator to control the matching on behalf of the PUs, and no information exchange among SUs. In contrast to [82], the proposed algorithm neither requires the learning of users in the network nor timely and precise information about them. In contrast to [53] and [61], we consider that SUs have different information regarding the activity of PUs over their licensed bands. Compared to [53], our proposed scheme enables the frequency band licensees in the network to be active players in the association process and, thus, make better informed spectrum association decisions that maximize their own payoffs. In addition, the performance analysis we provide is not based on bounds. As opposed to [61] in which the authors assume the existence of a central coordinator that responds to offers from all the SUs on behalf of the PUs, we propose a one-to-one stable matching for which we propose a completely distributed resource allocation algorithm.

To summarize, the main contributions of this work are as follows:

- We design a novel spectrum allocation approach in a CRN in which each SU perceives the availability of the spectrum differently.
- We devise the use of a measure of inference performance and rate to evaluate SUs' proposals which are used by PUs to rank SUs.
- We propose a novel distributed algorithm that enables SUs and PUs to self-organize into a stable and optimal matching.

## 3.3 System Model

Consider a single-hop CRN consisting of a set  $\mathcal{O} = \{1, \dots, O\}$  of  $O$  SU transmitter-receiver pairs and a set  $\mathcal{H} = \{1, \dots, H\}$  of  $H$  PU transmitter-receiver pairs, with  $O > H^1$ . For brevity, we use

---

<sup>1</sup>We consider this scenario for illustration purposes only. However, our work can be easily extended to  $O \leq H$ .

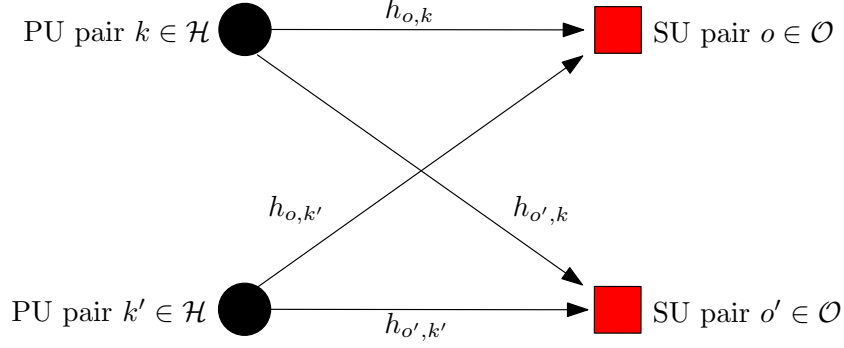


Fig. 3.1: An illustration of the system model. An arrow portrays the sensing mechanism of PUs activities performed at the transmitter's side of each SU pair.

the term SUs and PUs to denote, respectively, the SU and PU transmitter-receiver pairs. PUs are licensed users whose transmission behavior varies slowly over time. Each PU operates over 1 out of  $H$  orthogonal licensed frequency bands over which transmissions are assumed to be collision-free. At any point in time, a given PU may be active or inactive. However, from the perspective of any SU  $o \in \mathcal{O}$ , every PU  $k \in \mathcal{H}$  is considered to be active with a probability  $\pi_{o,k}$ . For a given PU  $k \in \mathcal{H}$ , two distinct SUs  $o, o' \in \mathcal{O}$ ,  $o \neq o'$  may have a different value of the probability that  $k$  is active, i.e., we may have  $\pi_{o,k} \neq \pi_{o',k}$ , depending on various factors such as the distance to the PU and the wireless channel state. Let  $\boldsymbol{\pi}_o = [\pi_{o,1} \cdots \pi_{o,H}]$  for any  $o \in \mathcal{O}$ . Furthermore, the wireless channel over which signals are transmitted is assumed to be frequency selective. We take into account a broad class of channel models which consist of a known distance-independent frequency selective component, and a deterministic distance-dependent path loss component with path loss exponent  $\gamma$  [92]. More specifically, let

$$h_{o,k} = \sqrt{\frac{\beta_k}{1 + Kd_{o,k}^\gamma}} \quad (3.1)$$

be the channel gain over a distance  $d_{o,k}$ , between the transmitters of SU  $o$  and PU  $k$ , with a deterministic frequency selective coefficient  $\beta_k$  and a constant  $K$ . Note that, for any two PU-owned frequency bands  $k$  and  $k'$ ,  $\beta_k \neq \beta_{k'}$ . Note that this path loss model is consistent with the one employed in [64] and it is valid even if  $d_{o,k}$  is close to or equal to 0.

Furthermore, we let  $\boldsymbol{\eta}_o = [\eta_{o,1} \cdots \eta_{o,H}]$  for any  $o \in \mathcal{O}$  denote the rates over the bands in  $\mathcal{H}$

where  $\eta_{o,k}$ , for  $k \in \mathcal{H}$ , is given by [40]:

$$\eta_{o,k} = \log_2 \left( 1 + \frac{P_{T_o} g_{o,k}^2}{\sigma^2} \right), \quad \forall o, k, \quad (3.2)$$

where  $P_{T_o}$  denotes SU  $o$ 's transmit power,  $g_{o,k} = \sqrt{\frac{\beta'_k}{1+Kd_{o,o}^\alpha}}$  is the channel gain of PU-owned band  $k$  over a distance  $d_{o,o}$  between SU transmitter-receiver pair  $o$  with a known frequency selective coefficient  $\beta'_k$ , and  $\sigma^2$  is the additive white Gaussian noise variance, assumed the same for all SUs over all bands.

In the model studied here, SUs can only communicate with PUs. In other words, there does not exist any negotiation or information exchange among SUs. We further assume that an SU is capable of transmitting over a single PU-owned frequency band at a time, but can sense the activities of all PUs in  $\mathcal{H}$ . In this chapter, the system is assumed to be slotted where each SU  $o \in \mathcal{O}$  makes a single observation every time slot and decides on the presence or absence of a PU  $k \in \mathcal{H}$  on its licensed channel based on this observation.

Local sensing for PU signal detection, done once every time slot, can be formulated as a binary hypothesis testing problem as follows [3]:

$$\begin{aligned} \text{under } H_0 : x_{o,k} &= w, \\ \text{under } H_1 : x_{o,k} &= h_{o,k}s_k + w, \end{aligned}$$

where, at SU  $o \in \mathcal{O}$  over PU-owned frequency band  $k \in \mathcal{H}$ ,  $x_{o,k}$  denotes the received signal,  $h_{o,k}$  is the  $k$ -th channel gain,  $s_k$  denotes the known signal of PU  $k$ , and  $w$  is the zero-mean additive white Gaussian noise.  $H_0$  and  $H_1$  denote the absence and the presence, respectively, of the PU signal in the frequency band.

In our model, we consider the above signal detection problem. We compute the logarithm of the *a posteriori* probability ratio that captures the inference performance. In other words, the sign of the logarithm of the *a posteriori* probability ratio yields the decision on  $H_1$  or  $H_0$  while its mag-

nitude determines the confidence regarding a decision on either one of the two hypotheses. More formally, we present this maximum *a posteriori* probability decision rule of the aforementioned binary hypothesis testing problem as follows:

$$\begin{aligned}\delta_{o,k} &= \log \left( \frac{P(H_1|x_{o,k})}{P(H_0|x_{o,k})} \right) \underset{H_0}{\overset{H_1}{\geq}} 0 \\ &= \log \left( \frac{\pi_{o,k} p(x_{o,k}|H_1)}{(1 - \pi_{o,k}) p(x_{o,k}|H_0)} \right) \underset{H_0}{\overset{H_1}{\geq}} 0,\end{aligned}\quad (3.3)$$

where  $P(H_1|x_{o,k})$  and  $P(H_0|x_{o,k})$  denote the *a posteriori* probabilities based on the SUs' observations.  $p(x_{o,k}|H_1)$  and  $p(x_{o,k}|H_0)$  represent the likelihood functions as computed by the SUs under  $H_1$  and  $H_0$  respectively, and, are given by:

$$p(x_{o,k}|H_1) = \frac{1}{\sigma\sqrt{2\pi}} e^{-\frac{(x_{o,k} - h_{o,k} s_k)^2}{2\sigma^2}}, \quad (3.4)$$

$$p(x_{o,k}|H_0) = \frac{1}{\sigma\sqrt{2\pi}} e^{-\frac{(x_{o,k})^2}{2\sigma^2}}. \quad (3.5)$$

We use the logarithm of the *a posteriori* probability ratio in our model to capture the confidence regarding the presence or absence of PU activity over a particular band. In fact, this measure constitutes the SU's ranking metric which, in turn, is used to order the PU-owned frequency bands in  $\mathcal{H}$ . For a given SU  $o \in \mathcal{O}$  and two distinct PU-owned frequency bands  $k, k' \in \mathcal{H}$ ,  $k \neq k'$  and  $\delta_{o,k} < \delta_{o,k'}$ , it prefers  $k$  over  $k'$ . As a result, the SU would prefer to use PU-owned frequency band  $k$  for its transmissions. It is, however, possible that the same band is the preferred choice of another SU. Hence, competitions exist among SUs for PU-owned bands and the problem of finding a stable allocation of each PU-owned band in  $\mathcal{H}$  to a unique SU in  $\mathcal{O}$  arises. For any SU  $o \in \mathcal{O}$  that is looking to transmit over any PU-owned frequency band  $k \in \mathcal{H}$ , we define  $v_{o,k}$ , a function of the ranking metric only, to serve as a measure of SU  $o$ 's utility:

$$v_{o,k} = f_1(\delta_{o,k}), \quad (3.6)$$

where  $f_1$  denotes a monotonically decreasing function of  $\delta_{o,k}$ , where  $\delta_{o,k}$  is the logarithm of the *a posteriori* probability ratio computed by SU  $o$  over PU  $k$ 's licensed band. In other words,  $f$  is chosen such that the utility of an SU decreases as  $\delta_{o,k}$  increases.

In our model, we assume that all the SUs and PUs participate in the association process. The SUs compute valuations that capture the ranking metric and rate over the licensed frequency bands as follows.

$$p_{o,k} = f_2(\delta_{o,k}, \eta_{o,k}), \quad (3.7)$$

where  $f_2$  is a monotonically decreasing function of  $\delta_{o,k}$  (since, an SU prefers a PU who is more likely to be inactive) and an increasing function of  $\eta_{o,k}$  (since, SUs seek to obtain good communication rates). In this game, the SUs propose this valuation to PUs. Using this proposal, a PU evaluates its utility. Accordingly, we define  $u_{k,o}$  as PU  $k$ 's utility when associated with SU  $o$ . It is assumed, in this framework, that  $u_{k,o}$  is monotonically increasing with  $p_{o,k}$  for PU  $k$  that is inactive and whose licensed band is available. One possible way of interpreting the aforementioned aspect is to consider  $u_{o,k}$  as a reward or credit that the SU proposes to give to the inactive PU based on the former's valuation of the latter's frequency band in (3.7). However, if PU  $k$  is active, we assume  $u_{k,o} = 0, \forall o$ , as it values its own transmission more than all SUs' proposals and, thus, it does not associate with any SU. This utility function serves as the incentive for a PU to participate in the association process and determines its preferences. For instance, a PU that is inactive prefers to allocate its licensed band to an SU with high valuation, e.g., an SU which is more likely to detect it as inactive and attains a high rate over the licensed band so that the PU gets a higher reward. An active PU, on the other hand, prefers to keep the licensed band for its own transmissions.

Here, we note that the PUs in the network do not have information about the SUs' inference performance levels as well as their rates. Hence, the valuations of SUs,  $p_{o,k}$  for all  $o$  and  $k$ , is unknown to the PUs initially. In other words, inactive PUs are unable to evaluate their utilities in the beginning and, therefore, cannot make association decisions that maximize their payoffs. In

this case, an inactive PU  $k$  can choose an SU  $o$  to associate with only when it acquires information on  $p_{o,k}$ . This is the main reason we require SUs to forward their proposals to PUs in our system according to their preference lists. Hence, our goal is to obtain a spectrum allocation strategy according to which each SU is associated with its most preferred PU-owned frequency band and vice versa. To do this, we formulate the problem as a *matching game* between PUs and SUs. We first define the game in Section 3.4 and, then, present the solution concept and propose a distributed resource allocation algorithm in Section 3.5.

### 3.4 Spectrum Allocation as a Matching Game

Using classical optimization techniques to solve the frequency allocation problem can yield significant overhead. As a matter of fact, it is NP-hard in general [49]. Therefore, the need for self-organizing solutions in CRNs along with the complexity of centralized optimization methods necessitate a distributed framework in which SUs and PUs autonomously determine, based on their individual objectives, the best SU-PU associations. One suitable mechanism for developing such an autonomous SU-PU associations is given by *matching theory* [75].

#### 3.4.1 Matching Concepts

A matching is defined as a pairing between SUs in  $\mathcal{O}$  and PUs in  $\mathcal{H}$  through a matching  $\xi: \mathcal{H} \rightarrow \mathcal{O}$ . We consider the pairing to be one-to-one in nature. In this case,  $O - H$  or more SUs will not be matched. We denote by  $\mathcal{K}$  the set of available bands where  $\mathcal{K} \subseteq \mathcal{H}$  and  $\mathcal{K}'$  is the set of matched SUs where  $\mathcal{K}' \subset \mathcal{O}$ . More formally, a matching game can be defined as in [37].

**Definition 3.1.** A matching game is defined by two sets of players  $(\mathcal{O}, \mathcal{H})$  and two preference relations  $\succ_o$  and  $\succ_k$ .  $\succ_o$  allows players of set  $\mathcal{O}$  to evaluate (rank) players of set  $\mathcal{H}$ , while  $\succ_k$  allows players of set  $\mathcal{H}$  to rank players of set  $\mathcal{O}$ .

The outcome of a matching game is a one-to-one association function  $\xi$  that bilaterally assigns to each player  $o \in \mathcal{K}'$ , a player  $k = \xi(o)$ ,  $k \in \mathcal{K}$ . Similarly, we have  $o = \xi(k)$ . To complete the

definition of the game, we must introduce a preference relation  $\succ$  which is defined as a complete, reflexive, and transitive binary relation between the players in  $\mathcal{O}$  and  $\mathcal{H}$ . Thus, for any SU  $o \in \mathcal{O}$ , a preference relation  $\succ_o$  is defined over the set of PUs  $\mathcal{H}$  such that, for any two PU-owned frequency bands  $k, k' \in \mathcal{H}, k \neq k'$ :

$$k \succ_o k' \Leftrightarrow \delta_{o,k} < \delta_{o,k'}, \quad (3.8)$$

where  $\delta_{o,k}$  and  $\delta_{o,k'}$  denote the logarithm of the *a posteriori* probability ratio of SU  $o$  corresponding to  $k$  and  $k'$  respectively. Similarly, for any available PU-owned frequency band  $k$ , a preference relation  $\succ_k$  over the set of SUs  $\mathcal{O}$  is defined as follows, for any two SUs  $o, o' \in \mathcal{O}, o \neq o'$ :

$$o \succ_k o' \Leftrightarrow u_{k,o}(p_{o,k}) > u_{k,o'}(p_{o',k}), \quad (3.9)$$

where  $u_{k,o}$  and  $u_{k,o'}$  denote PU  $k$ 's utility when it is inactive and grants its frequency band to SU  $o$  and  $o'$  respectively.

Next, we show how SUs build their preferences according to the preference relation defined in (3.8) and, accordingly, evaluate their proposals. Then, in Section 3.4.3, we present how PUs play an active role in the association process.

### 3.4.2 Preferences and Proposals of the SUs

So far, the logarithm of the *a posteriori* probability ratio for each of the SUs in  $\mathcal{O}$  has been computed according to (3.3), (3.4), and (3.5). Based on the results obtained, an SU  $o$  ranks the PU-owned frequency bands in an increasing order with the largest element being the least preferred. Accordingly, an SU  $o$  obtains a preference list  $\Delta_o$ , which is sorted based on (3.8).

Given  $\Delta_o$  and  $\eta_o$ , an SU  $o \in \mathcal{O}$  is able to better evaluate the benefit from using each of the PU-owned frequency bands. Intuitively, in addition to  $\eta_o$ , an SU values a frequency band less if it predicts the band to be occupied by a PU, i.e.,  $\delta_{o,k} > 0$ . On the other hand, an SU values a frequency band more if it predicts the band to have no PU activity on it. In other words, when  $\delta_{o,k} < 0$ ,  $p_{o,k}$  in (3.7) is higher than when  $\delta_{o,k} > 0$ . Hence,  $p_{o,k}$  should be defined in a way such



that the aforementioned properties are satisfied. We, in this chapter, express it as a weighted sum of the ranking metric and rate without loss of generality. More precisely, an SU  $o$ 's valuation that it proposes to PU  $k$  is given by:

$$p_{o,k} = -\alpha_o \delta_{o,k} + (1 - \alpha_o) \eta_{o,k}, \quad (3.10)$$

where  $\alpha_o$  is a positive weight chosen by SU  $o$  such that  $0 \leq \alpha_o \leq 1$ .

### 3.4.3 Preferences of the PUs

Initially, an inactive PU  $o \in \mathcal{K}$  has no known preferences as to which SU it should grant its licensed band to. It is, however, considered that its corresponding utility function is monotonically increasing with the valuation of the SU it is associated with. When the matching game starts, only inactive PUs start to build their preferences based on the proposals they receive from SUs in the form of their utility functions. In the case where  $p_{o,k} > 0 \forall o, k$ , every inactive PU will have a preferred SU while every active PU will keep the licensed band to itself. However, it is possible for an inactive PU  $k$  not to be matched. This happens in the following two scenarios: i)  $p_{o,k} < 0 \forall o$ , or ii) a restriction on the number of SUs' proposals to be made exists.

Inactive PUs are interested in getting associated with SUs presenting the highest reward. In this manner, an inactive PU maximizes its utility. In fact, it accepts or rejects SUs' proposals based on the preference relation defined in (3.9) and the fact that its utility is a monotonically increasing function with that of the SU. An active PU, on the other hand, simply rejects all the SUs' proposals.

We have defined the matching game and presented how SUs build their preferences and proposals. We have also shown how PUs adopt their preferences. Next, we present the solution concept and find a stable and optimal spectrum allocation.

### 3.5 Solution Concept and Proposed Algorithm

Having defined the preference relations of the SUs in (3.8) and the inactive PUs in (3.9) and articulated the modus operandi of active PUs, we study the matching between SUs and PUs next. First, we characterize the notion of stable spectrum matching in our model.

**Definition 3.2.** A matching  $\xi$  is said to be stable if there does not exist any two pairings  $(o, k), (o', k') \in \xi$ , such that,  $\delta_{o',k} < \delta_{o',k'}$  and  $u_{k,o'} > u_{k,o}$ .

In order to reach a stable matching in this framework, we propose a novel distributed algorithm shown in Algorithm 3.1. It consists of four main phases: detection of PUs' signals (Phase I), building SUs' preferences and constructing proposals (Phase II), matching evaluation (Phase III), and finally SU-PU associations (Phase IV). It is important to mention that the novelty of Algorithm 3.1 lies in its ability to address underlying uncertainties structures and lack of *a priori* known preferences in matching problems. This clearly distinguishes it from the deferred acceptance algorithm of Gale-Shapley [37] where all preferences are known *a priori* and resources are available deterministically.

Initially, each SU  $o$  computes the logarithm of the *a posteriori* probability ratio over PU-owned frequency band  $k$  ( $\delta_{o,k}, \forall o, k$ ). In the second phase, each SU  $m$  obtains its preference vector  $\Delta_o$  by ranking  $\delta_{o,k}$  based on (3.8)  $\forall k$ . Then, using  $\eta_o$  and  $\Delta_o$ , the SU evaluates  $p_{o,k}$  defined in (3.10) for all PU-owned frequency bands. In this model, an SU discards all the proposals with a negative valuation,  $p_{o,k}$ , from its preference list. That is, an SU in the network does not propose to a PU-owned frequency band for which  $p_{o,k} < 0$ . If an SU  $o$  is not currently allocated the most preferred frequency band  $k$ , it sends  $k$  a matching proposal. Upon receiving a proposal, PU  $k$ , if active, rejects the proposal. Otherwise, PU  $k$  updates its utility and accepts the request of the SU either when it has not been proposed to yet or when the reward is greater than what it gets from another SU's request. If the proposal is rejected, SU  $o$  proposes to the next PU-owned frequency band in its preference list. Once the algorithm terminates, a stable matching, that consists of  $H$  SU-PU associations, is reached as long as all PUs are inactive and there does not exist a scenario where,

---

**Algorithm 3.1** SU-PU Associations Algorithm
 

---

**Data:** Initially, no frequency band is assigned to any SU.

**Result:** A stable spectrum allocation (matching)  $\xi$ .

**Phase I - Detection of PUs Signals**

- Each SU  $o$  computes the logarithm of the *a posteriori* probability ratio over frequency band  $k$   $\delta_{o,k}$ ,  $\forall o, k$ .

**Phase II - Building SUs Preferences and Proposals**

- Each SU  $o$  constructs its preference vector  $\Delta_o$  based on  $\delta_{o,k}$ ,  $\forall k$ .  $\Delta_o$  is sorted based on  $\succ_o$ .
- Each SU  $o$  constructs its proposals, as shown in (3.10) for all  $k$ , and keeps it only if  $p_{o,k} > 0$ .

**Phase III - Matching Evaluation**

Initially, all PUs have no preferred SU.

**repeat**

**if**  $k \succ_o k'$ , then

    An SU  $o$  sends a proposal to PU  $k$ .

    PU  $k$  receives its proposal and, if active, rejects it.

    Otherwise, PU  $k$  accepts it if it hasn't been proposed to before.

    When PU  $k \in \mathcal{K}$  and it has been proposed to before,

**if**  $o \succ_k o'$  ( $p_{o,k} > p_{o',k}$  and  $u_{k,o}(p_{o,k}) > u_{k,o'}(p_{o',k})$ )

        PU  $k$  rejects  $o'$  proposal and adopts  $o$ 's.

**else**

        PU  $k$  keeps the proposal he has and rejects the new one.

**end**

**end**

**until** All positive proposals have been made.

**Phase IV - Spectrum Allocation**

---

for an inactive PU  $k$ , we have  $p_{o,k} < 0 \forall o$ . Otherwise, the number of associations in the stable matching is less than  $H$ . In this case, there are  $O - H$  or more SUs which are not associated with PUs. Once the proposals have been made, each active PU keeps its licensed band while each inactive PU remains associated with the most preferred SU and Phase III terminates.

The fundamental nature of the proposed algorithm is summarized in the following theorem:

**Theorem 3.1.** *For any given instance of the spectrum allocation problem, Algorithm 3.1 terminates, and, on termination, the associations between SUs and PUs form a stable matching.*

*Proof.* A PU in  $\mathcal{K}$  can reject SUs' proposals only when it is already associated with an SU, and once it is associated, the PU never becomes dissociated again. In this respect, the rejection of an SU by the last PU in its preference list would imply that all the PUs were already associated.

However, since  $O > H$ , and no SU can associate with two PU-owned frequency bands, then  $|\mathcal{K}|$  SUs would also be associated, which is a contradiction.

Each iteration involves sending one proposal and no SU ever proposes twice to the same PU, then the total number of iterations cannot exceed  $O \times H$ . On termination, the associated pairs specify a matching,  $\xi$ . If an SU  $o'$  prefers a PU-owned frequency band  $k$  to what it is currently associated with, then  $k$  must have rejected  $o'$  at some point during the execution of the algorithm. This rejection implies that  $k$  became, or was, associated with an SU that it prefers to  $o'$ , and any subsequent change of its association brings it still a better SU. So,  $k$  cannot prefer  $o'$  to the SU it is currently associated with. Therefore,  $\xi$  is a stable matching.  $\square$

The stable matching we obtain based on the aforementioned algorithm is said to be *optimal* for SUs and PUs at the same time.

**Theorem 3.2.** *All possible executions of Algorithm 3.1 yield the same stable matching in which each SU associates with its most preferred PU-owned band, and each PU associates with its best SU, that each can have in any stable matching.*

*Proof.* Our framework investigates one-to-one SU-PU associations for which we have proved the existence of a stable matching. Also, note that the convergence of Algorithm 3.1 follows from that of Phase III.

The order in which SUs propose to PUs is immaterial to the outcome of Algorithm 3.1 as the stable matching we obtain in this case is unique. Furthermore, this stable matching is said to be optimal for the SUs because every SU is associated with the best PU that it can possibly associate with. This observation is clear as a stable matching is always optimal for entities that propose [37]. Moreover, given the nature of our model where we assume that each PU builds its preferences based on the proposals it receives from SUs according to (3.9), it is obvious that a PU also associates with a SU that sends it a better proposal. Hence, it is clear that the stable matching we obtain is also optimal for the PUs. Therefore, the stable matching is *optimal* for SUs and PUs.  $\square$

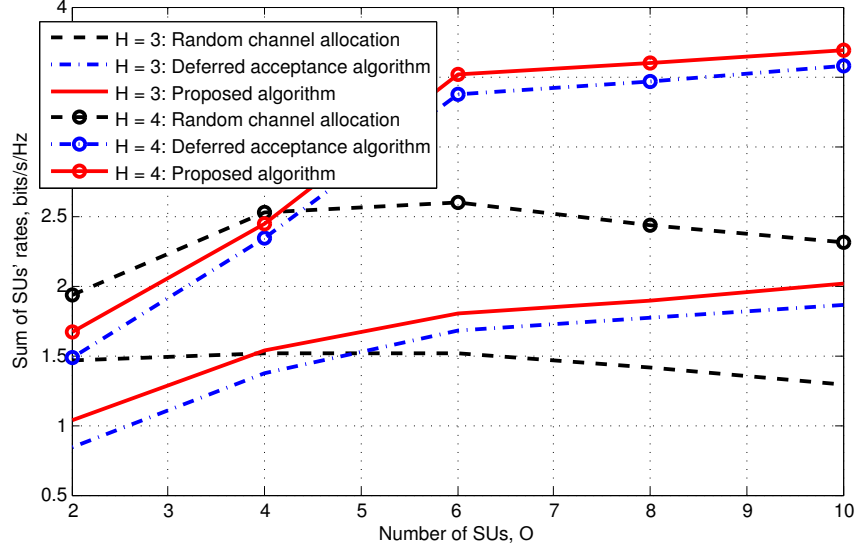


Fig. 3.2: The sum of SUs' rates with respect to the number of SUs in the network,  $O$ , for  $H = \{3, 4\}$ .

### 3.6 Numerical Results

We consider a CRN having  $O = 10$  SUs and  $H = 4$  PUs that are uniformly deployed in a square area of  $100 \text{ m} \times 100 \text{ m}$ . The transmit power of each SU is 13 dBm and of each PU is 17 dBm, and the noise level is given such that  $\sigma^2 = -90 \text{ dBm}$ . The path loss exponent is set to 3. Without loss of generality, we assume  $\pi_1 = \dots = \pi_{10} = [.1, .2, .3, .4]$ . Statistical results are averaged over a 100000 independent simulation runs. For illustration purposes, we assume that the PUs are inactive and  $u_{k,o}(p_{o,k}) = 1 - e^{-p_{o,k}}$ .

We present results on the performance of Algorithm 3.1 when compared to the algorithm in [61], the deferred acceptance algorithm [37], and a random channel allocation approach. For the algorithm in [61], we assume that the coordinator, responsible for responding on behalf of the PUs in the one-to-one matching process, is a simple but rational entity that expects to be rewarded by the PUs. For the sake of simplifying the analysis, we assume that the coordinator charges the PUs a percentage of what is being proposed to them. For the deferred acceptance algorithm (explained in our context), SUs include all PUs in their preference lists. For the random channel allocation approach where each SU randomly selects its channel to transmit on, we consider the transmit power of SUs to be twice as much as that considered in our proposed algorithm, the algorithm

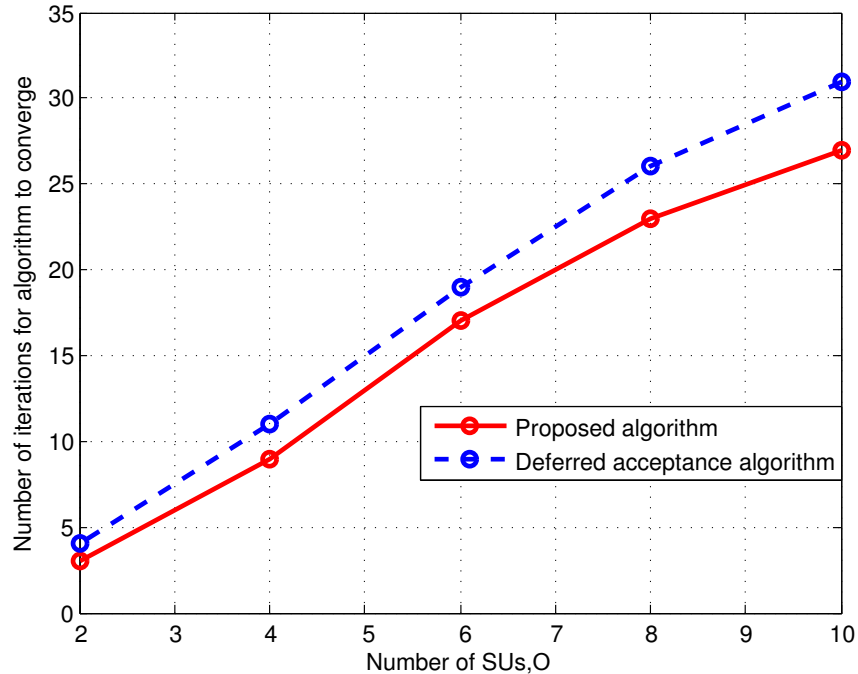


Fig. 3.3: The number of iterations required for an algorithm to converge with respect to the number of SUs,  $O$ , when  $H = 4$ .

in [61], and the deferred acceptance algorithm (assuming that sensing activity in both algorithms consumes the same amount of power as that needed for transmission).

Fig. 3.2 shows the sum of SUs' rates as the number of SUs  $O$  and PUs  $H$  vary. In the random channel allocation approach, it is possible for a group of SUs to randomly select the same channel to transmit on, the chances of which increase as  $O$  becomes larger than  $H$ . As a result, SUs may interfere with each other. Hence, the sum of rates decreases compared to the ones obtained by the deferred acceptance algorithm and Algorithm 3.1 where each frequency band is allocated to a unique SU. In Fig. 3.2, we can see that the proposed algorithm, in terms of the sum of SUs' rates, clearly outperforms both the deferred acceptance algorithm and random channel allocation approach when  $O > H$ . This is due to the following factors: i) higher number of collisions among SUs' transmissions as  $O$  increases that is expected to reduce the sum of rates that SUs achieve by following a random channel allocation, and ii) higher number of proposals (due to larger preference lists) to take into consideration when evaluating the value that the sum of SUs' rates converges to when adopting the deferred acceptance algorithm. In the latter case, the sum

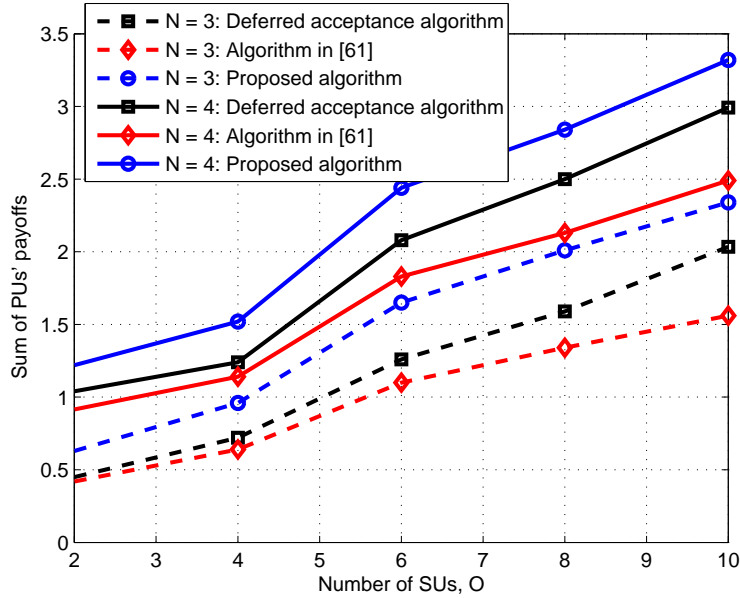


Fig. 3.4: The sum of PUs' payoffs with respect to the number of SUs in the network,  $O$ , for  $H = 3$  and 4.

of SUs' rates is expected to be higher than that of the deferred acceptance algorithm since SUs, according to Algorithm 3.1, discard proposals where  $p_{o,k} < 0$ . Fig. 3.2 also shows that the proposed algorithm attains up to 20% and 60% improvement in the sum of SUs' rates relative to the deferred acceptance algorithm ( $O = 2$  and  $H = 3$ ) and random channel allocation approach ( $O = 10$  and  $H = 4$ ), respectively.

In Fig. 3.3, we show the number of iterations required for the proposed and deferred acceptance algorithms to converge as  $O$  increases for  $H = 4$ . It is evident from this figure that our proposed algorithms to converge as  $O$  increases for  $H = 4$ . It is evident from this figure that our proposed algorithm outperforms the deferred acceptance algorithm. This is because the latter algorithm requires more iterations to converge. A similar and clear observation can be made from in Fig. 3.4 where we show the sum of PUs' payoffs as the number of SUs,  $O$ , and PUs,  $H$  vary. In Fig. 3.4, we also observe that the proposed algorithm outperforms the algorithm in [61]. It is important to mention here that both the proposed algorithm and the algorithm in [61] behave similarly when the coordinator does not charge PUs.

### 3.7 Summary

In this chapter, we introduced a distributed model for the allocation of PU-owned frequency bands to SUs in a CRN. In the proposed model, SUs sense the licensed spectrum looking for white spaces. We modeled the problem as a *matching game* between SUs and PUs. We proposed a novel distributed algorithm to obtain a stable and optimal matching. Moreover, we compared our proposed algorithm with the deferred acceptance algorithm and a random channel allocation approach. Simulation results showed that the proposed algorithm can improve: i) the sum of SUs' rates by up to 20% and 60% relative to the deferred acceptance algorithm and random channel allocation approach respectively, and ii) the sum of PUs' payoffs by up to 25% compared to the deferred acceptance algorithm. The results also showed an improved convergence time.

A novel and distributed spectrum allocation approach that is based on Matching theory was proposed in this chapter in order to mitigate the interference created by one or more SUs at each others' receivers in a CRN. In future work, we will assume that a jammer is present in the network and, accordingly, will present a jamming interference mitigation technique that is based on re-transmission protocols.



# CHAPTER 4

## MITIGATION OF JAMMING INTERFERENCE VIA ARQ PROTOCOLS

Data transmission (communication) is not only susceptible to interference from other transmitting nodes but is also vulnerable to jamming attacks from malicious users [7,67,76] given the broadcast nature of the wireless medium. In such adversarial environments, the reliability of communication further degrades due the destructive interference that a jammer may create at one or more of the receivers. For such systems, ARQ-based transmission mechanisms can be implemented as an interference mitigation technique in order to improve reliability in communication sessions.

In this chapter, we focus our attention on delay-sensitive Stop-and-Wait ARQ-based wireless systems in the presence of disruptions and performance degradation due to jammer's interference, Inter-symbol Interference (ISI), and AWGN. We model the framework as a constrained optimization problem in which the number of transmission attempts at the transmitter required to achieve a successful transfer of a data packet to the receiver is minimized such that the probability of successfully receiving it satisfies a prescribed guarantee.

## 4.1 Literature Review

As is well known, ARQ is as an error-control method for data transmission that uses acknowledgments and timeouts to achieve reliable data transmission over unreliable links [17, 20, 42, 48]. In the past, the authors in [74] and [87] considered ARQ mechanisms in the presence of a jammer, but failed to model the jammer to be strategic. Moreover, the jamming mechanism considered in [74] and [87] is limited to a simple ON-OFF model and the analysis provided ignores strategic (game-theoretic) considerations. While [74] focused on selective re-transmissions to improve communication performance over partial-time jamming channels, [87] discussed the detection and classification of jamming attacks in 802.11b wireless networks. Furthermore, in [101], the authors investigated the design of efficient ARQ schemes with anti-jamming coding techniques to improve the average throughput for secondary users prone to interference (jamming) from primary users in the network.

## 4.2 Motivation, Novelty, and Contributions

While [26, 31, 79] have considered a game-theoretic approach for optimal power allocation over different frequency bands, we, in this chapter, employ ARQ-based transmission mechanisms to improve the reliability of wireless P2P communication under jamming attacks. We consider both the transmitter and the jammer to be strategic in nature, thereby necessitating a game-theoretic analysis in which we first evaluate the probability of successfully receiving a data packet at the receiver as a function of system-latency<sup>1</sup> by formulating the optimal energy allocations at the transmitter and the jammer as a minimax game. For the sake of tractability, we analyze bounds on the probability of successfully receiving a data packet at the receiver to find an approximate optimal solution. Then, we minimize system-latency using approximate energy allocations that we obtained in the first stage. To the best of our knowledge, our work is the first attempt to

---

<sup>1</sup>The number of transmission attempts at the transmitter to achieve a successful transfer of a data packet to the receiver

analyze the problem of designing an ARQ-based system in the presence of a jammer within a game-theoretic framework. In the proposed setting, we provide a more realistic performance analysis of this re-transmission protocol implemented in the media access control layer of a P2P wireless communication link.

### 4.3 System Model and Problem Formulation

We consider a transmitter-receiver pair, with a perfect feedback channel, in the presence of a jammer as shown in Fig. 4.1. We assume that the transmitter communicates with the receiver by

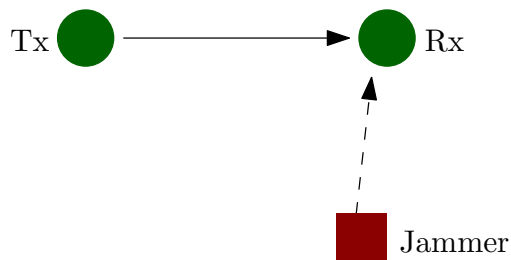


Fig. 4.1: A P2P communication system in the presence of a jammer.

sending a data packet (DATA) through an AWGN channel with perfect feedback in the presence of ISI. The receiver sends an acknowledgment packet (ACK) upon the reception of an error-free<sup>2</sup> DATA. Otherwise, the receiver stays quiet, in which case, the transmitter retransmits the same packet after a fixed wait-time. In this model, we allow a maximum of  $\mathcal{T}$  transmission attempts per data packet, i.e., original transmission and up to  $\mathcal{T} - 1$  retransmissions, where the total energy invested in communicating DATA cannot exceed  $\mathcal{E}_T$ , i.e.,  $\sum_{i=1}^{\mathcal{T}} E_{T_i} \leq \mathcal{E}_T$ . In practice, ACK packets are typically small in size, and therefore, the time required for an ACK to be received at the transmitter is negligible compared to the case of large DATA [43]. Therefore, we, in this chapter, consider jamming of DATA and not ACK.

We consider the communication between the transmitter and the receiver to be successful as long as the ACK is received within  $\mathcal{T}$  transmission attempts of DATA. Let  $\xi$  denote the number

<sup>2</sup>In practice, packet errors are detected by verifying the CRC checksums.

of transmissions attempted by the transmitter before DATA is received successfully. Note that, in practice, DATA has an upper limit on the number of retransmissions (Time To Live, in short, TTL) before it is dropped. Therefore, it is critical to study the minimum number of transmission attempts required for a successful transmission of a data packet. We assume that the transmitter strategically allocates its energy to minimize  $\mathcal{T}$  while the probability of successfully receiving DATA at the receiver satisfies a prescribed guarantee. Note that, consideration of the constraint requires a game-theoretic analysis of the competition between the transmitter (who wants to maximize the probability of successfully receiving DATA) and the jammer (that wants to minimize it) for a given  $\mathcal{T}$ . In fact, the jammer's objective lies in impairing the transmitter's communication session by injecting interference energy,  $\mathbf{E}_J = [E_{J_1} E_{J_2} \cdots E_{J_{\mathcal{T}}}]^T$ , where  $E_{J_i}$  is the interference at the  $(i-1)$ -th retransmission. Here, we assume the jammer to be powerful in the sense that it has complete knowledge of the protocol, and therefore, we consider a worst-case scenario in which the jammer knows precisely when the transmitter sends its information. We also assume that  $\mathcal{E}_J \geq \mathcal{E}_T$ . In practice, since any jammer is typically energy-constrained, we assume  $\sum_{i=1}^{\mathcal{T}} E_{J_i} \leq \mathcal{E}_J$ . Thus, the jammer allocates its energy to ensure that the constraint on the probability of successfully receiving a data packet at the receiver is not satisfied and, thereby, forces the transmitter to resend DATA as many times as possible.

### 4.3.1 Problem Formulation

We explore our problem framework in two stages. First, we investigate the probability of successfully receiving a data packet at the receiver as a function of  $\mathcal{T}$  by evaluating the optimal energy allocations at the transmitter and the jammer as a minimax game. In the next stage, we minimize  $\mathcal{T}$  using the equilibrium solution obtained in the first stage. Formally, we state the problem as follows. Find  $\mathcal{T}^*$  such that,

$$\begin{aligned} \min \quad & \mathcal{T} & (4.P1) \\ \text{subject to:} \quad & p^*(\mathcal{T}) \geq 1 - \delta \end{aligned}$$

where  $1 - \delta$  is a prescribed value above which the communication session between the transmitter and the receiver is considered successful, and,  $p^*(\mathcal{T})$ , for a fixed  $\mathcal{T}$ , is evaluated as follows.

$$p^*(\mathcal{T}) = \min_{\mathbf{E}_J} \max_{\mathbf{E}_T} Pr(\xi \leq \mathcal{T}) = \max_{\mathbf{E}_T} \min_{\mathbf{E}_J} Pr(\xi \leq \mathcal{T}) \quad (4.P2)$$

subject to:

$$\begin{aligned} \sum_{i=1}^{\mathcal{T}} E_{T_i} &\leq \mathcal{E}_T, \\ \sum_{i=1}^{\mathcal{T}} E_{J_i} &\leq \mathcal{E}_J. \end{aligned}$$

We attempt to solve 4.P1 by first solving 4.P2 and then using the optimal energy allocations obtained to evaluate the optimal number of transmission attempts  $\mathcal{T}^*$ .

## 4.4 Approximate Minimax Energy Allocations for a fixed $\mathcal{T}$

In order to solve 4.P2, we first present insights into the computation of  $Pr(\xi \leq \mathcal{T})$  which, in turn, is given by:

$$Pr(\xi \leq \mathcal{T}) = \sum_{i=1}^{\mathcal{T}} Pr(\xi = i), \quad (4.1)$$

where  $Pr(\xi = i)$  denotes the probability of the  $(i-1)$ -th retransmission being successful. Furthermore, the state diagram, presented in Fig. 4.2, describes the transitions a data packet transmission goes through before reaching a success or failure state. In Fig. 4.2, we denote by  $t_i$  and  $a_i$  the states in which DATA and ACK packets are to be transmitted at the  $i$ -th time respectively.  $s_i$  is the state in which the  $(i-1)$ -th retransmission of the information packet is successful while state  $f$  corresponds to the failure of DATA. Note that  $Pr(s_i)$  is equal to  $Pr(\xi = i)$  in Equation (4.1). The fact that the feedback channel is assumed to be perfect in our model, enforces  $p_i$  to be equal to 0.

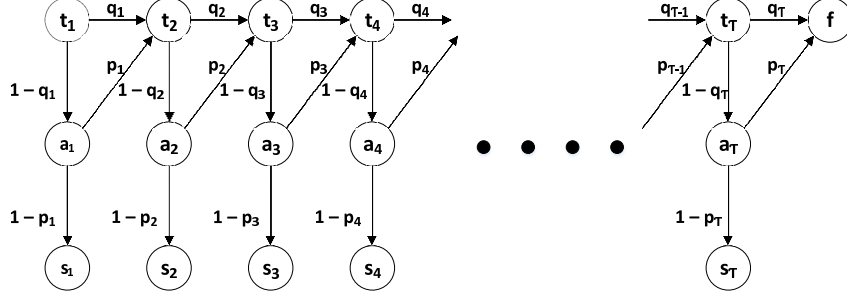


Fig. 4.2: A state diagram showing the transitions of a data packet transmission.

Accordingly, based on the state diagram provided in Fig. 4.2,  $\{Pr(s_i)\}_{i=1}^T$  is computed as follows.

$$Pr(s_1) = (1 - q_1), \quad (4.2)$$

$$\{Pr(s_i)\}_{i=2}^T = \{(1 - q_i) \prod_{k=1}^{i-1} q_k\}_{i=2}^T, \quad (4.3)$$

where  $q_i$  denotes the probability of error for the  $(i-1)$ -th retransmission of DATA and is a function of  $E_{T_i}$  and  $E_{J_i}$ . Substituting Equations (4.2) and (4.3) in Equation (4.1) yields the following:

$$Pr(\xi \leq T) = 1 - \prod_{i=1}^T q_i. \quad (4.4)$$

Hence, we write the equivalent of 4.P2 as follows.

$$1 - p^*(T) = \min_{\mathbf{E}_T} \max_{\mathbf{E}_J} \prod_{i=1}^T q_i = \max_{\mathbf{E}_J} \min_{\mathbf{E}_T} \prod_{i=1}^T q_i \quad (4.P2-A)$$

subject to:

$$\sum_{i=1}^T E_{T_i} \leq \mathcal{E}_T,$$

$$\sum_{i=1}^T E_{J_i} \leq \mathcal{E}_J.$$

Intuitively, the probability of error decreases as the signal-to-interference plus noise ratio (SINR) increases and vice versa. In this respect,  $q_i$  is monotonically decreasing in  $E_{T_i}$  and monotonically increasing in  $E_{J_i}$ . It is also true that the multiplication of monotonic non-negative functions pre-

serves monotonicity. Therefore, we take the natural logarithm of the objective function in 4.P2-A which reduces to the following *minimax* formulation.

$$\begin{aligned} & \log(1 - p^*(\mathcal{T})) = \\ & \min_{\mathbf{E}_T} \max_{\mathbf{E}_J} \sum_{i=1}^{\mathcal{T}} \log(q_i) = \max_{\mathbf{E}_J} \min_{\mathbf{E}_T} \sum_{i=1}^{\mathcal{T}} \log(q_i) \end{aligned} \quad (4.P2-B)$$

subject to:

$$\begin{aligned} & \sum_{i=1}^{\mathcal{T}} E_{T_i} \leq \mathcal{E}_T, \\ & \sum_{i=1}^{\mathcal{T}} E_{J_i} \leq \mathcal{E}_J. \end{aligned}$$

The solution to this *minimax* game is the Nash Equilibrium, which is a saddle point in the design metric,  $q_i$  for all  $i$ . Obtaining a closed form expression of  $q_i$  is intractable in the presence of ISI. Therefore, we investigate an approximate solution by considering both lower and upper bounds on 4.P2-B.

In [35], Forney provided an upper and lower bound expressions for the probability of error,  $q_i$ , as given below.

$$K_0 Q\left(\frac{d_{min,i}^2}{2\sigma_i}\right) \leq q_i \leq K_2 Q\left(\frac{d_{min,i}^2}{2\sigma_i}\right) \quad (4.5)$$

where  $d_{min,i}^2$  is the minimum energy of transmitter's signal,  $\sigma_i^2$  is the sum of the AWGN power spectral density and the energy of the jammer's signal,  $K_0$  and  $K_2$  are both constants with respect to the energy allocations of the transmitter and the jammer respectively. Forney's bound, not being restricted to a particular modulation scheme, allows us to analyse 4.P2-B in a very general sense. Since Q-functions do not have closed-form expressions, 4.P2-B still remains intractable. Therefore, we approximate 4.P2-B by using well-known bounds on  $Q\left(\frac{d_{min,i}^2}{2\sigma_i}\right)$  [21, 68] in order to devise a tractable problem. Since, we assume  $\mathcal{E}_J \geq \mathcal{E}_T$ , we consider bounds on Q-functions in the low SINR regime.

Note that the objectives of the transmitter-receiver pair and the jammer are conflicting. Therefore, the transmitter is interested in minimizing the upper-bound on  $\sum_{i=1}^{\mathcal{T}} \log(q_i)$  subject to a total energy constraint  $\mathcal{E}_T$ . On the other hand, the jammer attempts to maximize the lower-bound. In other words, the transmitter strategically allocates its energy to improve the worst-case probability of error performance, while the jammer tries to degrade the best-case probability of error performance of the transmitter.

Next, we relate the upper-bound as well as the lower-bound to system parameters to make them amenable to system design.

#### 4.4.1 Upper-bound

In order to find a tractable problem, we use the following upper bound on the Q-function, which is relatively tight in the low-SINR regime.

$$Q\left(\frac{d_{min,i}}{2\sigma_i}\right) \leq \frac{1}{2}e^{-\frac{d_{min,i}}{2\sigma_i}}. \quad (4.6)$$

Substituting Equation (4.6) in the right-hand side of Equation (4.5), we have

$$q_i \leq \frac{K_2}{2}e^{-\frac{d_{min,i}}{2\sigma_i}} = \frac{K_2}{2}e^{-\frac{1}{2}\sqrt{\frac{E_{T_i}}{N_0+E_{J_i}}}}. \quad (4.7)$$

Thus, the transmitter's utility is reduced to the following.

$$\sum_{i=1}^{\mathcal{T}} \log(q_i) \leq \underbrace{\mathcal{T} \log\left(\frac{K_2}{2}\right)}_{constant} - \frac{1}{2} \sum_{i=1}^{\mathcal{T}} \sqrt{\frac{E_{T_i}}{N_0 + E_{J_i}}}. \quad (4.8)$$

In this case, the transmitter's goal, which is to minimize the upper-bound on  $\sum_{i=1}^{\mathcal{T}} \log(q_i)$ , can be interpreted as the transmitter trying to maximize  $\sum_{i=1}^{\mathcal{T}} \sqrt{\frac{E_{T_i}}{N_0+E_{J_i}}}$  by strategically allocating its energy. In other words, the transmitter reduces 4.P2-B to the following, where the jammer is



assumed to play a given strategy,  $E_{J_i} = x$  for  $x \in [0, \mathcal{E}_J]$ .

$$\begin{aligned} \max_{\mathbf{E}_T} \sum_{i=1}^{\mathcal{T}} \sqrt{\frac{E_{T_i}}{N_0 + x}} \\ \text{subject to: } \sum_{i=1}^{\mathcal{T}} E_{T_i} \leq \mathcal{E}_T. \end{aligned} \quad (4.P3-A)$$

Since this is a standard convex-optimization problem [15], we solve 4.P3-A using Karush-Kuhn-Tucker (KKT) multipliers method. Given the jammer's strategy  $E_{J_i} = x$ , the auxiliary function, in this case, is given by

$$L_U(E_{T_i}, \lambda) = \sum_{i=1}^{\mathcal{T}} \sqrt{\frac{E_{T_i}}{N_0 + x}} + \lambda \left( \mathcal{E}_T - \sum_{i=1}^{\mathcal{T}} E_{T_i} \right). \quad (4.9)$$

Therefore,  $E_{T_i}^*$  satisfies the necessary condition:  $\nabla L_U(E_{T_i}^T) = 0$ . On substituting Equation (4.9) in the necessary condition, we get

$$E_{T_i}^* = \frac{1}{4\lambda^2(N_0 + x)}, \quad (4.10)$$

where  $\lambda$  is a constant for all  $i$ .

#### 4.4.2 Lower-bound

In contrast to the transmitter's view on 4.P2-B, the jammer wishes to maximize the lower-bound on the probability of error. A tight lower-bound on the Gaussian Q-function has been presented in the form of a single exponential function with parametric order and weight in [21]. In this chapter, we use this lower-bound to obtain the following:

$$\sum_{i=1}^{\mathcal{T}} \log(q_i) \geq \underbrace{\mathcal{T} \log\left(\frac{e}{2\pi} \frac{\kappa - 1}{2\kappa - 1}\right)}_{\text{constant}} - \frac{\kappa}{2} \sum_{i=1}^{\mathcal{T}} \frac{E_{T_i}}{N_0 + E_{J_i}}. \quad (4.11)$$

where  $e = \exp(1)$  and  $\kappa \geq 1$ . Therefore, the jammer's goal, which is to maximize the lower-bound on  $\sum_{i=1}^{\mathcal{T}} \log(q_i)$ , is equivalent to minimizing  $\sum_{i=1}^{\mathcal{T}} \frac{E_{T_i}}{N_0 + E_{J_i}}$ .

Thus, the jammer reduces 4.P2-B to the following, where the transmitter is assumed to play a given strategy,  $E_{T_i} = y$ , for  $y \in [0, \mathcal{E}_T]$ .

$$\begin{aligned} \min_{\mathbf{E}_J} \quad & \sum_{i=1}^{\mathcal{T}} \frac{y}{N_0 + E_{J_i}} \\ \text{subject to:} \quad & \sum_{i=1}^{\mathcal{T}} E_{J_i} \leq \mathcal{E}_J \end{aligned} \quad (4.P3-B)$$

Here, we also apply the KKT multipliers method to 4.P3-B in order to obtain  $E_{J_i}^*$ . We have the following auxiliary function:

$$L_L(E_{J_i}, \mu) = \sum_{i=1}^{\mathcal{T}} \frac{y}{N_0 + E_{J_i}} - \mu \left( \mathcal{E}_J - \sum_{i=1}^{\mathcal{T}} E_{J_i} \right). \quad (4.12)$$

The necessary condition for a stationary point in 4.P3-B is  $\nabla L_L(E_{J_i}) = 0$ , which, in turn, yields

$$E_{J_i}^* = \sqrt{\frac{y}{\mu}} - N_0, \quad (4.13)$$

where  $\mu$  is a constant for all  $i$  and the transmitter is playing  $E_{T_i} = y$ .

### 4.4.3 Equilibrium Analysis of Problem 4.P2-B

Intuitively, one may argue that the equilibrium solution to 4.P2-B is reached when both players uniformly allocate their energy resources. However, in this chapter, we show it formally by formulating the problem as a *minimax* game.

**Theorem 4.1.** *Given a fixed number of transmission attempts  $\mathcal{T}$ ,  $(\frac{\mathcal{E}_T}{\mathcal{T}}, \frac{\mathcal{E}_J}{\mathcal{T}})$  is the equilibrium strategy of this game in every attempt of the transmitter to retransmit DATA.*

*Proof.* A saddle point is the strategy at which both min-max and max-min solutions (Equations (4.10) and (4.13) respectively) coincide. In other words,  $x = E_{J_i}^*$  and  $y = E_{T_i}^*$ . Therefore, we

substitute Equation (4.13) in Equation (4.10) in order to obtain the transmitter's best-response as follows:

$$E_{T_i}^* = \left( \frac{\mu}{(4\lambda^2)^2} \right)^{\frac{1}{3}}. \quad (4.14)$$

Notice that, in Equation (4.14),  $E_{T_i}^*$  is a constant and independent of  $i$ . Substituting Equation (4.14) in the transmitter's energy constraint, we obtain a uniform energy allocation across  $\mathcal{T}$  transmission attempts. In other words, we have  $E_{T_i}^* = \frac{\mathcal{E}_T}{\mathcal{T}}$  for all  $i$ . Moreover, given the transmitter's uniform energy allocation and  $\mu$  is a constant for all  $i$ , then the jammer also distributes its energy resources uniformly across all the retransmission attempts. Thus, we have  $E_{J_i}^* = \frac{\mathcal{E}_J}{\mathcal{T}}$  for all  $i$ . Hence, we obtain  $(\frac{\mathcal{E}_T}{\mathcal{T}}, \frac{\mathcal{E}_J}{\mathcal{T}})$  to be the equilibrium strategy of this simultaneous-move game, described in 4.P3-A and 4.P3-B, in every attempt of the transmitter to retransmit DATA and the jammer to block DATA, given a fixed  $\mathcal{T}$ .  $\square$

Given that this point,  $(\frac{\mathcal{E}_T}{\mathcal{T}}, \frac{\mathcal{E}_J}{\mathcal{T}})$ , is the equilibrium strategy (solution) based on the analysis of 4.P3-A and 4.P3-B provided in Sections 4.4.1 and 4.4.2, we adopt  $(\frac{\mathcal{E}_T}{\mathcal{T}}, \frac{\mathcal{E}_J}{\mathcal{T}})$  as an approximate Nash equilibrium solution to 4.P2-B because of the bounds considered on packet error probability as was described earlier.

#### 4.4.4 Discussion: Impact of Retransmissions on System-Performance

Note that, at the equilibrium point, the objective functions of 4.P3-A and 4.P3-B are both functions of the receiver SINR,  $\frac{E_{T_i}^*}{N_0 + E_{J_i}^*}$ , at the  $i$ -th time instant. Upon substituting  $E_{T_i}^* = \frac{\mathcal{E}_T}{\mathcal{T}}$  and  $E_{J_i}^* = \frac{\mathcal{E}_J}{\mathcal{T}}$ , the overall receiver's SINR is given as follows.

$$\sum_{i=1}^{\mathcal{T}} \frac{E_{T_i}^*}{N_0 + E_{J_i}^*} = \mathcal{T} \frac{\frac{\mathcal{E}_T}{\mathcal{T}}}{N_0 + \frac{\mathcal{E}_J}{\mathcal{T}}} = \frac{\mathcal{E}_T}{N_0 + \frac{\mathcal{E}_J}{\mathcal{T}}}. \quad (4.15)$$

Note that the impact of jammer reduces significantly with increasing number of transmission attempts,  $\mathcal{T}$ . As  $\mathcal{T}$  tends to  $\infty$ , the jammer's energy has no absolute impact on the overall re-

ceiver's SINR. Thus, the proposed solution approach can be interpreted as a scheme that mitigates jamming attacks over time. The cost that the transmitter-receiver pair incurs, as a consequence of the mitigation scheme, is the latency involved in delivering DATA successfully with high probability. Therefore, such analysis when  $\mathcal{T}$  tends to  $\infty$  is neither realistic nor practical for the transmitter with a finite energy budget, while simultaneously being interested in guaranteeing a successful data transfer in as few transmissions attempts as possible. We will investigate this problem, as stated in 4.P1, in Section 4.5.

## 4.5 Minimization of the Number of Transmission Attempts for Successful Communication

Having analyzed 4.P2 and obtained the optimal energy allocation adopted by the transmitter and the jammer in Section 4.4 for a fixed number of transmission attempts, we now investigate 4.P1.

Since the maximum number of allowable transmission attempts,  $\mathcal{T}$ , is chosen at the transmitter, we relax  $p^*(\mathcal{T})$  using the upper-bound expression in Equation (4.7), similar to our analysis in Section 4.4.1. As a result, the relaxed expression is a lower bound on  $p^*(\mathcal{T})$  and it is denoted by  $p_L^*(\mathcal{T})$ . Then,

$$1 - \delta \leq p_L^*(\mathcal{T}) \leq p^*(\mathcal{T}) \text{ or } 1 - p_L^*(\mathcal{T}) \leq \delta \quad (4.16)$$

Applying logarithms on both sides, and substituting Equation (4.8), we have

$$\underbrace{\mathcal{T} \sqrt{\frac{\mathcal{E}_T}{N_0 \mathcal{T} + \mathcal{E}_J}} + 2\mathcal{T} \log \left( \frac{2}{K_2} \right) + 2 \log \delta}_{f(\mathcal{T})} \geq 0. \quad (4.17)$$

Taking the first order derivative of  $f(\mathcal{T})$  with respect to  $\mathcal{T}$  yields the following:

$$\frac{df(\mathcal{T})}{d\mathcal{T}} = \sqrt{\frac{\mathcal{E}_T}{N_0\mathcal{T} + \mathcal{E}_J}} \left( \frac{N_0\mathcal{T} + 2\mathcal{E}_J}{2(N_0\mathcal{T} + \mathcal{E}_J)} \right) + 2 \log\left(\frac{2}{K_2}\right) \quad (4.18)$$

where  $K_2$  is a small positive constant less than 1. In this case, we have  $\frac{df(\mathcal{T})}{d\mathcal{T}} \geq 0$ . Therefore,  $f(\mathcal{T})$  is a monotonically increasing function in  $\mathcal{T}$ . In other words, there exists a unique solution,  $\mathcal{T}^*$ , at which  $f(\mathcal{T}^*) = 0$ .

Next, we present simulation results on the optimal energy allocations to be adopted by both players at equilibrium and numerically find the optimal number of transmission attempts using a combination of bisection, secant, and inverse quadratic interpolation methods.

## 4.6 Numerical Results

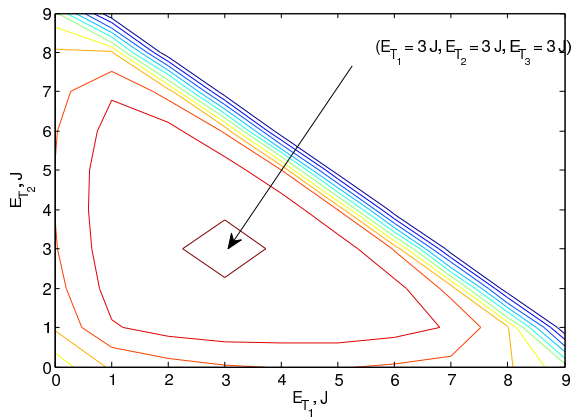


Fig. 4.3: Energy allocation of the transmitter when  $\mathcal{T} = 3$ .

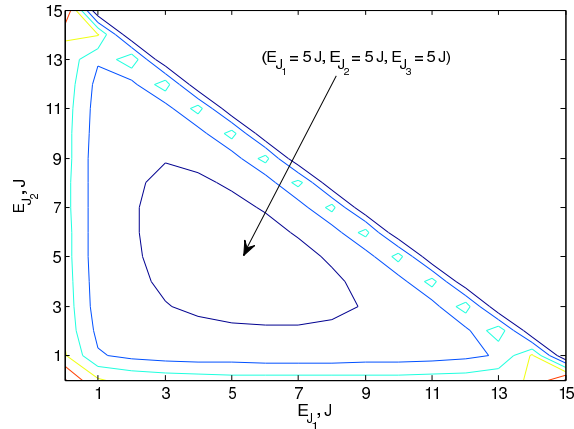


Fig. 4.4: Energy allocation of the jammer when  $\mathcal{T} = 3$ .

In this section, we assume  $N_0 = .5$  J/Hz and a jamming energy budget of 15 J to be efficiently distributed among  $\mathcal{T}$  transmission attempts which, in turn, is first assumed to be equal to 3 for simulation purposes. The transmitter's attempts to send DATA is also subject to a total energy budget of 9 J.

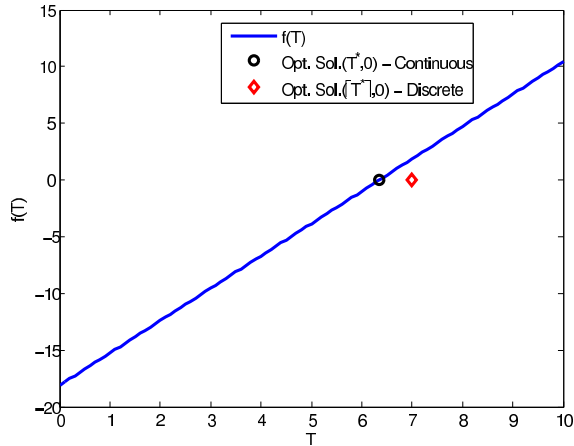


Fig. 4.5: The behavior of  $f(\mathcal{T})$  with respect to  $\mathcal{T}$ .

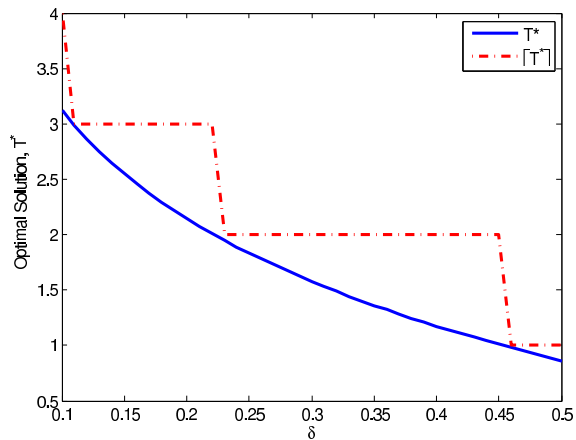


Fig. 4.6: The variation of  $\mathcal{T}^*$  with respect to  $\delta$ .

We numerically verify the saddle point at  $\{(3J,3J,3J),(5J,5J,5J)\}$  as an equilibrium solution by presenting the contour plots of the transmitter and the jammer energy allocations. This is demonstrated in Figs. 4.3 and 4.4 respectively, where it is clear that the transmitter adopts a uniform energy allocation  $(3J,3J,3J)$  as an optimal strategy in response to the jammer also uniformly allocating its energy according to  $(5J,5J,5J)$ .

In our problem formulation, we treat  $\mathcal{T}$  as the number of transmission attempts of a data packet (a discrete number). Thus, we denote the optimal solution of the relaxed problem of 4.P1 by  $\lceil \mathcal{T}^* \rceil$  for  $f(\lceil \mathcal{T}^* \rceil) < 0$  where  $\lceil \cdot \rceil$  and  $\lfloor \cdot \rfloor$  denote the *ceil* and *floor* functions that map a real number to the smallest following or the largest previous integer, respectively. In order to find the minimum value of  $\mathcal{T}$  that satisfies the relaxed constraint in 4.P1, we first numerically plot Equation (4.17) with respect to increasing values of  $\mathcal{T}$  to show that  $f(\mathcal{T})$  is a monotonically increasing function and admits a unique solution at  $f(\mathcal{T}^*) = 0$ . This is clearly shown in Fig. 4.5 where the optimal number of transmission attempts is equal to 7 ( $\lceil \mathcal{T}^* \rceil = 7$ ) for  $\delta = 0.01$ .

It is known that the number of retransmissions of a data packet decreases as  $\delta$  increases ( $1 - \delta$  decreases). This is clearly shown in Fig. 4.6 where we plot the optimal number of transmission attempts with respect to increasing values of  $\delta$ . This result is intuitive in the sense that a transmitter requires a lower number of retransmissions when the constraint on probability of successful reception at the receiver is less stringent and vice versa.

## 4.7 Summary

We presented an approximate minimum-latency analysis of ARQ-based wireless P2P communication links with perfect feedback channels and ISI in the presence of a jammer. We also proved that the optimal energy allocation is uniform across the transmission attempts. Furthermore, we provided an algorithmic solution to find the minimum latency that is required in order to guarantee a prescribed performance at the receiver.

In this chapter, the design and performance of ARQ protocols were investigated in the presence of a strategic jammer. Motivated by the famous Colonel-Blotto model [73], we propose to investigate another jamming interference mitigation technique using power allocation in future work.

# CHAPTER 5

## MITIGATION OF JAMMING INTERFERENCE VIA A STRATEGIC POWER ALLOCATION

With the open nature of the DSA paradigm, less restrictions are imposed on spectrum access. This not only results in competition for spectrum among SUs [25], but also makes such networks highly susceptible to jamming interference created by jammers.

In this chapter, we consider the competitive interactions between an SU transmitter-receiver pair and a jammer under physical interference restrictions e.g., a minimum SINR, power budget constraints, and incomplete knowledge of the channel gains. This can be formulated as a power allocation game between the SU and the jammer, which is considered a game with incomplete information (i.e., of Bayesian nature according to Harsanyi's observation [44]). Note that these interactions between the SU and the jammer over a set of channels are analogous to the interactions between two colonels over a set of battlefields in a Colonel Blotto game [73].

### 5.1 Literature Review

There exists vast literature on the design and analysis of dynamic spectrum sharing, some of which has investigated power allocation games in the presence of a jammer [10, 38, 46, 77, 78, 94, 96, 99].



The authors investigate equilibrium points in the form of pure strategies [10,46,77,78,99] as well as mixed strategies [94,96] and examine optimal power allocations that maximize the utility functions defined. Under the assumption of full knowledge of the system, the authors in [10] formulate a zero-sum power allocation game between a transmitter and a jammer and prove the existence of pure strategy NE points and characterize them in the form of optimized secrecy capacity in the presence of a passive eavesdropper. In [99], the authors study a defense strategy against a jamming attack in which a smart jammer quickly learns the transmission strategy of the user and, adaptively, adjusts its transmission strategy so as to maximize the damage. The authors model the problem as a complete and perfect information Stackelberg game where the user behaves like a foresighted player (leader) and the jammer (follower) plays its optimal strategy given the leader's strategy. In [77], the authors consider game theoretic models of wireless medium access control (MAC) in which each transmitter makes individual decisions regarding their power level or transmission probability. The authors investigate NE points for MAC Bayesian and MAC dynamic repeated games and consider incomplete information regarding the users' types. In [78], the authors consider stochastically varying packet traffic and evaluate the effects of traffic uncertainty on jamming attacks. In order to study the conflicting interests of selfish transmitters and malicious jammers, they consider a model in which transmitters and jammers play a non-cooperative game of optimizing their individual performance objectives. The authors evaluate the NE strategies of the resulting games when different levels of queue state information are available to jammers. The authors in [46] consider a jamming game in which a malicious user tries to jam the transmissions of a user over multiple channels with Gaussian fading. Having complete information of the game, both players allocate power based on the obtained minimax solution to multiple channels with their total power constraints in order to maximize their utilities.

Different from pure strategy solutions, the authors in [94] investigate an anti-jamming defense mechanism in a CRN by means of random power allocation while considering SINR constraints at the receiver. In fact, the authors in [94] formulate the random power allocation problem as a Colonel Blotto game [73] with perfect and complete information, and derive the equilibrium

strategy in terms of the probability distribution of allocated power. The defense strategy obtained in [94] from the equilibrium minimizes the worst-case damage caused by the jammer. In [96], the authors apply prospect theory to analyze anti-jamming communications in CRNs from a user-centric viewpoint. As a matter of fact, they formulate the interactions between a smart jammer and an SU with mixed transmission strategies and apply weighting functions to model the subjectivity of both players in the transmission. Gao *et al.* in [38] investigate the interaction between a statistical multiple-input multiple-output (MIMO) radar and an intelligent target equipped with a jammer. They consider a two-person zero-sum game and a Bayesian game to model the adversarial interaction where assumptions of complete and incomplete information are considered respectively. The utility functions are formulated based on the mutual information and the equilibria to these two games in the form of mixed strategies are derived.

Optimal power control approaches have also been examined using learning mechanisms and classical optimization techniques instead of using game theory. Wang *et al.*, in [89], consider the interactions between an adaptive jammer and a user from a non-game theoretical perspective to study the joint control of transmission power and channel switching. As a matter of fact, the authors adopt an online learning perspective to model the reasoning of the attacker as well as the defender in order to develop an explicit form of optimal power control when the user is aware of the type of learning algorithm used by the jammer and when it has no such information and, thus, also tries to learn the jammer's strategies. In [84], the authors investigate the design of an adversary with optimal power allocation for spoofing and jamming under a Rayleigh fading channel. Assuming that the adversary has full knowledge of the SU system, the authors determine a worst-case optimal energy allocation for spoofing and jamming that the SU adopts using classical optimization techniques. Furthermore, Bayram *et al.* in [11] determine the optimum power allocation policy for an average power constrained jammer operating over an arbitrary additive noisy channel and fully adaptive receiver. They show that the optimum jamming performance can be achieved via power randomization between at most two different power levels.

## 5.2 Motivation, Novelty, and Contributions

Although numerous aspects of the jamming problem have been investigated when it comes to power allocation, the authors have considered rather ideal and/or impractical scenarios or even non-optimal ones by: i) focusing only on games that have a pure strategy solution [10,46,77,78,99], ii) assuming complete information of the system in their equilibrium analysis [10,46,94,99], iii) considering a descriptive system model in which it tries to model real-life choices rather than optimal ones [96], or iv) presenting the jammer as a non-strategic user in the network [11,89]. These drawbacks, to a large extent, limit the practicality and applicability of any spectrum sharing protocol that takes the malicious intent of a rational user into consideration. It should also be pointed out that there exist in the literature works on jamming that study practical problems related to the detection or mitigation of jamming attacks in the context of Bayesian games [23,91]. However, they do not investigate the interactions between players in terms of optimal power allocations, which is an effective technique to mitigate jamming attacks. Specifically, the authors in [91] formulate a malicious node detection game and a post-detection game to isolate it in wireless networks. Furthermore, in [23], the authors focus on mitigating the jammer's effect through channel hopping and power alteration from a predefined set. In this chapter, we address the aforementioned limitations of past works on power allocation games with regards to: i) the system model, ii) the channel model, and iii) the level of information available to each player. Therefore, we not only generalize past works in terms of the solution space we obtain (e.g., pure strategy is a special case of mixed strategy), but also make it applicable to more practical scenarios.

In a nutshell, the main contributions of this chapter are summarized as follows:

- We formulate the power allocation problem over multiple orthogonal channels at both the SU and the jammer as one-shot Bayesian games under different channel scenarios, where both the SU and the jammer have incomplete information regarding channel gains.
- We compute the NE for these Bayesian games by finding the optimal mixed strategy (probability distributions) power allocations at both the SU and the jammer. In particular, we

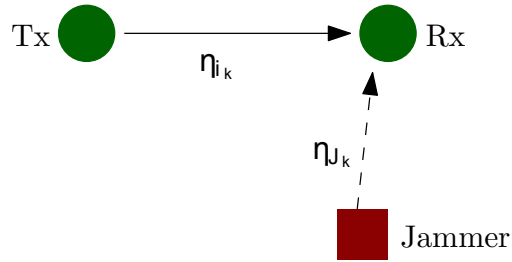


Fig. 5.1: A CRN with one SU Tx-Rx pair in the presence of a jammer.

consider two practical channel models as examples, namely multi-path fading model and the path-loss model, and study their impact on the NE in order to get practical insights of our proposed framework.

- We address different incomplete information settings based on the level of knowledge available at each player, including uncertainties regarding instantaneous channel gains as well as uncertainties associated with spectrum sensing. Such an analysis spans a wide range of practical scenarios from worst-case to real-world performance.
- We present simulation results that corroborate our theoretical results as well as provide insights into the dynamics of the strategic power allocation problem and its equilibrium.

### 5.3 System Model and Problem Formulation

We consider a single-hop CRN model comprising of an SU transmitter-receiver pair and a jammer as shown in Fig. 5.1. The SU<sup>1</sup>, equipped with a multi-channel radio consisting of  $H$  orthogonal channels that are independent and available<sup>2</sup>, is subject to a power budget  $P$  and is assumed to transmit different messages over the channels. These messages experience different channel-independent and channel-dependent physical phenomena that may be deterministic or random

<sup>1</sup>The term SU is used to denote an SU transmitter-receiver pair.

<sup>2</sup>This assumption is valid since the Federal Communication Commission (FCC) has mandated the existence of a database in which all licensed frequency bands are registered. In this respect, through an incorporated geo-location capability for example, the SU can access this database and acquire information about which frequencies are available and which are not [Second Memorandum Opinion and Order, 174 FCC (2010)].

(e.g., propagation losses, fading, and so forth). We write the signal's received power as follows.

$$p_{r_k} = p_{i_k} \eta_{i_k}, \quad (5.1)$$

where  $p_{r_k}$  is the power received at the intended receiver over a given channel  $k$ ,  $p_{i_k}$  is the transmitting power of the SU on the  $k$ -th channel, and  $\eta_{i_k}$  represents the  $k$ -th channel gain. The SINR condition for successful reception at the SU's receiver is, thus, given by:

$$\frac{p_{i_k} \eta_{i_k}}{N_0 + p_{J_k} \eta_{J_k}} \geq \beta, \quad (5.2)$$

where  $N_0$  is the variance of the additive noise and assumed to be the same for all the channels,  $p_{J_k}$  is the jamming power on the  $k$ -th channel,  $\eta_{J_k}$  represents the gain of channel  $k$  between the jammer and the SU's receiver, and  $\beta$  denotes the minimum required SINR to declare a successful reception at the SU's receiver. We model the SU's payoff per channel as an indicator function whose value of 1 denotes a successful reception. Accordingly, the SU's payoff is defined as the number of SU's successful receptions over  $N$  available channels, i.e.,

$$\mathcal{U}_i = \sum_{k=1}^H \mathbb{1}\left\{\frac{p_{i_k} \eta_{i_k}}{N_0 + p_{J_k} \eta_{J_k}} \geq \beta\right\}, \quad (5.3)$$

where  $\mathbb{1}\{\cdot\}$  is the indicator function.

On the other hand, the jammer, with a jamming power budget  $J$ , is assumed to be more powerful ( $J \geq P$ ) and is interested in sabotaging the SU's transmissions over  $H$  channels by adopting a power allocation strategy so that the condition in (5.2) is not satisfied. Hence, we quantify the jammer's payoff over channel  $k$  as an indicator function whose value of 1 denotes an unsuccessful SU's reception and, accordingly, write the attacker's payoff as:

$$\mathcal{U}_J = \sum_{k=1}^H \mathbb{1}\left\{\frac{p_{i_k} \eta_{i_k}}{N_0 + p_{J_k} \eta_{J_k}} < \beta\right\}. \quad (5.4)$$

From (5.3) and (5.4), it is evident that a player's payoff is dependent on its own choice of power and that of the opponent's over the channels of interest in addition to  $\eta_{i_k}$  and  $\eta_{J_k}$ . This is the main reason we employ game theory as a tool to solve the strategic one-shot power allocation problem at hand. In this chapter, mixed strategies are investigated. Therefore, both players model the power to be allocated over each channel (e.g.,  $p_{i_k}$  and  $p_{J_k}$ ) as a random variable whose distribution is to be determined. At this point, it is important to mention that this game is similar to the Colonel Blotto game in [73] where two colonels distributively allocate their troops in a strategic manner over a set of battlefields.

Furthermore, knowledge regarding the channel gains, in practice, may vary among users (players) in the network. A player may have complete or incomplete information of any element of the game's characteristic function. In this chapter, we consider a power allocation problem between the SU transmitter and the jammer in the most general sense in which we assume that both players have incomplete information.

In this problem formulation, both players are assumed to have incomplete information of the channel gains in the power allocation game. In other words, the SU is assumed to have incomplete knowledge of  $\eta_{J_k}$  for all  $k$  and, therefore, treats it as a random variable with an arbitrary probability density function (pdf). Similarly, we assume that the jammer has incomplete knowledge of  $\eta_{i_k}$  for all  $k$  and also treats it as a random variable with an arbitrary pdf.

Given this framework, the SU's expected utility,  $\bar{U}_i$ , to be maximized is written as follows.

$$\begin{aligned}\bar{U}_i &= \sum_{k=1}^H \int_0^\infty Pr \left( x \geq \underbrace{\frac{\beta}{\eta_{i_k}} (N_0 + p_{J_k} \eta_{J_k})}_{\mathcal{I}_k} \right) dF_{p_{i_k}}(x) \\ &= \sum_{k=1}^H \int_0^\infty F_{\mathcal{I}_k}(x) dF_{p_{i_k}}(x),\end{aligned}\tag{5.5}$$

where  $\eta_{J_k}$  is the  $k$ -th channel gain between the jammer and the SU receiver that is unknown to the SU transmitter who, in turn, treats it as a random variable with an arbitrary pdf,  $f_{\eta_{J_k}}$ . Also,  $p_{i_k}$  and  $p_{J_k}$  are two random variables with  $F_{p_{i_k}}$  and  $F_{p_{J_k}}$  as their corresponding Cumulative Distribution

Functions (CDFs) respectively. In a similar manner, the jammer's expected utility is given by:

$$\bar{U}_J = \sum_{k=1}^H \int_{\beta N_0}^{\infty} F_{\mathcal{P}_k}(I) dF_{\mathcal{S}_k}(I), \quad (5.6)$$

where  $\mathcal{P}_k = p_{i_k} \eta_{i_k}$ ,  $\eta_{i_k}$  is the  $k$ -th channel gain that is assumed to be unknown to the jammer and  $\mathcal{S}_k = \beta(N_0 + p_{J_k} \eta_{J_k})$ . The power allocation game, at hand in this case, between the SU and the jammer involves the solution of two optimization problems – one from the SU's perspective and another from the jammer's perspective.

## SU's Perspective

Find the optimal marginal CDF,  $F_{p_{i_k}}$  for all  $k$ , such that:

$$\begin{aligned} & \underset{\{F_{p_{i_k}}\}_{k=1}^H}{\text{maximize}} && \sum_{k=1}^H \int_0^{\infty} F_{\mathcal{I}_k}(x) dF_{p_{i_k}}(x) \\ & \text{subject to:} && \sum_{k=1}^H \int_0^{\infty} x dF_{p_{i_k}}(x) \leq P \end{aligned} \quad (5.P1)$$

## Jammer's Perspective

Find the optimal marginal CDF,  $F_{p_{J_k}}$  for all  $k$ , such that:

$$\begin{aligned} & \underset{\{F_{p_{J_k}}\}_{k=1}^H}{\text{maximize}} && \sum_{k=1}^H \int_{\beta N_0}^{\infty} F_{\mathcal{P}_k}(I) dF_{\mathcal{S}_k}(I) \\ & \text{subject to:} && \sum_{k=1}^H \int_{\beta N_0}^{\infty} I dF_{\mathcal{S}_k}(I) \leq \beta(HN_0 + J\eta_{J_k}) \end{aligned} \quad (5.P2)$$

The determination of both players' optimal marginal strategies are dependent on the choice of  $f_{\eta_{i_k}}$  and  $f_{\eta_{J_k}}$ . Therefore, in order to solve for the equilibria points of this power allocation game,  $f_{\eta_{i_k}}$  and  $f_{\eta_{J_k}}$  need to be known.

At this point, it is important to mention that other scenarios, that depend on which player the element of uncertainty arises at, can also be studied. For example, a special case of the aforemen-

tioned scenario is when both players are assumed to have complete information of channel gains in the game. This framework was investigated in [94] where the authors studied the attack and defense strategies of the jammer and the SU respectively in the form of power allocations. They showed that the strategies of both players should be randomized. They also derived the NE for this game. For more details on this framework in terms of problem formulation and analysis, we refer the reader to [94]. There also exists an SU-worst case scenario where only the SU has incomplete information in the power allocation game [26]. Note that, in this particular case, the equilibrium analysis and the derivation of the optimal marginal distributions for both players can be derived from those of the general case we investigate next.

## 5.4 Equilibrium Analysis: Channels are available

In this section, we consider the general problem framework given in Section 5.3 and analyze the average performances from the SU's and the jammer's perspectives based on their incomplete knowledge of the channel gains in the power allocation game,  $\eta_{J_k}$  and  $\eta_{i_k}$ , respectively.

It is critical, however, to define and characterize the NE of the game to be analyzed in the form of mixed strategies [62] as a pure strategy NE may not exist in general in games of allocative strategic mismatch. For example, in Colonel Blotto [73], a pure strategy NE does not exist when  $\frac{X_B}{H} < X_A \leq X_B$  where  $X_A$  and  $X_B$  denote the troop forces of colonels  $A$  and  $B$  respectively. It has also been shown that a pure strategy NE trivially exists only when  $X_A \leq \frac{X_B}{H}$ , which means that Colonel  $B$  wins all of the battlefields. In this chapter, we assume that the jammer's power budget is larger than the transmitter's power budget, i.e.,  $P \leq J$ . Furthermore, it can be noted that the scenario when  $P \leq \frac{J}{H}$  is trivial because any transmitter's power allocation strategy in this case is defeated by the jammer, and is thus ignored in this chapter. Hence, we investigate optimal power allocations in the form of mixed strategy solutions.

At this point, it is important to recall that the reason behind formulating the problem as a Bayesian game lies in the basic definition of Bayesian games as a model of interactive decision



situations in which each player has only partial information about the payoff relevant parameters of a given situation. In this respect, a player who has only partial knowledge about the state of nature is assumed to have some beliefs, namely prior distributions, about the parameters which he does not know or he is uncertain about. For more information on Bayesian games and their equilibrium analysis, we refer the reader to [44, 62].

**Definition 5.1** (Bayesian NE). *A strategy  $(F_i, F_J) \in \mathcal{S}$  is a Bayesian Nash Equilibrium for the game if and only if:*

$$\bar{U}_i(F_i, F_J) \geq \bar{U}_i(\hat{F}_i, F_J), \forall \hat{F}_i \in \{\mathcal{S}\}/F_i$$

$$\bar{U}_J(F_i, F_J) \geq \bar{U}_J(F_i, \hat{F}_J), \forall \hat{F}_J \in \{\mathcal{S}\}/F_J$$

where  $(F_i, F_J) = \left( (F_{p_{i_1}}, \dots, F_{p_{i_H}}), (F_{p_{J_1}}, \dots, F_{p_{J_H}}) \right)$  is a pair of  $H$  marginal distributions that maximize the players' expected utility function, e.g.,  $\bar{U}_i$ , from which no player can unilaterally deviate to increase its payoff.

At equilibrium,  $F_i$  and  $F_J$  respectively denote the SU and the jammer optimal power distributions. In order to solve for these optimal distributions, we recall that the SU is assumed to be uncertain of  $\eta_{J_k}$  and the jammer to be uncertain of  $\eta_{i_k}$ . In this regard, both the SU and the jammer employ probability distributions to model the uncertainties regarding the channel gains and, eventually, obtain closed form expressions of the marginal distributions.

### 5.4.1 Solution of 5.P1

In order to maximize the SU's expected utility, we apply the Karush-Kuhn-Tucker (KKT) method to the optimization problem, defined in 5.P1 of Section 5.3, according to:

$$\bar{U}_i = \sum_{k=1}^H \int_0^\infty (F_{\mathcal{I}_k}(x) - \lambda_i x) dF_{p_{i_k}}(x) + \lambda_i P, \quad (5.7)$$

where  $\lambda_i$  is the KKT multiplier involved in maximizing the SU's expected utility.

**Theorem 5.1.** *The optimal marginal CDF,  $F_{p_{J_k}}$ , of the jammer's allocated power over channel  $k$  is given by:*

$$F_{p_{J_k}}(y) = \lambda_i \beta (N_0 + y\eta_{J_k}) \mathbb{E} \left[ \frac{1}{\eta_{i_k}} \right], \quad (5.8)$$

for  $y \in \left[ 0, \left( \frac{1}{\beta \lambda_i \mathbb{E} \left[ \frac{1}{\eta_{i_k}} \right]} - N_0 \right) / \eta_{J_k} \right]$  and  $k = \{1, 2, \dots, H\}$ .  $F_{p_{J_k}}$  admits a discontinuity point at 0 with mass point  $\lambda_i \beta N_0 \mathbb{E} \left[ \frac{1}{\eta_{i_k}} \right]$ .

*Proof.* The SU's power per frequency band is lower bounded by  $\frac{\beta N_0}{\eta_{i_k}}$  when the jammer does not attempt to block SU transmissions and upper bounded by  $1/\lambda_i$  knowing  $F_{\mathcal{I}_k}(x) - \lambda_i x \geq 0$ . So, in order for the SU to have a successful communication session,  $x \in \left[ \frac{\beta N_0}{\eta_{i_k}}, \lambda_i^{-1} \right]$  as the jammer cannot allocate a negative power for  $x < \frac{\beta N_0}{\eta_{i_k}}$ . In other words,  $\left[ \frac{\beta N_0}{\eta_{i_k}}, \lambda_i^{-1} \right]$  dominates  $\left[ 0, \frac{\beta N_0}{\eta_{i_k}} \right) \cup (\lambda_i^{-1}, P]$ .

Since we are considering the mixed strategy space knowing that a player is indifferent over choosing an action among its strategies, we have  $F_{\mathcal{I}_k}(x) - \lambda_i x = c$  where  $c$  is a positive constant. For  $x = \lambda_i^{-1}$ ,  $F_{\mathcal{I}_k}(\lambda_i^{-1}) = c + 1$ . Knowing  $F_{\mathcal{I}_k}$  is a CDF admitting a maximum of 1, we have  $c = 0$ . Thus,  $F_{\mathcal{I}_k}(x) = \lambda_i x$  is obtained.

Next, we find the marginal CDF that models the jammer's allocated power over channel  $k$  for a given realization of the unknown random channel gain between the SU's transmitter and receiver,  $\eta_{i_k} = \eta$ .

$$\begin{aligned} F_{p_{J_k}}(y|\eta_{i_k} = \eta) &= Pr(\mathcal{I}_k \leq \frac{\beta}{\eta}(N_0 + y\eta_{J_k})|\eta_{i_k} = \eta) \\ &= \frac{\lambda_i \beta}{\eta} (N_0 + y\eta_{J_k}). \end{aligned} \quad (5.9)$$

Accordingly, the jammer's strategy is given by,

$$F_{p_{J_k}}(y|\eta_{i_k}) = \frac{\lambda_i \beta}{\eta_{i_k}} (N_0 + y\eta_{J_k}). \quad (5.10)$$

However, since there is uncertainty regarding the gains, to characterize the jammer's strategy at

equilibrium,  $F_{p_{J_k}}$  is shown below as

$$\begin{aligned} F_{p_{J_k}}(y) &= \int_{\eta} F_{p_{J_k}}(y|\eta_{i_k} = \eta) f_{\eta_{i_k}}(\eta) d\eta \\ &= \lambda_i \beta (N_0 + y\eta_{J_k}) \mathbb{E} \left[ \frac{1}{\eta_{i_k}} \right], \end{aligned} \quad (5.11)$$

where, in this case,  $f_{\eta_{i_k}}$  is the pdf that the jammer assumes to govern  $\eta_{i_k}$ ,  $y \in \left[ 0, \left( \frac{1}{\beta \lambda_i \mathbb{E}[\frac{1}{\eta_{i_k}}]} - N_0 \right) / \eta_{J_k} \right]$ , and  $\mathbb{E}[\cdot]$  represents the expectation. Also,  $F_{p_{J_k}}$  admits a discontinuity point at 0 with mass point  $\lambda_i \beta N_0 \mathbb{E}[\frac{1}{\eta_{i_k}}]$ .  $\square$

## 5.4.2 Solution of 5.P2

In order to maximize the expected utility of the jammer, the KKT multipliers approach is employed in 5.P2. In this respect, we write the following:

$$\begin{aligned} \bar{u}_J &= \sum_{k=1}^H \int_{\beta N_0}^{\infty} (F_{p_k}(I) - \lambda_J I) dF_{S_k}(I) \\ &\quad + \lambda_J \beta (HN_0 + J\eta_{J_k}), \end{aligned} \quad (5.12)$$

where  $\lambda_J$  is the KKT multiplier that is to be determined.

**Theorem 5.2.** *The optimal marginal CDF,  $F_{p_{i_k}}$ , of the SU's allocated power over channel  $k$  is given by:*

$$F_{p_{i_k}}(x) = 1 - \lambda_J \left( \frac{1}{\lambda_i} - x \right) \eta_{i_k}, \quad (5.13)$$

for  $x \in \left[ \frac{\beta N_0}{\eta_{i_k}}, \lambda_i^{-1} \right]$  for  $k = \{1, 2, \dots, H\}$ .  $F_{p_{i_k}}$  admits a discontinuity point at  $\frac{\beta N_0}{\eta_{i_k}}$  with mass point  $\lambda_J \beta N_0 + 1 - \lambda_J \lambda_i^{-1} \eta_{i_k}$ .

*Proof.* The interference power per frequency band,  $S_k = \beta(N_0 + p_{J_k} \eta_{J_k})$  is lower bounded by  $\beta N_0$  when the jammer does not attempt to block SU transmissions and, otherwise, upper bounded by  $1/\lambda_J$  knowing the expected utility is a positive quantity.

$F_{\mathcal{P}_k}(I) - \lambda_J I = c$  in the range over which  $I$  is defined and  $c$  is a positive constant. This is because the player is indifferent over choosing any of its strategies over the range of  $I$ . At the same time,  $F_{\mathcal{P}_k}(I) - \lambda_J I \neq 0$  for the value of  $F_{\mathcal{P}_k}(I) - \lambda_J I$  is influenced by the relation between the upper limits of both random variables  $\mathcal{P}_k$  and  $\mathcal{S}_k$ ,  $\eta_{i_k} \lambda_i^{-1}$  and  $\lambda_J^{-1}$  respectively. In this framework, we assume that the jammer is superior to the SU in terms of power at the receiver side. In other words, we assume  $\frac{1}{\lambda_J} \geq \frac{\eta_{i_k}}{\lambda_i}$ . In this case, it is obvious that  $F_{\mathcal{P}_k}(\eta_{i_k} \lambda_i^{-1}) - \lambda_J \eta_{i_k} \lambda_i^{-1} = c$ . Then,  $c = 1 - \lambda_J \eta_{i_k} \lambda_i^{-1}$ . Accordingly, we write  $F_{\mathcal{P}_k}(I) = \lambda_J I + 1 - \lambda_J \eta_{i_k} \lambda_i^{-1}$ . With a simple change of notation  $x = I$ , we have  $F_{\mathcal{P}_k}(x) = \lambda_J x + 1 - \lambda_J \eta_{i_k} \lambda_i^{-1}$ .

Accordingly, we obtain the optimal marginal CDF that models the SU allocated power over channel  $k$  as follows:

$$\begin{aligned}
F_{\mathcal{P}_{i_k}}(x) &= Pr(\mathcal{P}_k \leq x \eta_{i_k}) \\
&= F_{\mathcal{P}_k}(x \eta_{i_k}) \\
&= \lambda_J x \eta_{i_k} + 1 - \lambda_J \eta_{i_k} \lambda_i^{-1} \\
&= 1 - \lambda_J \left( \frac{1}{\lambda_i} - x \right) \eta_{i_k}, \tag{5.14}
\end{aligned}$$

where  $x \in [\frac{\beta N_0}{\eta_{i_k}}, \lambda_i^{-1}]$  for  $k = \{1, 2, \dots, N\}$ . Note that  $F_{\mathcal{P}_{i_k}}$  admits a discontinuity point at  $\frac{\beta N_0}{\eta_{i_k}}$  with mass point  $\lambda_J \beta N_0 + 1 - \lambda_J \lambda_i^{-1} \eta_{i_k}$ .  $\square$

## 5.5 Optimal Power Allocation for Different Instantiations and Knowledge Level

So far, the optimal marginal CDFs have been derived for both players given their power budget constraints as presented earlier in 5.P1 and 5.P2. However, they are dependent on KKT multipliers which, in turn, depend on the probability distributions that the players assume to model their incomplete information and need to be evaluated.

At this point, it is important to mention that the KKT multipliers are computed by substituting

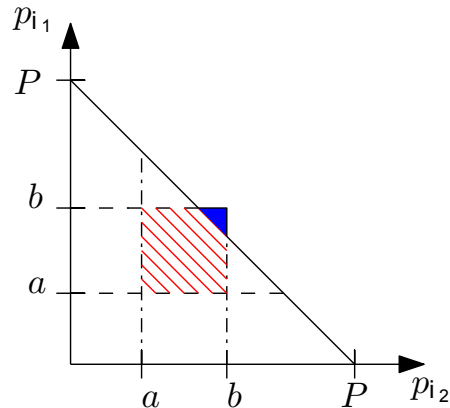


Fig. 5.2: [a, b] presents the support over which the marginal CDFs of the SU are defined when  $H = 2$  in the absence of a power budget. The red-shaded region denotes all power allocations of the SU that satisfy a power budget  $P$ , if it exists. The blue region, on the other hand, corresponds to those allocations that don't. Solving for KKT multipliers in the power budget will guarantee the existence of a power allocation strategy that always lies in the red shaded region.

each player's optimal marginals, obtained in Section 5.4, in the corresponding power budgets. This will guarantee that a player's power allocation strategy will satisfy its power budget constraint on an average. Hence, the marginal distributions we obtain for each player from solving the corresponding optimization problem constitute its equilibrium strategy.

For the sake of illustration, we consider a specific example of the scenario in Section 5.3 where we study the competitive interactions between the SU and the jammer over two independent and orthogonal channels, i.e.,  $H = 2$ . In this case,  $((F_{p_{i_1}}, F_{p_{i_2}}), (F_{p_{j_1}}, F_{p_{j_2}}))$  is a pair of 2 marginal distributions that maximize each player's expected utility function. This represents our mixed strategy NE as long as the power budget constraint for each player is satisfied. In order to clarify our point, we pictorially illustrate this observation in Fig. 5.2.

Next, we consider two different instantiations of the channel gains for the general scenario analyzed earlier in this chapter and the SU-worst case scenario where the jammer is put at an advantage. Depending on the probability distributions that players in the game of each scenario assume to model their uncertainties regarding the gains of the channels, we compute KKT multipliers and evaluate equilibrium solutions accordingly.

### 5.5.1 Multi-path Fading Model with Incomplete Knowledge of Channel Gains

In a wireless communication system, a signal can travel from the transmitter to receiver over multiple reflective paths; this phenomenon is referred to as multi-path propagation. The effect can cause fluctuations in the received signal's amplitude, phase, and angle of arrival, causing multi-path fading. In this case,  $\eta_{i_k}$  in (5.1) is given by:

$$\eta_{i_k} = h_k^2, \quad (5.15)$$

where  $h_k$  is a real value that denotes the fading gain of the  $k$ -th channel between the SU transmitter and its receiver. Similarly, we write  $\eta_{J_k}$  according to:

$$\eta_{J_k} = g_k^2, \quad (5.16)$$

where  $g_k$  is a real value that denotes the fading gain of the  $k$ -th channel between the jammer and the SU receiver. Note that the gains of the channels need not necessarily be real in general.

In this subsection, the jammer is assumed to have incomplete knowledge of  $h_k$  for all  $k$  and, therefore, treats it as a random variable with an arbitrary pdf  $f_{h_k}$ . Similarly, we assume that the SU has incomplete knowledge of  $g_k$  for all  $k$  and treats it as a random variable with an arbitrary pdf  $f_{g_k}$ . Accordingly, we rewrite the jammer's marginal distribution at equilibrium according to:

$$F_{p_{J_k}}(y) = \lambda_i \beta (N_0 + y g_k^2) \mathbb{E} [h_k^{-2}], \quad (5.17)$$

where, in this particular case, the range over which  $y$  varies is  $\left[0, \left(\frac{1}{\beta \lambda_i \mathbb{E}[h_k^{-2}]} - N_0\right) / g_k^2\right]$ . Note that  $F_{p_{J_k}}$  admits a discontinuity point with mass point  $\lambda_i \beta N_0 \mathbb{E} [h_k^{-2}]$  at 0. In a similar fashion, the SU's marginal distribution at equilibrium is written as follows:

$$F_{p_{i_k}}(x) = 1 - \lambda_J \left(\frac{1}{\lambda_i} - x\right) h_k^2. \quad (5.18)$$

where, in this case,  $x$  is defined over  $[\frac{\beta N_0}{h_k^2}, \lambda_i^{-1}]$ . Also, note that  $F_{p_{i_k}}$  admits a discontinuity point at  $\frac{\beta N_0}{h_k^2}$  with mass point  $\lambda_J \beta N_0 + 1 - \lambda_J \lambda_i^{-1} h_k^2$ .

The evaluation of KKT parameters is provided next for a given  $f_{h_k}$  and  $f_{g_k}$ .

In this subsection, we highlight the analysis and the results of the power allocation game presented earlier by evaluating the KKT parameters. Without loss of generality, we consider a particular example in which we assume that  $h_k \sim \text{Rayleigh}(\sigma_1)$  and  $g_k \sim \text{Rayleigh}(\sigma_2)$  where  $\sigma_1$  and  $\sigma_2$  are the scale parameters of the distributions and they are strictly positive. Accordingly, we obtain  $h_k^{-2}$  and  $g_k^{-2}$  and observe that they follow an inverse Gamma distribution for which the means are not defined. Thus, for the sake of making the problem tractable, we use Jensen's Inequality to write  $\mathbb{E}[\frac{1}{h_k^2}] \geq \frac{1}{\mathbb{E}[h_k^2]} = \frac{1}{2\sigma_1^2}$  and obtain a lower bound on the jammer's optimal power strategy. That said, we rewrite (5.17) as follows:

$$F_{p_{j_k}}(y) = \frac{\lambda_i \beta}{2\sigma_1^2} (N_0 + y g_k^2). \quad (5.19)$$

**Lemma 5.1.** *Given  $h_k$  and  $g_k$  follow Rayleigh distributions with  $\sigma_1$  and  $\sigma_2$  respectively, then the KKT parameters are given as follows:*

$$\lambda_i = \frac{2\beta N_0 + \frac{2}{H}\beta g_k^2 J - \sqrt{[\frac{2}{H}\beta g_k^2 J] [4\beta N_0 + \frac{2}{H}\beta g_k^2 J]}}{\frac{(\beta N_0)^2}{\sigma_1^2}}, \quad (5.20)$$

and

$$\lambda_J = \frac{\frac{P}{H}}{\frac{\beta N_0}{h_k^2} + \frac{h_k^2}{2} \left( \left( \frac{1}{\lambda_i} \right)^2 - \left( \frac{\beta N_0}{2\sigma_1^2} \right)^2 \right)}. \quad (5.21)$$

*Proof.* The necessary slackness condition of the KKT multiplier method with positive parameters results in  $\sum_{k=1}^H \int_y y dF_{p_{j_k}}(y) = J$ . In order to find  $\lambda_i$ , solving the latter yields the following quadratic equation,

$$\frac{(\beta N_0)^2}{2\sigma_1^2} \lambda_i^2 - [2\beta N_0 + \frac{2}{H}\beta g_k^2 J] \lambda_i + 2\sigma_1^2 = 0, \quad (5.22)$$

with a discriminant  $\Delta = [\frac{2}{H}\beta g_k^2 J] [4\beta N_0 + \frac{2}{H}\beta g_k^2 J]$ . It is clear that  $\Delta > 0$ . Therefore, (5.22) admits two real roots,  $\lambda_{i,2}$ , such that:

$$\lambda_{i,2} = \frac{2\beta N_0 + \frac{2}{H}\beta g_k^2 J \pm \sqrt{\Delta}}{\frac{(\beta N_0)^2}{\sigma_1^2}}. \quad (5.23)$$

But, we need  $\frac{1}{\lambda_i} \geq \frac{\beta N_0}{2\sigma_1^2}$ , then

$$\lambda_i = \frac{2\beta N_0 + \frac{2}{H}\beta g_k^2 J - \sqrt{\Delta}}{\frac{(\beta N_0)^2}{\sigma_1^2}}. \quad (5.24)$$

In a similar fashion, we find  $\lambda_J$  according to:

$$\lambda_J = \frac{\frac{P}{H}}{\frac{\beta N_0}{h_k^2} + \frac{h_k^2}{2} \left( \left( \frac{1}{\lambda_i} \right)^2 - \left( \frac{\beta N_0}{2\sigma_1^2} \right)^2 \right)}, \quad (5.25)$$

where, due to the SU incomplete knowledge of  $g_k$ ,  $\lambda_i$  in (5.25) is given by:

$$\lambda_i = \frac{2\beta N_0 + \frac{4}{H}\beta\sigma_2^2 J - \sqrt{\left[ \frac{4}{H}\beta\sigma_2^2 J \right] \left[ 4\beta N_0 + \frac{4}{H}\beta\sigma_2^2 J \right]}}{2\frac{(\beta N_0)^2}{h_k^2}}. \quad (5.26)$$

□

## 5.5.2 Simplified Path-Loss Model and Incomplete Knowledge of $d_{J_i}$

In this model, channel gains are a function of distance only. For the sake of simplicity, we use  $\eta_{i_k} = d_{ii}^{-\gamma}$  and  $\eta_{J_k} = d_{J_i}^{-\gamma}$  where  $d_{ii}$  is the distance between the SU's transmitter and receiver,  $d_{J_i}$  is the distance between the SU's receiver and the jammer, and  $\gamma$  is the path-loss exponent.

In this subsection, the SU is assumed to have an incomplete knowledge of  $d_{J_i}$  and, therefore, treats it as a random variable with an arbitrary pdf  $f_{d_{J_i}}$ . The jammer in this model is assumed to have complete knowledge of the system model. That said, we rewrite the jammer's marginal



distribution at equilibrium according to:

$$F_{p_{J_k}}(y) = \lambda_i \beta d_{ii}^\gamma (N_0 + y d_{ji}^{-\gamma}), \quad (5.27)$$

where, in this case,  $y \in \left[0, \left(\frac{1}{\beta \lambda_i d_{ii}^\gamma} - N_0\right) / d_{ji}^{-\gamma}\right]$  and  $F_{p_{J_k}}$  admits a discontinuity point at 0 with mass point  $\lambda_i \beta N_0 d_{ii}^\gamma$ .

Similarly, we can write the SU's marginal distribution at equilibrium as follows:

$$F_{p_{i_k}}(x) = 1 - \lambda_J \left(\frac{1}{\lambda_i} - x\right) \quad (5.28)$$

where  $x \in [\beta N_0 d_{ii}^\gamma, \lambda_i^{-1}]$  for all  $k$ .  $F_{p_{i_k}}$  admits a discontinuity point at  $\beta N_0 d_{ii}^\gamma$  with mass point  $\lambda_J \beta N_0 d_{ii}^\gamma + 1 - \lambda_J / \lambda_i$ .

As assumed earlier, the SU transmitter has incomplete knowledge of the distance between the jammer and the SU receiver. Accordingly, the SU transmitter treats this distance as a random variable with an arbitrary pdf  $f_{d_{J_i}}$ . In this subsection, we consider a particular pdf that is described by:

$$f_{d_{J_i}}(d) = \frac{2d}{R^2}, \text{ for } 0 \leq d \leq R, \quad (5.29)$$

where  $R$  is the maximum distance that a jammer can be located at.

By substituting (5.29) in (5.27), we evaluate the expected value of  $d_{ji}^{-\gamma}$  and, thereby, compute SU's view on the CDF that governs the jammer's power over a given channel  $k$ ,  $\forall k$ , according to:

$$F'_{p_{J_k}}(y) = \lambda_i \beta d_{ii}^\gamma \left( N_0 + \frac{2R^{-\gamma}}{|2-\gamma|} y \right), \quad (5.30)$$

where  $\gamma \neq 2$  and  $|\cdot|$  is used to ensure the increasing monotonicity of  $F'_{p_{J_k}}$  for  $\gamma > 2$ . Note that the aforementioned condition and the closed-form expression of the averaged jammer's marginal by the SU transmitter are a result of the particular pdf we are considering.

So far, we have analyzed the game and derived closed form expressions for both players' optimal marginal CDFs modeling their power allocation schemes. In order to find these strategies and, eventually, evaluate the expected utility of each player, we need to find the KKT parameters ( $\lambda_i$  and  $\lambda_j$ ) which, in our model, are dependent on  $f_{d_{J_i}}$  due to the lack of complete knowledge at the SU transmitter's side.

**Lemma 5.2.** *Given  $f_{d_{J_i}}$  is provided by (5.29), the KKT multipliers are evaluated as follows,*

$$\lambda_i = \frac{\beta N_0 d_{ii}^{-\gamma} + \frac{\beta J d_{J_i}^{-\gamma}}{d_{ii}^\gamma H}}{(\beta N_0)^2} - \frac{\sqrt{\left[ \frac{\beta J d_{J_i}^{-\gamma}}{d_{ii}^\gamma H} \right] \left[ \frac{\beta J d_{J_i}^{-\gamma}}{d_{ii}^\gamma H} + 2\beta N_0 d_{ii}^{-\gamma} \right]}}{(\beta N_0)^2}, \quad (5.31)$$

and

$$\lambda_j = \frac{\frac{P}{H}}{\beta N_0 d_{ii}^\gamma + \frac{1}{2} \left( \left( \frac{1}{\lambda_i} \right)^2 - (\beta N_0 d_{ii}^\gamma)^2 \right)}. \quad (5.32)$$

*Proof.* The necessary slackness condition of the KKT multiplier method for  $\lambda_j > 0$  implies that  $\sum_{k=1}^H \int_{I'} I' dF_{I'_k}(I') = \beta d_{ii}^\gamma (HN_0 + Jd_{J_i}^{-\gamma})$  which is equivalent to  $\sum_{k=1}^H \int_y y dF_{p_{J_k}}(y) = J$ . Solving this yields the following quadratic equation,

$$(\beta N_0)^2 \lambda_i^2 - \left[ 2\beta N_0 d_{ii}^{-\gamma} + \frac{2\beta J d_{J_i}^{-\gamma}}{d_{ii}^\gamma H} \right] \lambda_i + d_{ii}^{-2\gamma} = 0, \quad (5.33)$$

with a discriminant  $\Delta = \left[ \frac{2\beta J d_{J_i}^{-\gamma}}{d_{ii}^\gamma H} \right] \left[ \frac{2\beta J d_{J_i}^{-\gamma}}{d_{ii}^\gamma H} + 4\beta N_0 d_{ii}^{-\gamma} \right]$ . It is clear that  $\Delta > 0$ . Therefore, (5.33) admits two real roots,  $\lambda_{i,1,2}$ , such that:

$$\lambda_{i,1,2} = \frac{\beta N_0 d_{ii}^{-\gamma} + \frac{\beta J d_{J_i}^{-\gamma}}{d_{ii}^\gamma H} \pm 0.5\sqrt{\Delta}}{(\beta N_0)^2}. \quad (5.34)$$

But, we need  $\frac{1}{\lambda_i} \geq \beta N_0 d_{ii}^\gamma$ , then

$$\lambda_i = \frac{\beta N_0 d_{ii}^{-\gamma} + \frac{\beta J d_{Ji}^{-\gamma}}{d_{ii}^\gamma H} - 0.5\sqrt{\Delta}}{(\beta N_0)^2}. \quad (5.35)$$

In order to evaluate  $\lambda_J$ , the necessary slackness condition of the KKT multiplier method for  $\lambda_i > 0$ , applied to the utility function in (5.7) yields  $\sum_{k=1}^H \int_x x dF_{p_{i_k}}(x) = P$  from which we obtain  $\lambda_J = \frac{\frac{P}{H}}{\beta N_0 d_{ii}^\gamma + \frac{1}{2} \left( \left( \frac{1}{\lambda_i} \right)^2 - (\beta N_0 d_{ii}^\gamma)^2 \right)}$ , where  $\lambda_i$ , due to SU's incomplete knowledge about the jammer's location in this case, is given by

$$\lambda_i = \frac{\beta N_0 d_{ii}^{-\gamma} + \frac{2\beta J R^{-\gamma}}{|2-\gamma| d_{ii}^\gamma H}}{(\beta N_0)^2} - \frac{0.5\sqrt{16 \left[ \frac{\beta J R^{-\gamma}}{|2-\gamma| d_{ii}^\gamma H} \right] \left[ \frac{\beta J R^{-\gamma}}{|2-\gamma| d_{ii}^\gamma H} + \beta N_0 d_{ii}^{-\gamma} \right]}}{(\beta N_0)^2}. \quad (5.36)$$

□

## 5.6 Sensing-based Spectrum Access

So far, we have investigated the scenario where both the SU and the jammer strategically allocate their powers over  $H$  orthogonal channels which are assumed available.

### 5.6.1 Problem Formulation

In this section, we no longer assume that the set of  $N$  channels are always available. In other words, we consider each of these channels to be licensed to a unique PU whose activity is intermittent and follows an On-Off model [27]. In Fig. 5.3, we show a set of  $H$  PUs and a single-hop CRN comprising of the SU transmitter-receiver pair and the jammer. We assume that the SU's transmitter performs spectrum sensing on each frequency band and makes a decision on the absence or presence of the corresponding PU. Therefore, the following scenarios arise for every PU

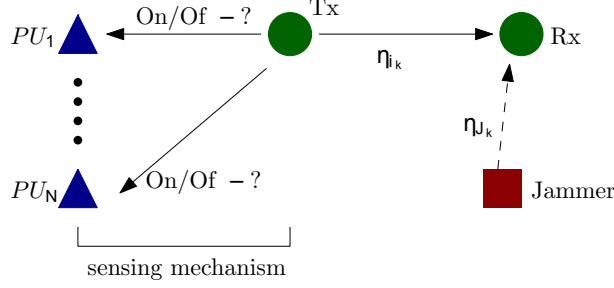


Fig. 5.3: A set of  $H$  PUs and a single-hop CRN with one SU Tx-Rx pair in the presence of a jammer.

channel: i) the PU is inactive and the SU infers the same, ii) the PU is inactive and the SU infers the opposite, iii) the PU is active and the SU infers the opposite, and iv) the PU is active and the SU infers the same. We denote the probabilities of each of the aforementioned scenarios by  $q_{00_k}$ ,  $q_{01_k}$ ,  $q_{10_k}$ , and  $q_{11_k}$  respectively corresponding to the  $k$ -th PU-owned channel. Furthermore, we, in this chapter, assume that the PU transmit power is sufficiently large so that the SU's payoff is zero whenever a collision takes place. Therefore, the SU's payoff is defined as follows:

$$\mathcal{U}_i = \sum_{k \in \mathcal{K}} q_{00_k} \mathbb{1} \left\{ \frac{p_{i_k} \eta_{i_k}}{N_0 + p_{J_k} \eta_{J_k}} \geq \beta \right\}, \quad (5.37)$$

where  $\mathcal{K}$  is the set of frequency bands deemed available by the SU transmitter.

On the other hand, the jammer is assumed to be aware of SU's sensing decisions, e.g., the jammer is of reactive type [98] or it simply listens to the transmitter-receiver pair handshake process on which channels to tune to [4, 6, 13]. In other words, it acquires full knowledge of the set of frequency bands that are deemed available by the SU and their corresponding information regarding PUs' activities and, thereby, is interested in disrupting SU's transmissions over each of these channels by adopting a power allocation strategy so that the condition in (5.2) is not satisfied. Accordingly, we write the jammer's payoff as:

$$\mathcal{U}_J = \sum_{k \in \mathcal{K}} q_{00_k} \mathbb{1} \left\{ \frac{p_{i_k} \eta_{i_k}}{N_0 + p_{J_k} \eta_{J_k}} < \beta \right\} + q_{10_k}. \quad (5.38)$$

In this respect, note that the jammer does not allocate power over  $k$  if  $k \notin \mathcal{K}$ . Note also that

the jammer's payoff on channel  $k$ , when the PU is active and SU's inference on its activity is the opposite, is equal to  $q_{10_k}$  given the large PU interference at the SU receiver that is sufficiently high so that (5.2) is not satisfied.

In this section, not only the jammer is assumed to have incomplete information of  $\eta_{i_k}$ , but also  $\eta_{J_k}$ . Following a similar reasoning to that discussed in Section 5.3, the power allocation game, at hand in this case, between the SU and the jammer also involves solving two optimization problems – one from the SU's perspective and another from the jammer's perspective.

### *SU's Perspective*

Find the optimal marginal CDF,  $F_{p_{i_k}}$  for all  $k$ , such that:

$$\begin{aligned} & \underset{\{F_{p_{i_k}}\}_{k \in \mathcal{K}}}{\text{maximize}} && \sum_{k \in \mathcal{K}} q_{00_k} \int_0^\infty F_{\mathcal{I}_k}(x) dF_{p_{i_k}}(x) \\ & \text{subject to:} && \sum_{k \in \mathcal{K}} \pi_k \int_0^\infty x dF_{p_{i_k}}(x) \leq P, \end{aligned} \quad (5.P3)$$

where  $\pi_k = q_{00_k} + q_{10_k}$  is the probability of Scenarios i or iii occurring.

### *Jammer's Perspective*

Find the optimal marginal CDF,  $F_{p_{J_k}}$  for all  $k$ , such that:

$$\begin{aligned} & \underset{\{F_{p_{J_k}}\}_{k \in \mathcal{K}}}{\text{maximize}} && \sum_{k \in \mathcal{K}} q_{00_k} \left( \int_{\eta} \int_{\beta N_0}^{\infty} F_{\mathcal{P}_k}(I) dF_{\mathcal{S}_k}(I) f_{\eta} d\eta \right) + q_{10_k} \\ & \text{subject to:} && \sum_{k \in \mathcal{K}} \pi_k \int_{\eta} \int_{\beta N_0}^{\infty} I dF_{\mathcal{S}_k}(I) f_{\eta} d\eta \leq \beta \left( |\mathcal{K}| N_0 + J \int_{\eta} \eta f_{\eta} d\eta \right), \end{aligned} \quad (5.P4)$$

where, in this case,  $\mathcal{S}_k = \beta(N_0 + p_{J_k}\eta)$ ,  $|\mathcal{K}|$  is the cardinality of  $\mathcal{K}$ , and  $\eta \sim f_{\eta}$ .

### 5.6.2 Equilibrium Analysis

The SU and the jammer need to employ probability distributions to model the uncertainties regarding the channel gains in order to solve for the optimal marginal distributions.

#### *Solution of 5.P3*

In order to maximize the SU's expected utility in this case, we apply the KKT method to the optimization problem, defined in 5.P3, according to:

$$\bar{U}_i = \sum_{k \in \mathcal{K}} \int_0^\infty (q_{00_k} F_{\mathcal{I}_k}(x) - \lambda_i \pi_k x) dF_{p_{i_k}}(x) + \lambda_i P. \quad (5.39)$$

**Theorem 5.3.** *The optimal marginal CDF,  $F_{p_{J_k}}$ , of the jammer's allocated power over channel  $k$ ,  $\forall k \in \mathcal{K}$ , is given by:*

$$F_{p_{J_k}}(y) = \frac{\lambda_i \beta}{\alpha_k} \mathbb{E}\left[\frac{1}{\eta_{i_k}}\right] (N_0 + y \mathbb{E}[\eta_{J_k}]), \quad (5.40)$$

where  $\alpha_k = \frac{q_{00_k}}{\pi_k}$  and  $y \in \left[0, \left(\frac{\alpha_k}{\beta \lambda_i \mathbb{E}\left[\frac{1}{\eta_{i_k}}\right]} - N_0\right) / \mathbb{E}[\eta_{J_k}]\right]$ .  $F_{p_{J_k}}$  admits a discontinuity point at 0 with mass point  $\lambda_i \beta N_0 \mathbb{E}\left[\frac{1}{\eta_{i_k}}\right]$ .

*Proof.* For brevity, we omit the proof since it similar to that of Theorem 5.1. □

#### *Solution of 5.P4*

The KKT multipliers approach is employed in 5.P4 in order to maximize the expected utility of the jammer. In this respect, we write the following:

$$\begin{aligned} \bar{U}_J = \sum_{k \in \mathcal{K}} \int_{\beta N_0}^\infty \int_\eta^\infty (q_{00_k} F_{\mathcal{P}_k}(I) - \lambda_J \pi_k I) dF_{S_k}(I) f_\eta d\eta \\ + \sum_{k \in \mathcal{K}} q_{10_k} + \lambda_J \beta \left( |\mathcal{K}| N_0 + J \int_\eta f_\eta d\eta \right). \end{aligned} \quad (5.41)$$

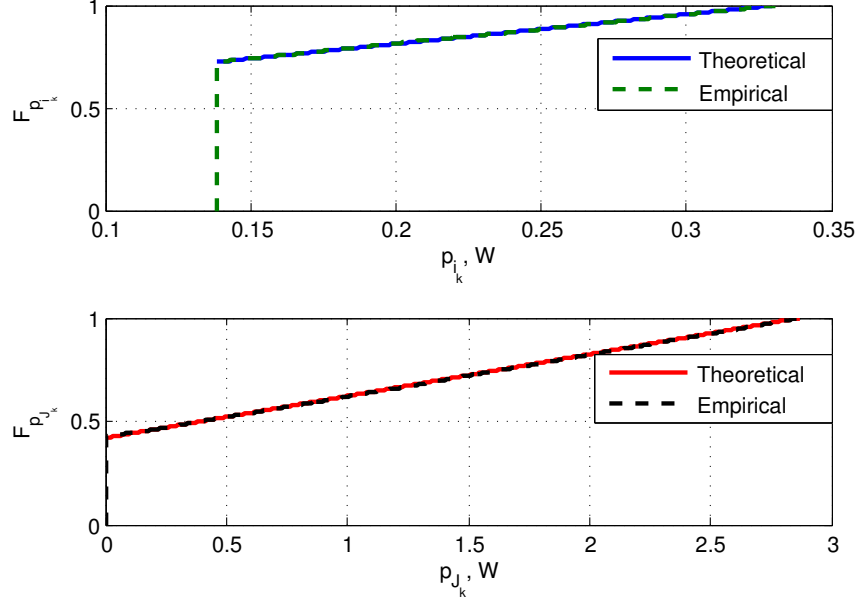


Fig. 5.4: Marginal CDFs of both players under incomplete knowledge of the jammer's location.

**Theorem 5.4.** *The optimal marginal CDF,  $F_{p_{i_k}}$ , of the SU's allocated power over channel  $k$ ,  $\forall k \in \mathcal{K}$ , is given by:*

$$F_{p_{i_k}}(x) = 1 - \lambda_J \left( \frac{\alpha_k}{\lambda_i} - x \right) \eta_{i_k}, \quad (5.42)$$

for  $x \in \left[ \frac{\beta N_0}{\eta_{i_k}}, \frac{\alpha_k}{\lambda_i} \right]$ .  $F_{p_{i_k}}$  admits a discontinuity point at  $\frac{\beta N_0}{\eta_{i_k}}$  with mass point  $\lambda_J \beta N_0 + 1 - \lambda_J \frac{\alpha_k}{\lambda_i} \eta_{i_k}$ .

*Proof.* For brevity, we also omit the proof here since it is similar to that of Theorem 5.2.  $\square$

Note that the evaluation of  $\lambda_i$  and  $\lambda_J$  is dependent on the specific prior distribution that each player assumes to model its uncertainty.

## 5.7 Numerical Results

In this section, we present numerical results to illustrate the game-theoretic equilibrium analysis presented in the chapter. For simplicity, we assume that both players have equal power budgets to be strategically distributed among  $H = 20$  channels. In this respect, we consider  $P = J = 40$  dBm. The SU transmissions subject to an SINR constraint, e.g.,  $\beta = -20$  dB, are assumed to

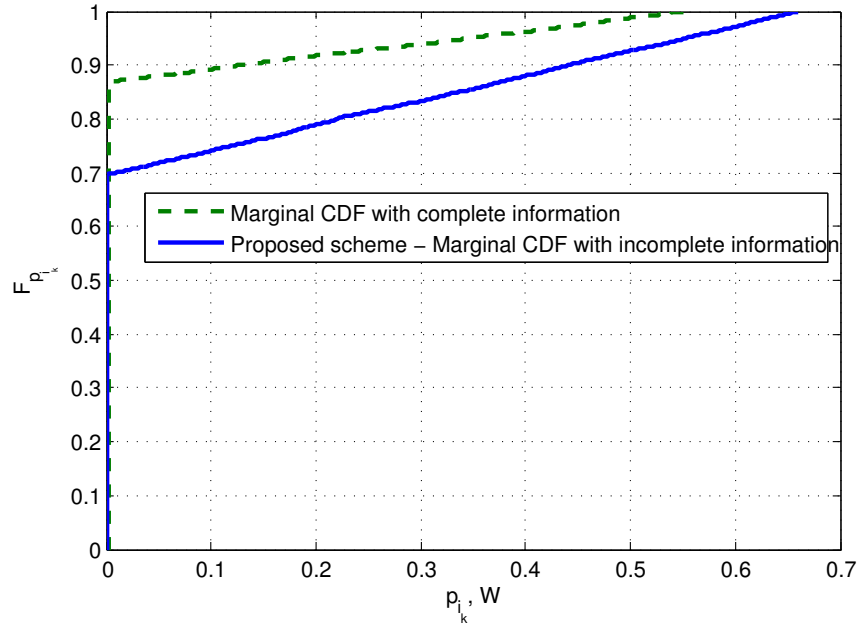


Fig. 5.5: SU's Marginal CDFs with complete and incomplete knowledge of channels' fading gains,  $g_k$  for all  $k$ .

undergo propagation losses and reduction in power based on: i) a multi-path fading channel model, and ii) a simplified path-loss channel model with a path-loss exponent, e.g.,  $\gamma = 1.8$ . In the former model, we consider the channel coefficients to be Rayleigh-distributed. Without loss of generality, we assume that  $h = h_1 = \dots = h_H$  and  $g = g_1 = \dots = g_H$ , while  $\sigma_1 = 0.5$  and  $\sigma_2 = 1$  in  $f_{h_k}$  and  $f_{g_k}$  respectively. Furthermore, in the latter model, we set the distance between the SU transmitter and its corresponding receiver,  $d_{ii}$ , to be equal to 200 m, and  $R$  in (5.29) to be equal to 250 m.

In Fig. 5.4, we plot the marginal CDFs of both players based on the closed form expressions obtained in our equilibrium analysis. We verify our theoretical results by comparing them to the ones obtained via simulations. It is clear in this figure that the results corroborate each other.

In Figs. 5.5 and 5.6, we consider the players' behaviors in the system given complete and incomplete information of the channel gains and, accordingly, plot the SU's and the jammer's marginal CDFs respectively. Fig. 5.5 portrays the advantage, characterized by higher expected utility of the SU, that our proposed power allocation approach has over complete knowledge of the channel gains. This is intuitive as the SU is expected to randomize its power over a larger range when it has incomplete information of the system. This incomplete level of knowledge also



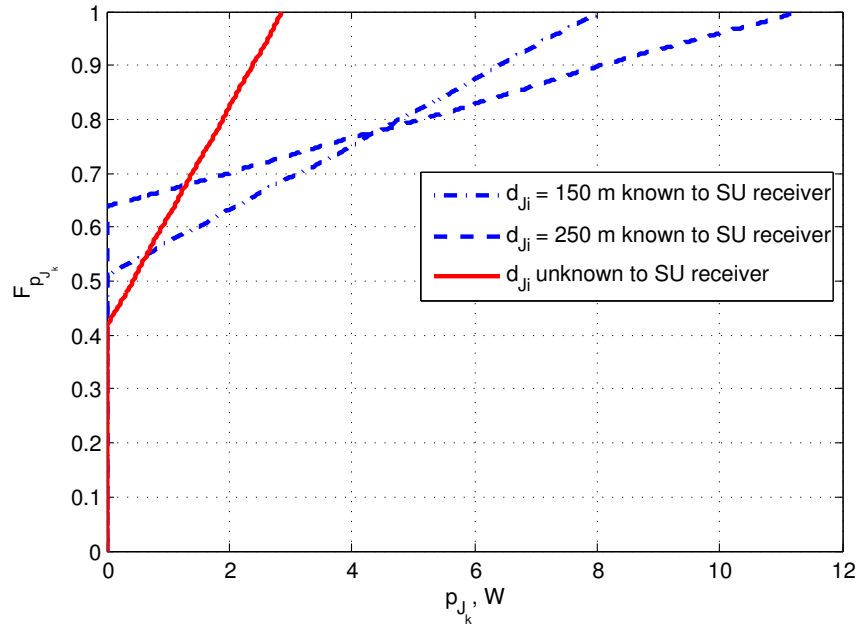


Fig. 5.6: Jammer's Marginal CDFs with complete and incomplete knowledge of the jammer's location.

imposes another advantage in terms of the probability of successful reception at the SU receiver. In Fig. 5.6, we plot the jammer's marginal CDF for the scenario where only the SU has incomplete information of the channel gains. In this case, the jammer tends to randomize its power over a larger power range as  $d_{J_i}$  increases in order to enhance its chances of bringing down the SU transmissions. The results obtained are intuitive as more resources are required by the jammer to block the SU transmissions when the jammer is farther apart from the SU receiver. It is also shown in this figure that the jammer randomizes its power over a smaller power range for  $R = 250$  m when the SU receiver follows a Bayesian approach to model  $d_{J_i}$ . In fact, the jammer needs less power resources to block the SU transmissions since the jammer, on an average, is located at a distance that is less than what we consider in the other two cases where the SU exactly knows  $d_{J_i}$ .

In Figs. 5.7 and 5.8, we plot the SU's expected utility with respect to increasing values of  $P$  for different instantiations of the channel gains as explained in Sections 5.5.1 and 5.5.2 respectively. Intuitively, the expected utility of the SU increases when its power budget increases. This is due to the increase in the available power resources to be strategically distributed. The results obtained in both figures match our intuition. For the scenario in Section 5.5.1, we, in Fig. 5.7, also compare

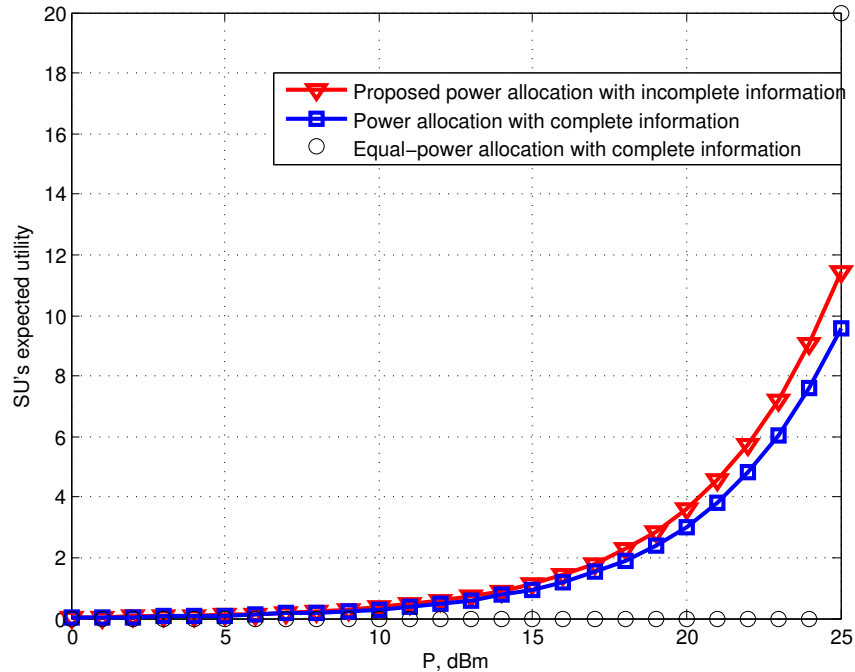


Fig. 5.7: SU's expected utility with respect to  $P$  and different power allocation schemes.

the performance of our proposed power allocation scheme with the power distribution described in [95] and a simple equal-power distribution given complete information of the channel gains. The SU's expected utility, evaluated in [94], is smaller than what we would obtain in the proposed power allocation scheme since the authors in [94] investigated the worst-case damage caused by the jammer. At the same time, the simple equal-power distribution is also expected to present a weaker performance unless the SU increases its transmit power so that the SINR constraint is satisfied. Fig. 5.7 corroborates the same intuition stated earlier. For the scenario in Section 5.5.2, the SU is expected to obtain a larger payoff when it assumes that the average location of the jammer is farther away. This is clearly shown in Fig. 5.8. It is also evident in Fig. 5.8 that the value of  $R$  chosen by the SU in (5.29) determines its payoff. For example, the SU, for  $R = 200$  m, is expected to obtain a payoff that is smaller than what it gets when it either exactly knows the location of the jammer ( $d_{J_i} = 200$  m) or  $R > 200$  m.

The expected utility of the SU is presented in Figs. 5.9 and 5.10 versus increasing values of the SINR threshold  $\beta$  above which an SU transmission is declared successful. Intuitively, it is known that the SU's expected utility decreases as  $\beta$  increases since more power resources are required

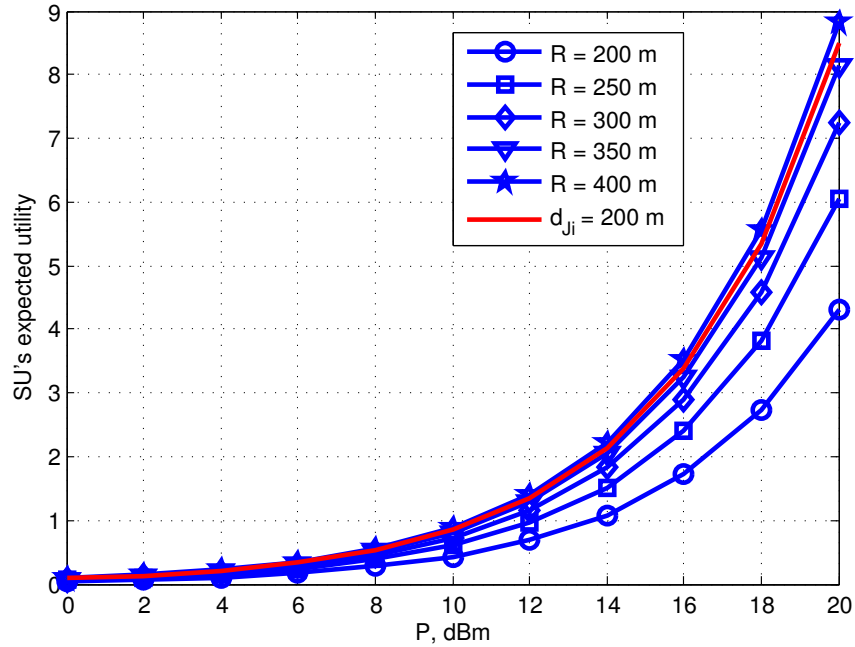


Fig. 5.8: SU's expected utility versus  $P$  under complete and incomplete knowledge of jammer's location.

to guarantee a successful communication session in this case. The results obtained corroborate our observation as smaller expected utility is presented in both figures. In Fig. 5.9, we further compare the performance of our proposed power allocation scheme with the power distribution described in [94] and the simple equal-power distribution presented earlier. It is clear in this figure that the SU's expected utility evaluated according to the proposed power allocation scheme outperforms the other two schemes. This is mainly because the jammer is considered to have incomplete information about channel gains and, accordingly, the opponent player is expected to achieve a better payoff than when the jammer exactly knows the game. Furthermore, in Fig. 5.10, we notice that the SU obtains a higher expected utility when the jammer, on an average, is farther away (or as  $R$  increases).

In Fig. 5.11, we plot the behavior of SU's expected utility with respect to increasing values of the jammer's power budget and compare it to that of [94] and the simple equal-power distribution. It is clear in Fig. 5.11 that smaller expected utility is obtained for all three allocation strategies when the jammer becomes more powerful (e.g.,  $J$  increases). In addition, a similar observation is made from the results in Figs. 5.7 and 5.9 as the expected utility of the SU evaluated based on our

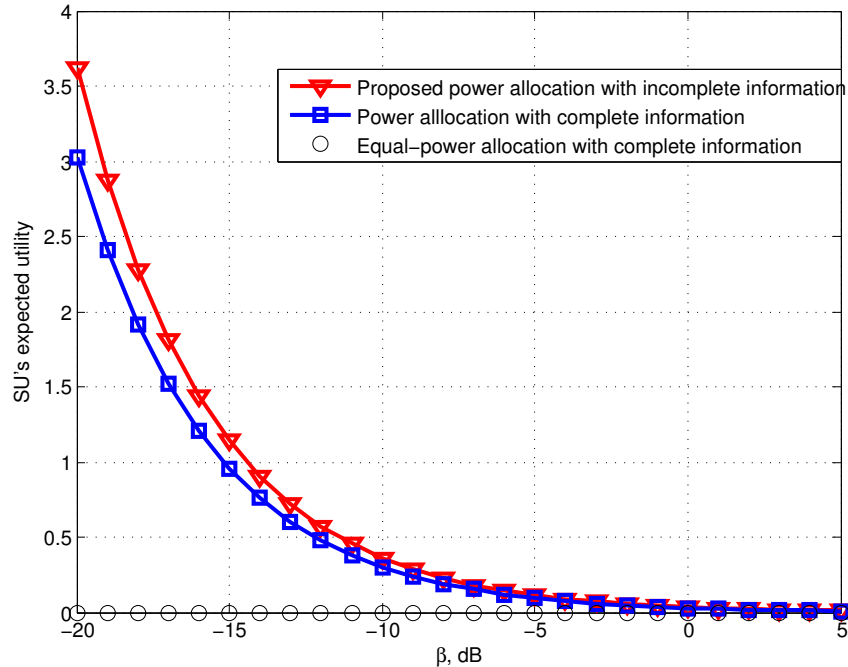


Fig. 5.9: SU's expected utility with respect to increasing values of  $\beta$  and different power allocation schemes.

proposed approach is greater than that in [94] and the equal-power strategies. Also, note that the equal power allocation outperforms the other two schemes when  $J = 15$  dBm. This is intuitive because the SINR constraint at SU's receiver is satisfied for such value of  $J$ .

So far, we have presented simulation results for the case where the SU assumes that all  $H$  channel are available for it to transmit on. For the case where the SU senses these channels before it transmits, we set  $q_k = 0.1$  and  $\pi_k = 0.25$  for all  $k$  for simplicity. If active, the PU transmitting power over each channel is chosen to be equal to 90 dBm, i.e., it is sufficiently high so that (5.2) is not satisfied. In Fig. 5.12, we present the SU's expected utility versus  $\alpha_k$  which, in turn, varies with  $q_{10_k}$  given  $q_k = 0.1$  and  $q_{10_k} = [0, 0.1, 0.2, 0.3, 0.4, 0.5]$ . It is intuitive to say that the expected utility of the SU increases when the probability of SU's transmissions colliding with PUs gets smaller or  $q_{10_k}$  decreases (i.e.,  $\alpha_k$  increases in this case), and vice-versa. It is clear in this figure that our intuition matches our simulation results.

At this point, it is, however, essential to mention that ignoring the channel imperfections in the signal propagation model [94] is not realistic. Therefore, our proposed Bayesian NE strategies are

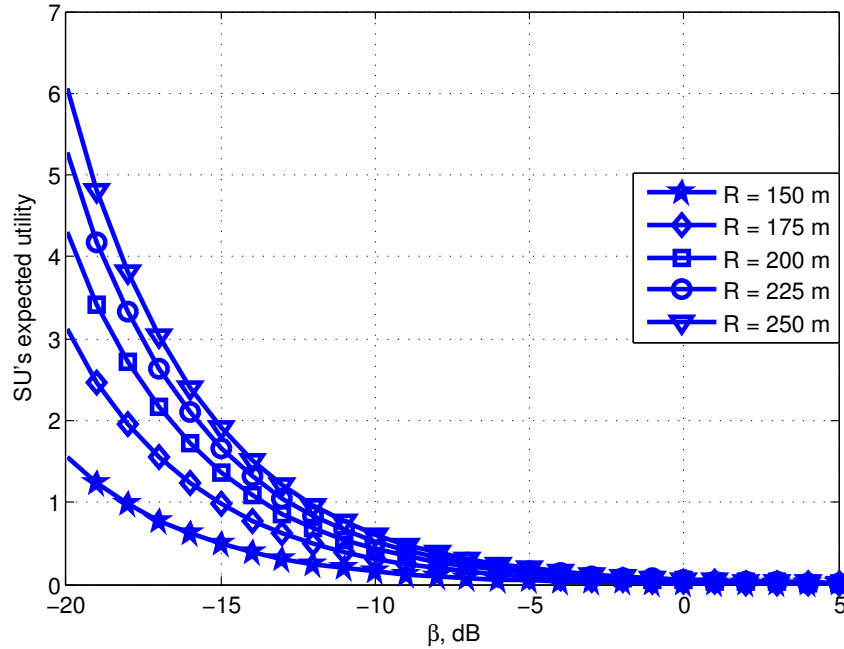


Fig. 5.10: SU's expected utility versus  $\beta$  for different values of  $R$ .

more practical and rewarding for the players than the other two schemes' strategies, and, therefore, the SU has to choose its as the optimal power allocation strategy (i.e., defense strategy) against the malicious jammer.

## 5.8 Summary

In this chapter, we considered the problem of competitive communications of a SU in the presence of a jammer with incomplete knowledge of the gains of the channels. In our work, the SU chooses its transmission strategy with the intention of satisfying the SINR constraint at the intended receiver. On the other hand, the jammer tries to sabotage the SU transmissions by strategically adopting a power allocation strategy. We further assumed that both players consider probability distributions to model the incomplete information in the framework and, hence, treat the power allocation game as imperfect. Furthermore, we investigated the mixed strategy solution space under two instantiations of the channel gains. Specifically, as the mixed strategy solution, we provided the marginal distributions of the SU and the jammer according to which they would select their

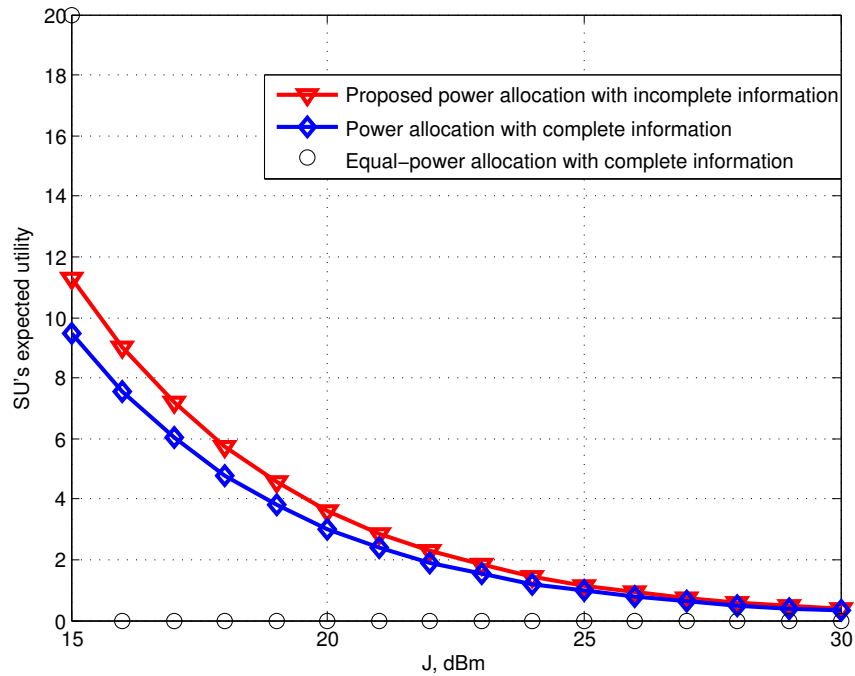


Fig. 5.11: SU's expected utility versus  $J$  for different power allocation schemes.

transmission powers in equilibrium.

Motivated by the famous Colonel-Blotto game [73], we presented a novel strategic power allocation game with different levels of uncertainties between the SU transmitter and the jammer. We next summarize the dissertation and present few work directions that can be pursued in the future.

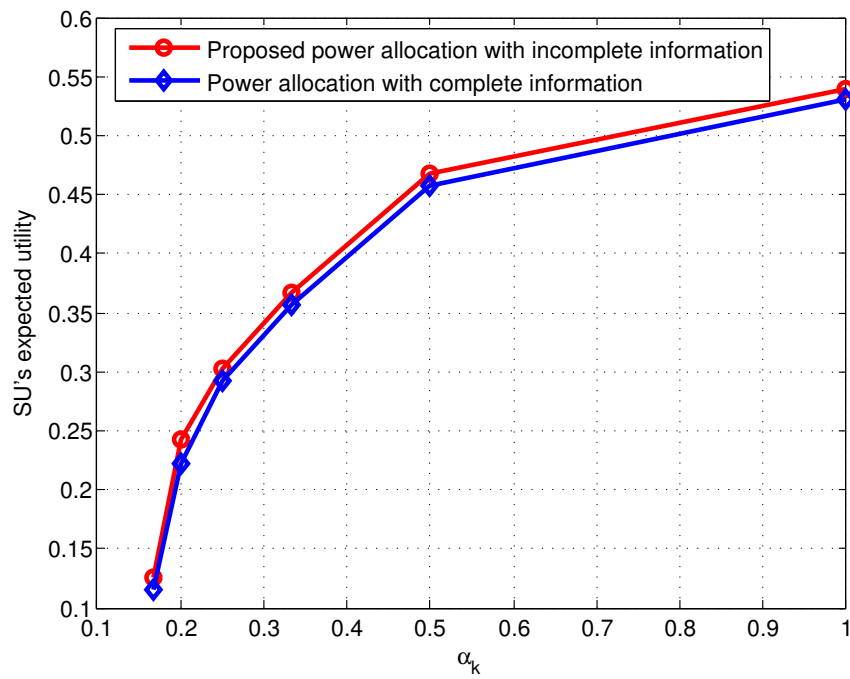


Fig. 5.12: SU's expected utility versus  $\alpha_k$ .

# CHAPTER 6

## CONCLUSION

### 6.1 Summary

We presented four different interference mitigation techniques to deal with communication and jamming interference in this dissertation. For communication interference, we presented two techniques. In order to make SU transmissions resilient to PUs' interference, the first technique exploited PTC combined with  $M$ -ary frequency shift keying. The other one utilized a novel frequency allocation approach using Matching theory in an attempt to mitigate SU interference. Furthermore, two jamming interference mitigation techniques were investigated. One technique exploited ARQ protocols and adopted a uniform energy allocation strategy to mitigate the jammer's effect. The other one was based on a game-theoretic framework where we employed a defense strategy against jamming using a strategic power allocation.

In Chapter 2, we employed a PTC based framework to mitigate the impact of PUs modeled using a practical *dynamic* channel occupancy model in CRNs. We computed the SU link's BER approximately which was shown to be quite accurate. This approximation allows one to use BER as a QoS metric to determine the link quality of an SU link for applications such as link adaptation. Furthermore, in order to assess the effectiveness of the proposed PTC based multi-level FSK communication scheme, we compared the performance to that of an uncoded opportunistic



$M$ -FSK system, a coded  $M$ -FSK system, a coded BPSK modulated system deploying parallel transmissions, and a  $\frac{1}{2}$ -rate LDPC encoding with an  $M$ -FSK modulation system. Based on the comparisons described in Section 2.6, we showed that the proposed scheme outperforms the latter two under relatively heavy PU interference. We also presented results that exhibit the resiliency of an SU link to interference for PTCs in the presence of multiple *dynamic* PUs activities.

We introduced a distributed model in Chapter 3 for the allocation of PU-owned frequency bands to SUs in a CRN. In the proposed model, SUs sense the licensed spectrum looking for white spaces. We modeled the problem as a *matching game* between SUs and PUs. We proposed a novel distributed algorithm to obtain a stable and optimal matching. Moreover, we compared our proposed algorithm with the deferred acceptance algorithm and a random channel allocation approach and showed the superior performance of our approach.

In Chapter 4, we investigated the design and performance analysis of a stop-and-wait ARQ protocol with a perfect feedback channel in the presence of jammer interference and ISI. We defined system-latency as the maximum number of transmission attempts required at the transmitter to achieve successful reception of a data packet and attempted to minimize it by modeling our framework as a constrained optimization problem in which system-latency is to be minimized such that the probability of successfully receiving a data packet satisfies a prescribed quality-of-service. Furthermore, a game-theoretic formulation was taken into account in the form of a minimax game between the transmitter and the strategic jammer. An NE solution was provided in the form of uniform energy allocations for both the transmitter and the jammer which, in turn, were used to minimize system-latency.

In Chapter 5, we considered the problem of competitive communications of a SU in the presence of a jammer with incomplete knowledge of the gains of the channels. In this work, the SU chooses its transmission strategy with the intention of satisfying the SINR constraint at the intended receiver. On the other hand, the jammer tries to sabotage the SU transmissions by strategically adopting a power allocation strategy. We further assumed that both players consider probability distributions to model the incomplete information in the framework and, hence, treat the power al-

location game as imperfect. Furthermore, we investigated the mixed strategy solution space under two instantiations of the channel gains. Specifically, as the mixed strategy solution, we provided the marginal distributions of the SU and the jammer according to which they would select their transmission powers in equilibrium. We showed that our approach outperforms a scenario employing an equal-power allocation with complete information of the system. We also showed that the proposed approach relatively lags behind in performance when compared with a similar approach with complete information. It is important to mention here that our proposed Bayesian NE strategies are more practical and rewarding for the players because ignoring the channel imperfections in the signal propagation model or assuming complete information is available to players are not realistic.

## 6.2 Future Work

In the modulation scheme proposed in Chapter 2, when the ON-OFF keying is replaced with antipodal signaling, we have a coded-OFDM framework at hand. This can be combined together with state-of-the-art OFDM-based spectrum overlay techniques in order to design hybrid cognitive radio networks and improve spectrum efficiency and the overall network throughput. One can analyze the aforementioned system design in future work. Furthermore, in the case of multiple SUs, PTCs employed at different SUs may interfere with each other. This motivates future investigation of PTCs that minimally interfere with each other when employed by spatially distributed SUs. One can also investigate optimal threshold selection in the case of hard-decision decoding and soft-decision decoding as a more effective decoding technique. Based on the promising results we obtained in a CRN, generalizing the proposed scheme to tackle wireless networks subject to jamming attacks and malicious nodes' activities is an interesting direction to pursue in future work.

Exploring SUs' extreme selfishness is a compelling extension of the problem investigated in Chapter 3. In this case, an SU can send untruthful valuations in order to increase its chances in matching to the most preferred frequency bands. At the same time, generalizing the scheme to

include other matching forms constitutes another future work direction to pursue.

A similar design and performance analysis to what we provided in Chapter 4 for more practical re-transmission protocols, e.g., HARQ-RR and HARQ-IR protocols, and system models, e.g., energy harvesting capabilities at the transmitter and the jammer, can be pursued in future work. Another interesting direction to pursue includes the design of the analyzed system while considering some other performance metrics, e.g., average delay of a data packet, that relate directly to the type of application.

An interesting extension of the problem that is highlighted in Chapter 5 lies in studying the interactions between the SU and the jammer in a repeated Bayesian game setting where both players converge to the NE in an online manner. Considering the scenario where a jammer is capable of jamming SU's sensing block as well as transmissions is also another exciting direction that can be pursued.

## REFERENCES

- [1] “Federal Communications Commission: Spectrum Policy Task Force,” Nov. 2002.
- [2] F. Abrishamkar and Z. Siveski, “Pcs global mobile satellites,” *Comm. Mag.*, vol. 34, no. 9, pp. 132–136, Sep. 1996. [Online]. Available: <http://dx.doi.org/10.1109/35.536561>
- [3] I. F. Akyildiz, W.-Y. Lee, and K. R. Chowdhury, “Crahns: Cognitive radio ad hoc networks,” *Ad Hoc Netw.*, vol. 7, no. 5, pp. 810–836, Jul. 2009. [Online]. Available: <http://dx.doi.org/10.1016/j.adhoc.2009.01.001>
- [4] I. F. Akyildiz, W.-Y. Lee, M. C. Vuran, and S. Mohanty, “Next generation/dynamic spectrum access/cognitive radio wireless networks: A survey,” *Computer Networks*, vol. 50, no. 13, pp. 2127–2159, 2006.
- [5] I. Akyildiz, W.-Y. Lee, M. C. Vuran, and S. Mohanty, “A survey on spectrum management in cognitive radio networks,” *IEEE Communications Magazine*, vol. 46, no. 4, pp. 40–48, Apr. 2008.
- [6] H. M. Almasaeid and A. E. Kamal, “Receiver-based channel allocation for wireless cognitive radio mesh networks,” in *IEEE Symposium on New Frontiers in Dynamic Spectrum*, Apr. 2010, pp. 1–10.
- [7] E. Altman, K. Avrachenkov, and A. Garnaev, “Jamming in wireless networks: The case of several jammers,” in *International Conference on Game Theory for Networks*, 2009, pp. 585–592.

- [8] F. Ananasso and F. Delli Priscoli, "The role of satellites in personal communication services," *IEEE Journal on Selected Areas in Communications*, vol. 13, no. 2, pp. 180–196, Feb 1995.
- [9] W.-C. Ao and K.-C. Chen, "End-to-end HARQ in cognitive radio networks," in *Proc. IEEE Wireless Comm. and Networking Conf. (WCNC)*, Apr. 2010, pp. 1–6.
- [10] M. Ara, H. Reboredo, S. A. M. Ghanem, and M. R. D. Rodrigues, "A zero-sum power allocation game in the parallel gaussian wiretap channel with an unfriendly jammer," in *IEEE International Conference on Communication Systems*, 2012, pp. 60–64.
- [11] S. Bayram, N. D. Vanli, B. Dulek, I. Sezer, and S. Gezici, "Optimum power allocation for average power constrained jammers in the presence of non-gaussian noise," *IEEE Communications Letters*, vol. 16, no. 8, pp. 1153–1156, 2012.
- [12] A. Bharathidasan, V. An, and S. Ponduru, "Sensor networks: An overview," Department of Computer Science, University of California, Davis, Tech. Rep., 2002.
- [13] V. K. Bhargava and E. Hossain, *Cognitive Wireless Communication Networks*. Secaucus, NJ, USA: Springer-Verlag New York, Inc., 2007.
- [14] J. Boksiner, Y. Posherstnik, B. May, M. Saltzman, and S. Kamal, "Centrally controlled dynamic spectrum access for manets," in *IEEE Military Communications Conference*, Nov. 2013, pp. 641–646.
- [15] S. Boyd and L. Vandenberghe, *Convex Optimization*. New York, NY, USA: Cambridge University Press, 2004.
- [16] L. Cao and H. Zheng, "Distributed spectrum allocation via local bargaining," in *Second Annual IEEE Communications Society Conference on Sensor and Ad Hoc Communications and Networks*, Sep. 2005, pp. 475–486.

- [17] L. Carrasco, G. Femenias, and J. Ramis, "Channel-aware mac performance of AMC-ARQ-based wireless systems," *EURASIP Journal on Wireless Communications and Networking*, vol. 2013, no. 1, p. 213, 2013. [Online]. Available: <http://jwcn.erasipjournals.com/content/2013/1/213>
- [18] C.-S. Chang, *Performance Guarantees in Communication Networks*. London, UK, UK: Springer-Verlag, 2000.
- [19] T. C. Clancy, "Formalizing the interference temperature model," *Wiley J. on Wireless Comm. and Mobile Computing*, vol. 7, no. 9, pp. 1077–1086, Nov. 2007.
- [20] R. Comroe and J. Costello, D.J., "ARQ schemes for data transmission in mobile radio systems," *IEEE Journal on Selected Areas in Communications*, vol. 2, no. 4, pp. 472–481, July 1984.
- [21] F. D. Cote, I. N. Psaromiligkos, and W. J. Gross, "A chernoff-type lower bound for the Gaussian Q-function," Tech. Rep. arXiv:1202.6483, Mar 2012, comments: 7 pages, 2 figures.
- [22] D. Cox, "Wireless personal communications: what is it?" *IEEE Personal Communications*, vol. 2, no. 2, pp. 20–35, Apr 1995.
- [23] K. Dabcevic, A. Betancourt, L. Marcenaro, and C. S. Regazzoni, "Intelligent cognitive radio jamming - a game-theoretical approach," *EURASIP Journal on Advances in Signal Processing*, vol. 2014, no. 1, pp. 1–18, 2014.
- [24] V. H. M. Donald, "Advanced mobile phone service: The cellular concept," *Bell System Technical Journal*, vol. 58, no. 1, pp. 15–41, 1979. [Online]. Available: <http://dx.doi.org/10.1002/j.1538-7305.1979.tb02209.x>
- [25] R. El-Bardan, S. Brahma, and P. K. Varshney, "A game theoretic power control framework for spectrum sharing in competitive environments," in *Signals, Systems and Comput-*

- ers (ASILOMAR), 2013 Conference Record of the Forty Seventh Asilomar Conference on, 2013.
- [26] ———, “Power control with jammer location uncertainty: A game theoretic perspective,” in *48th Annual Conference on Information Sciences and Systems (CISS)*, March 2014, pp. 1–6.
- [27] R. El-Bardan, E. Masazade, O. Ozdemir, Y. S. Han, and P. K. Varshney, “Permutation trellis coded multi-level fsk signaling to mitigate primary user interference in cognitive radio networks,” *IEEE Transactions on Communications*, vol. 64, no. 1, pp. 104–116, Jan 2016.
- [28] R. El Bardan, E. Masazade, O. Ozdemir, and P. K. Varshney, “Performance of permutation trellis codes in cognitive radio networks,” in *Proc. IEEE Sarnoff Symp.*, May 2012, pp. 1–6.
- [29] M. Elalem, L. Zhao, and Z. Liao, “Interference mitigation using power control in cognitive radio networks,” in *Proc. IEEE Vehicular Tech. Conf.*, May 2010.
- [30] D. Estrin, R. Govindan, J. Heidemann, and S. Kumar, “Next century challenges: Scalable coordination in sensor networks,” in *Proceedings of the 5th Annual ACM/IEEE International Conference on Mobile Computing and Networking*, ser. MobiCom ’99. New York, NY, USA: ACM, 1999, pp. 263–270. [Online]. Available: <http://doi.acm.org/10.1145/313451.313556>
- [31] R. Etkin, A. Parekh, and D. Tse, “Spectrum sharing for unlicensed bands,” *IEEE Journal on Selected Areas in Communications*, vol. 25, no. 3, pp. 517–528, 2007.
- [32] Federal Communications Commission, “Establishment of interference temperature metric to quantify and manage interference and to expand available unlicensed operation in certain fixed mobile and satellite frequency bands,” *Et Docket 03-289, Notice of Inquiry and Proposed Rulemaking*, 2003.

- [33] D. Feng, C. Jiang, G. Lim, J. Cimini, L.J., G. Feng, and G. Li, "A survey of energy-efficient wireless communications," *IEEE Communications Surveys Tutorials*, vol. 15, no. 1, pp. 167–178, First 2013.
- [34] H. C. Ferreira, A. J. H. Vinck, T. G. Swart, and I. De Beer, "Permutation trellis codes," *IEEE Trans. Communications*, vol. 53, no. 11, pp. 1782–1789, Nov. 2005.
- [35] G. D. Forney, "Maximum-likelihood sequence estimation of digital sequences in the presence of intersymbol interference," *IEEE Transactions on Information Theory*, vol. 18, no. 3, pp. 363–378, 1972.
- [36] G. Forney, "Geometrically uniform codes," *Information Theory, IEEE Transactions on*, vol. 37, no. 5, pp. 1241–1260, Sep 1991.
- [37] D. Gale and L. S. Shapley, "College admissions and the stability of marriage," *The American Mathematical Monthly*, vol. 69, no. 1, pp. 9–15, 1962.
- [38] H. Gao, J. Wang, C. Jiang, and X. Zhang, "Equilibrium between a statistical mimo radar and a jammer," in *IEEE Radar Conference (RadarCon)*, May 2015, pp. 0461–0466.
- [39] A. Goldsmith, S. A. Jafar, I. Maric, and S. Srinivasa, "Breaking spectrum gridlock with cognitive radios: An information theoretic perspective," *Proceedings of the IEEE*, vol. 97, no. 5, pp. 894–914, May 2009.
- [40] A. Goldsmith, *Wireless Communications*. New York, NY, USA: Cambridge University Press, 2005.
- [41] M. Grossglauser and D. Tse, "Mobility increases the capacity of ad-hoc wireless networks," in *Twentieth Annual Joint Conference of the IEEE Computer and Communications Societies*, vol. 3, 2001, pp. 1360–1369.



- [42] N. Gunaseelan, L. Liu, J. Chamberland, and G. Huff, "Performance analysis of wireless hybrid-arq systems with delay-sensitive traffic," *IEEE Transactions on Communications*, vol. 58, no. 4, pp. 1262–1272, April 2010.
- [43] K. Guth and T. Ha, "An adaptive stop-and-wait ARQ strategy for mobile data communications," in *IEEE 40th Vehicular Technology Conference*, May 1990, pp. 656–661.
- [44] J. Harsanyi, "Games with incomplete information played by "bayesian" players, i-iii part i. the basic model," *Management Science*, vol. 14, no. 3, pp. 159–182, 1967.
- [45] E. Hossain, D. Niyato, and Z. Han, *Dynamic Spectrum Access and Management in Cognitive Radio Networks*, 1st ed. New York, NY, USA: Cambridge University Press, 2009.
- [46] F.-T. Hsu and H.-J. Su, "Power allocation strategy against jamming attacks in Gaussian fading multichannel," in *IEEE 25th Annual International Symposium on Personal, Indoor, and Mobile Radio Communication (PIMRC)*, Sept 2014, pp. 1062–1066.
- [47] J. Huang, R. Berry, and M. Honig, "Distributed interference compensation for wireless networks," *IEEE Journal on Selected Areas in Communications*, vol. 24, no. 5, pp. 1074–1084, May 2006.
- [48] S.-Y. Jeon and D.-H. Cho, "Modelling and analysis of arq mechanisms for wireless multi-hop relay system," in *IEEE Vehicular Technology Conference*, May 2008, pp. 2436–2440.
- [49] E. Jorswieck, "Stable matchings for resource allocation in wireless networks," in *17th International Conference on Digital Signal Processing*, Jul. 2011, pp. 1–8.
- [50] J. Ko and C. Kim, "Communication method between spectrum heterogeneous secondary users in OFDM-based cognitive radio," *Electronics Letters*, vol. 47, no. 14, pp. 827–829, Jul. 2011.

- [51] Y.-S. Kwon, H.-S. Kim, J.-H. Yoo, and J.-H. Chung, "A non-interfering cognitive radio system for spectrum sharing," in *Proc. Int. Symp. on Comm. and Information Technology*, Sep. 2009, pp. 664–665.
- [52] J. Laneman, D. Tse, and G. W. Wornell, "Cooperative diversity in wireless networks: Efficient protocols and outage behavior," *IEEE Transactions on Information Theory*, vol. 50, no. 12, pp. 3062–3080, Dec. 2004.
- [53] A. Leshem, E. Zehavi, and Y. Yaffe, "Multichannel opportunistic carrier sensing for stable channel access control in cognitive radio systems," *IEEE Journal on Selected Areas in Communications*, vol. 30, no. 1, pp. 82–95, Jan. 2012.
- [54] G. Li, Z. Xu, C. Xiong, C. Yang, S. Zhang, Y. Chen, and S. Xu, "Energy-efficient wireless communications: tutorial, survey, and open issues," *IEEE Wireless Communications*, vol. 18, no. 6, pp. 28–35, December 2011.
- [55] Y.-C. Liang, Y. Zeng, E. Peh, and A. T. Hoang, "Sensing-throughput tradeoff for cognitive radio networks," *IEEE Trans. Wireless Comm.*, vol. 7, no. 4, pp. 1326–1337, Apr. 2008.
- [56] S. Lin and D. J. Costello, Jr., *Error Control Coding: Fundamentals and Applications*. Prentice-Hall, 1983.
- [57] D. Lopez-Perez, X. Chu, A. Vasilakos, and H. Claussen, "Power minimization based resource allocation for interference mitigation in ofdma femtocell networks," *IEEE Journal on Selected Areas in Communications*, vol. 32, no. 2, pp. 333–344, Feb. 2014.
- [58] H. Mahmoud, T. Yucek, and H. Arslan, "OFDM for cognitive radio: merits and challenges," *IEEE Trans. Wireless Comm.*, vol. 16, no. 2, pp. 6–15, Apr. 2009.
- [59] J. Mitola and G. Q. Maguire, "Cognitive radio: making software radios more personal," *IEEE Personal Comm.*, vol. 6, no. 4, pp. 13–18, Aug. 1999.

- [60] J. Mitola, “Cognitive Radio — An Integrated Agent Architecture for Software Defined Radio,” DTech thesis, Royal Institute of Technology (KTH), Kista, Sweden, may 2000.
- [61] R. Mochaourab, B. Holfeld, and T. Wirth, “Distributed channel assignment in cognitive radio networks: Stable matching and walrasian equilibrium,” *IEEE Transactions on Wireless Communications*, vol. 14, no. 7, pp. 3924–3936, July 2015.
- [62] R. B. Myerson, *Game Theory: Analysis of Conflict*. Harvard University Press, 1991.
- [63] C. Nicola, H. Mercier, and V. K. Bhargava, “Error-correcting codes for dynamic spectrum allocation in cognitive radio systems,” in *Proc. Int. Symp. on Signals, Syst. and Electron.*, Aug. 2007, pp. 247–250.
- [64] R. Niu and P. Varshney, “Target location estimation in sensor networks with quantized data,” *IEEE Transactions on Signal Processing*, vol. 54, no. 12, pp. 4519–4528, Dec 2006.
- [65] G. Ozcan and M. C. Gursoy, “Throughput of cognitive radio systems with finite blocklength codes,” in *Proc. IEEE Annual Conf. on Inf. Sciences and Systems (CISS)*, Mar. 2012, pp. 1–6.
- [66] K. Pahlavan and P. Krishnamurthy, *Principles of Wireless Networks: A Unified Approach*, 1st ed. Upper Saddle River, NJ, USA: Prentice Hall PTR, 2001.
- [67] S. Prasad and D. J. Thunte, “Jamming attacks in 802.11g— a cognitive radio based approach,” in *Military Communications Conference*, 2011, pp. 1219–1224.
- [68] J. G. Proakis, *Digital communications*. McGraw-Hill New York, 1983.
- [69] ———, *Digital Communications*. McGraw -Hill, 2000.
- [70] D. Puccinelli and M. Haenggi, “Wireless sensor networks: applications and challenges of ubiquitous sensing,” *IEEE Circuits and Systems Magazine*, vol. 5, p. 2005, 2005.

- [71] T. Rappaport, *Wireless Communications: Principles and Practice*, 2nd ed. Upper Saddle River, NJ, USA: Prentice Hall PTR, 2001.
- [72] P. Ren, Y. Wang, Q. Du, and J. Xu, “A survey on dynamic spectrum access protocols for distributed cognitive wireless networks.” *EURASIP J. Wireless Comm. and Networking*, vol. 2012, p. 60, 2012.
- [73] B. Roberson, “The colonel blotto game,” *Economic Theory*, vol. 29, no. 1, pp. 1–24, September 2006. [Online]. Available: <http://ideas.repec.org/a/spr/joecth/v29y2006i1p1-24.html>
- [74] A. Roongta, J.-W. Moon, and J. Shea, “Reliability-based hybrid ARQ as an adaptive response to jamming,” *IEEE Journal on Selected Areas in Communications*, vol. 23, no. 5, pp. 1045–1055, May 2005.
- [75] A. E. Roth and M. A. Oliveira Sotomayor, *Two-sided matching : a study in game-theoretic modeling and analysis*, ser. Econometric society monographs. Cambridge, Mass.: Cambridge university press, 1992, 1990. [Online]. Available: <http://opac.inria.fr/record=b1127621>
- [76] G. Rucker, R. G. Cole, D. Cansever, and A. Mishra, “Games applied to jam resistant DSA radios,” in *Military Communications Conference*, 2012, pp. 1–6.
- [77] Y. Sagduyu, R. Berry, and A. Ephremides, “MAC games for distributed wireless network security with incomplete information of selfish and malicious user types,” in *International Conference on Game Theory for Networks*, 2009, pp. 130–139.
- [78] ———, “Wireless jamming attacks under dynamic traffic uncertainty,” in *Proceedings of the 8th International Symposium on Modeling and Optimization in Mobile, Ad Hoc and Wireless Networks (WiOpt)*, 2010, pp. 303–312.

- [79] G. Scutari and J.-S. Pang, "Joint sensing and power allocation in nonconvex cognitive radio games: Nash equilibria and distributed algorithms," *IEEE Transactions on Information Theory*, vol. 59, no. 7, pp. 4626–4661, 2013.
- [80] B. Shahrabi and N. Rahnavard, "Rateless-coding-based cooperative cognitive radio networks: Design and analysis," in *Proc. Annual IEEE on Comm. Society Conf. on Sensor, Mesh and Ad Hoc Comm. and Networking (SECON)*, June 2011, pp. 224–232.
- [81] F. Shayegh and M. R. Soleymani, "Rateless codes for cognitive radio in a virtual unlicensed spectrum," in *Proc. IEEE Sarnoff Symp.*, May 2011, pp. 1–5.
- [82] H.-P. Shiang and M. van der Schaar, "Distributed resource management in multihop cognitive radio networks for delay-sensitive transmission," *IEEE Transactions on Vehicular Technology*, vol. 58, no. 2, pp. 941–953, Feb. 2009.
- [83] M. K. Simon, *Probability Distributions Involving Gaussian Random Variables: A Handbook for Engineers, Scientists and Mathematicians*. Springer-Verlag New York, 2006.
- [84] M. Soysa, P. Cosman, and L. Milstein, "Optimized spoofing and jamming a cognitive radio," *IEEE Transactions on Communications*, vol. 62, no. 8, pp. 2681–2695, Aug 2014.
- [85] W. Stallings, *Wireless Communications and Networks*, 1st ed. Prentice Hall Professional Technical Reference, 2001.
- [86] C. Stevenson, G. Chouinard, Z. Lei, W. Hu, S. J. Shellhammer, and W. Caldwell, "IEEE 802.22: The first cognitive radio wireless regional area network standard," *IEEE Comm. Mag.*, vol. 47, no. 1, pp. 130–138, Jan. 2009.
- [87] N. Sufyan, N. Saqib, and M. Zia, "Detection of jamming attacks in 802.11b wireless networks," *EURASIP Journal on Wireless Communications and Networking*, vol. 2013, no. 1, p. 208, 2013. [Online]. Available: <http://jwcn.urasipjournals.com/content/2013/1/208>

- [88] T. G. Swart, I. De Beer, H. C. Ferreira, and A. J. H. Vinck, "Simulation results for permutation trellis codes using M-ary FSK," in *Proc. Int. Symp. on Power Line Comm. and its Applications*, Apr. 2005, pp. 317–321.
- [89] Q. Wang and M. Liu, "Joint control of transmission power and channel switching against adaptive jamming," in *Proc. of the 51st Annual Allerton Conference on Communication, Control, and Computing*, Oct. 2013, pp. 909–916.
- [90] S. Wang, Y. Wang, J. P. Coon, and A. Doufexi, "Energy-efficient spectrum sensing and access for cognitive radio networks," *IEEE Trans. Veh. Technol.*, vol. 61, no. 2, pp. 906–912, Feb. 2012.
- [91] W. Wang, M. Chatterjee, K. Kwiat, and Q. Li, "A game theoretic approach to detect and co-exist with malicious nodes in wireless networks," *Computer Networks*, vol. 71, pp. 63 – 83, 2014.
- [92] S. Weber, J. G. Andrews, S. Member, and N. Jindal, "The effect of fading, channel inversion, and threshold scheduling on ad hoc networks," *IEEE Trans. Inf. Theory*, vol. 53, pp. 4127–4149, 2007.
- [93] Y. Wu and Z. Yang, "Spectrum sharing under interference temperature and SINR constraints," in *Proc. Int. Conf. on Wireless Comm., Networking and Mobile Computing*, Oct. 2008, pp. 1–4.
- [94] Y. Wu, B. Wang, K. J. R. Liu, and T. C. Clancy, "Anti-jamming games in multi-channel cognitive radio networks," *IEEE Journal on Selected Areas in Communications*, vol. 30, no. 1, pp. 4–15, 2012.
- [95] Y. Wu, B. Wang, K. Liu, and T. Clancy, "Anti-jamming games in multi-channel cognitive radio networks," *IEEE Journal on Selected Areas in Communications*, vol. 30, no. 1, pp. 4–15, 2012.

- [96] L. Xiao, J. Liu, Y. Li, N. Mandayam, and H. Poor, "Prospect theoretic analysis of anti-jamming communications in cognitive radio networks," in *IEEE Global Communications Conference (GLOBECOM)*, Dec 2014, pp. 746–751.
- [97] Y. Xing, R. Chandramouli, S. Mangold, and N. Sai Shankar, "Dynamic spectrum access in open spectrum wireless networks," *IEEE Journal on Selected Areas in Communications*, vol. 24, no. 3, pp. 626–637, Mar. 2006.
- [98] W. Xu, W. Trappe, Y. Zhang, and T. Wood, "The feasibility of launching and detecting jamming attacks in wireless networks," in *Proceedings of the 6th ACM International Symposium on Mobile Ad Hoc Networking and Computing*, ser. MobiHoc '05. New York, NY, USA: ACM, 2005, pp. 46–57.
- [99] D. Yang, J. Zhang, X. Fang, A. Richa, and G. Xue, "Optimal transmission power control in the presence of a smart jammer," in *IEEE Global Communications Conference*, 2012, pp. 5506–5511.
- [100] G. Yue and X. Wang, "Anti-jamming coding techniques with application to cognitive radio," *IEEE Trans. Wireless Comm.*, vol. 8, no. 12, pp. 5996–6007, Dec. 2009.
- [101] —, "Design of efficient arq schemes with anti-jamming coding for cognitive radios," in *IEEE Wireless Communications and Networking Conference*, April 2009, pp. 1–6.
- [102] J. Zander, "Radio resource management in future wireless networks: requirements and limitations," *IEEE Communications Magazine*, vol. 35, no. 8, pp. 30–36, Aug. 1997.
- [103] Q. Zhao, B. Krishnamachari, and K. Liu, "On myopic sensing for multi-channel opportunistic access: structure, optimality, and performance," *IEEE Trans. Wireless Comm.*, vol. 7, no. 12, pp. 5431–5440, Dec. 2008.

# VITA

NAME OF AUTHOR: Raghed Ahmad El Bardan

PLACE OF BIRTH: Tyre, Lebanon

DATE OF BIRTH: November 02, 1985

GRADUATE AND UNDERGRADUATE SCHOOLS ATTENDED:

Lebanese American University, Lebanon

DEGREES AWARDED:

B. E., 2007, Lebanese American University, Lebanon

M. Sc., 2009, Lebanese American University, Lebanon

PROFESSIONAL EXPERIENCE:

- Research Intern (2015), ANDRO Computational Solutions
- Instructor (2009-2010), American University of Technology
- Intern (2006), International Turnkey Systems